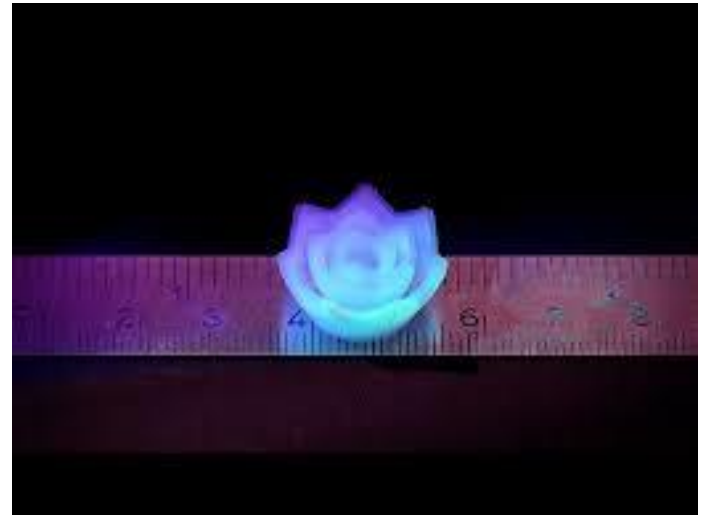
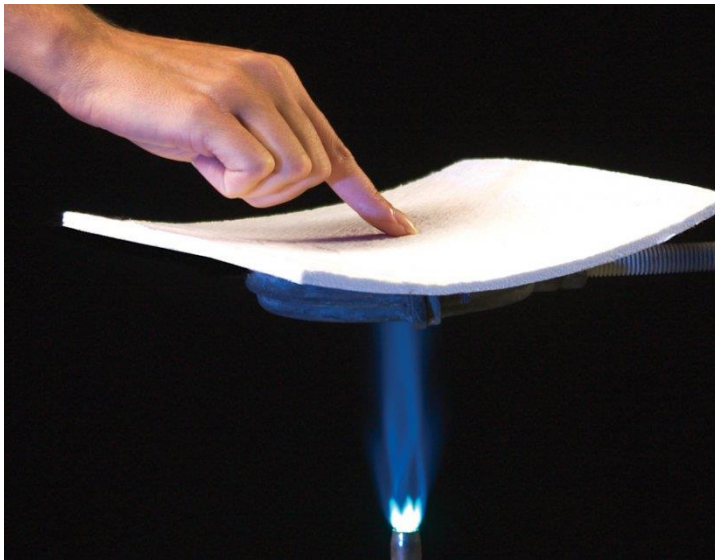


Aerogels



PART 1

Nanotechnology and Nanomaterials

3-dimensional ⇒ ...

- **Aerogels** (...are 3D nanomaterials!)

2-dimensional ⇒ **Atom arrays, thin sheets...**

- Graphene
- Metals
- Oxides

1-dimensional ⇒ **Nanotubes, nanowires, nanorods...**

- Carbon
- Silicon
- Oxides

0-dimensional ⇒ **Nanoparticles**

- Metals (Au, Pt, Ag etc.)
- Oxides (SiO₂, TiO₂, ZnO etc.)
- Semiconductors (CdS, CdSe, HgS etc.)

RECENT POSTS

IUPAC Concentrate – sample 2022-11-22

IUPAC Elections for the 2024–2025 Term

eTOC Alert 'Pure and Applied Chemistry' –
September 2022

Best Practices in Chemistry Education and
around e-Waste

IUPAC welcomes its new Executive
Director, Dr. Greta Heydenrych

CATEGORIES

RECENT RELEASES

FOR PUBLIC REVIEW

UPCOMING DEADLINES

AWARDS & PRIZES

GRANTS

UTHINGS

DIVISION BLOG POST

UPCOMING EVENTS

ANNOUNCEMENTS

CALL FOR INPUT

IUPAC ANNOUNCES THE 2022 TOP TEN EMERGING
TECHNOLOGIES IN CHEMISTRY

17 Oct 2022

Facebook Tweet Pin

The International Union of Pure and Applied Chemistry (IUPAC) has released the 2022 Top Ten Emerging Technologies in Chemistry. The goal of this initiative is to showcase the transformative value of chemistry and to inform the general public about the potential of chemical sciences to foster the well-being of Society and the sustainability of our planet. The Jury* –an international panel of prestigious scientists with a varied and broad range of expertise– reviewed and discussed the diverse pool of nominations of emerging technologies submitted by researchers from around the globe and selected the final top ten. These technologies are defined as transformative innovations in between a discovery and a fully-commercialized technology, having outstanding potential to open new opportunities in chemistry, sustainability, and beyond.

The **2022 finalists** are (in alphabetical order):

- Aerogels
- Fibre batteries
- Film-based fluorescent sensors
- Liquid solar fuel synthesis
- Nanoparticle mega libraries
- Nanozymes
- Rational vaccines with SNA
- Sodium-ion batteries
- Textile displays
- VR-enable interactive modeling



Aerogels

Aerogel is an open non-fluid colloidal network or polymer network that is expanded throughout its whole volume by a gas, and is formed by the removal of all swelling agents from a gel without substantial volume reduction or network compaction.

Aerogels were first reported in 1931 by S. S. Kistler, who was studying the properties of wet-gels. The term was introduced in order to describe gels in which the solvent was replaced by a gas without collapse of the solid network.

COHERENT EXPANDED AEROGELS

BY. S. S. KISTLER

Summary

It was predicted from general considerations and demonstrated experimentally that in general after a gel is formed the liquid phase is accidental and unnecessary.

Aerogels of silica, alumina, tungstic oxide, ferric oxide, stannic oxide, nickel tartrate, cellulose, nitrocellulose, gelatin, agar and egg albumin were made by removal of the water from the normal gels. Rubber offered difficulties not yet surmounted, but the way has been indicated.

The preparation and properties of these aerogels have been briefly described, and some discussion of structure has been included.

*College of the Pacific,
Stockton, California,
and
Stanford University.*

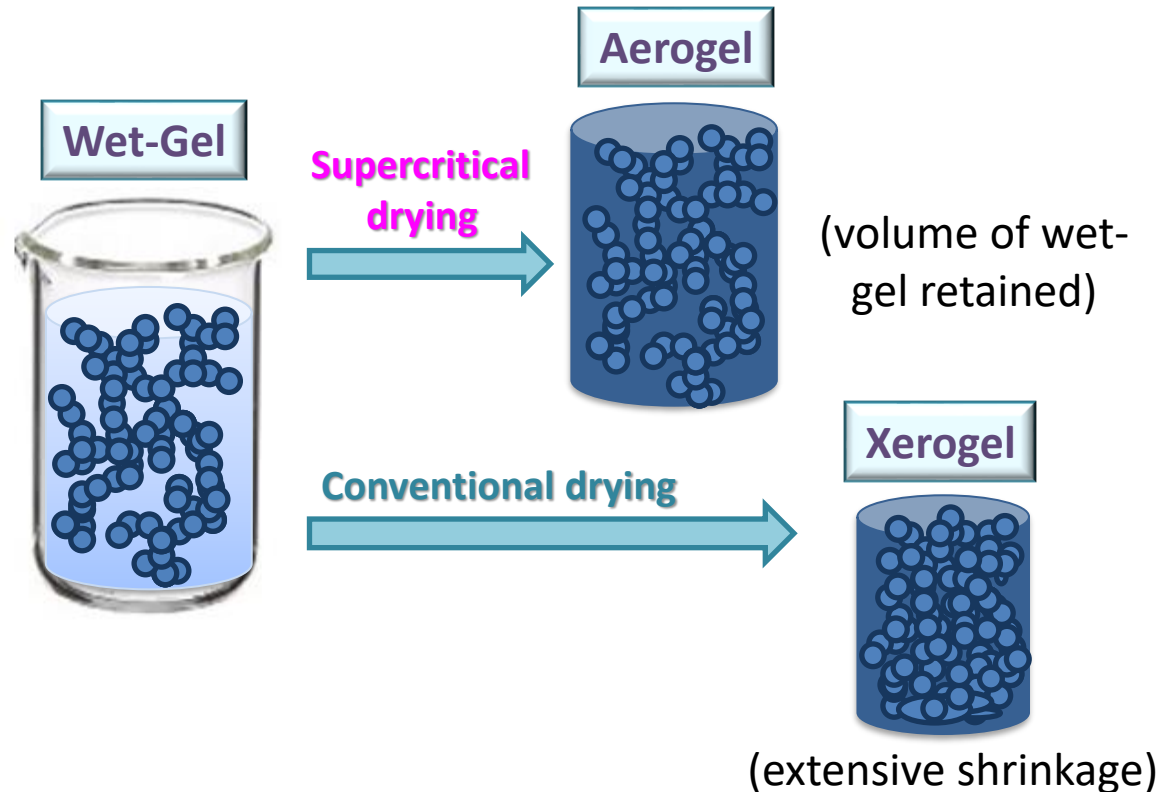
S. S. Kistler, *Nature*, **1931**, 127, 741

Aerogels

Aerogel is an open non-fluid colloidal network or polymer network that is expanded throughout its whole volume by a gas, and is formed by the removal of all swelling agents from a gel without substantial volume reduction or network compaction.

Aerogels were first reported in 1931 by S. S. Kistler, who was studying the properties of wet-gels. The term was introduced in order to describe gels in which the solvent was replaced by a gas without collapse of the solid network.

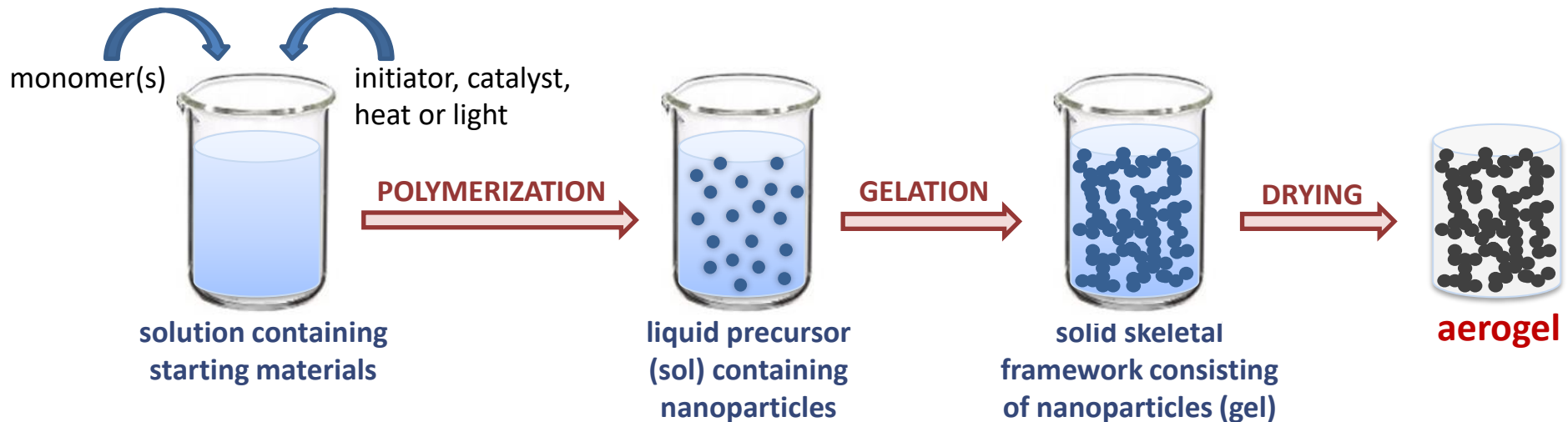
Aerogel vs Xerogel



Aerogels

Nanotechnology (in 3D)

They allow use of molecular science (chemistry, physics) to manipulate nanostructured matter (1-100 nm) in order to furnish useful macroscopic (engineering) properties that, in turn, allow application in thermal and acoustic insulation, dielectrics, as catalysts and catalyst supports, in drug delivery etc.



Aerogels

Aerogels can be classified as:

- Inorganic (oxides, metals, ceramics and carbons)
- Organic (polymers and biopolymers)
- Hybrid (organic/inorganic, metal-doped carbons and ceramics)

Aerogels

Aerogels can be prepared in in any desirable form factor:



powders



beads



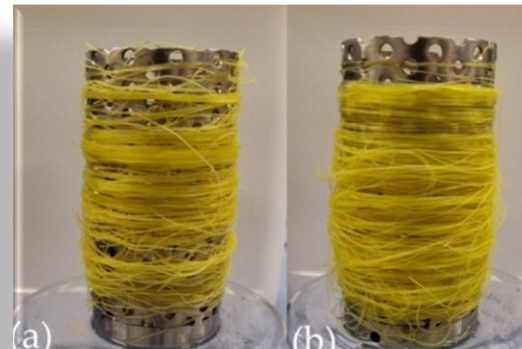
monoliths



films



blankets

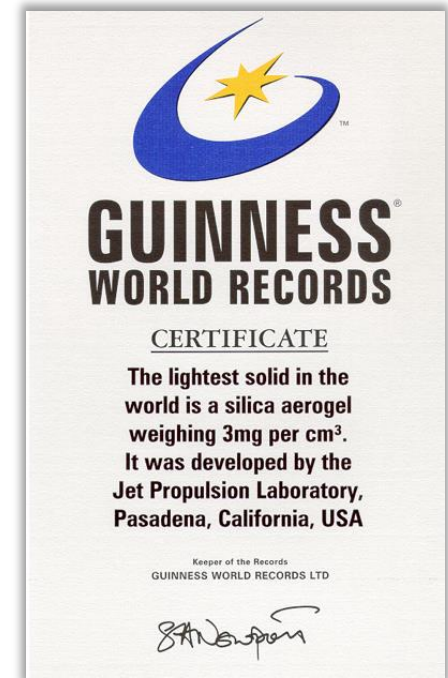


fibers

Aspen Aerogels Spaceloft®

Characteristic properties of aerogels

Extremely lightweight materials!



extremely low bulk densities

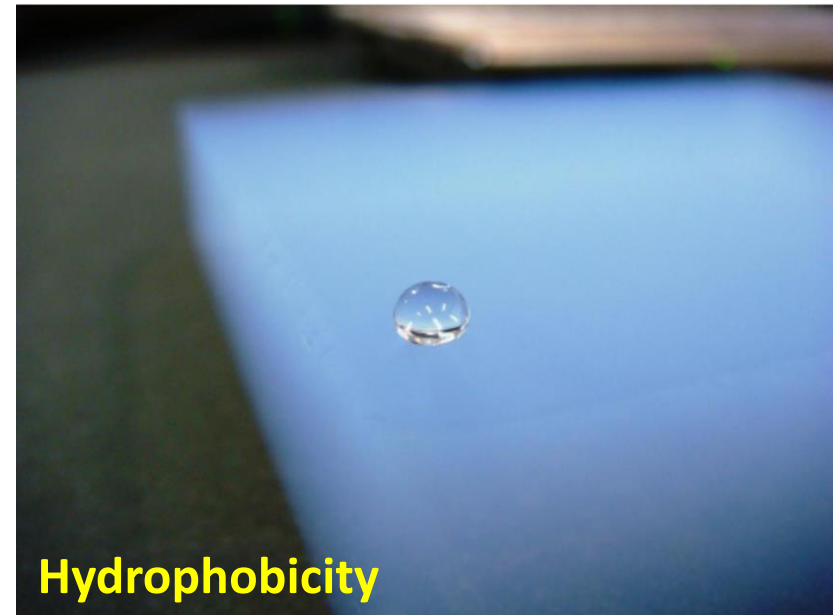


- high porosity
- high surface area
- slow sound propagation

low thermal conductivity



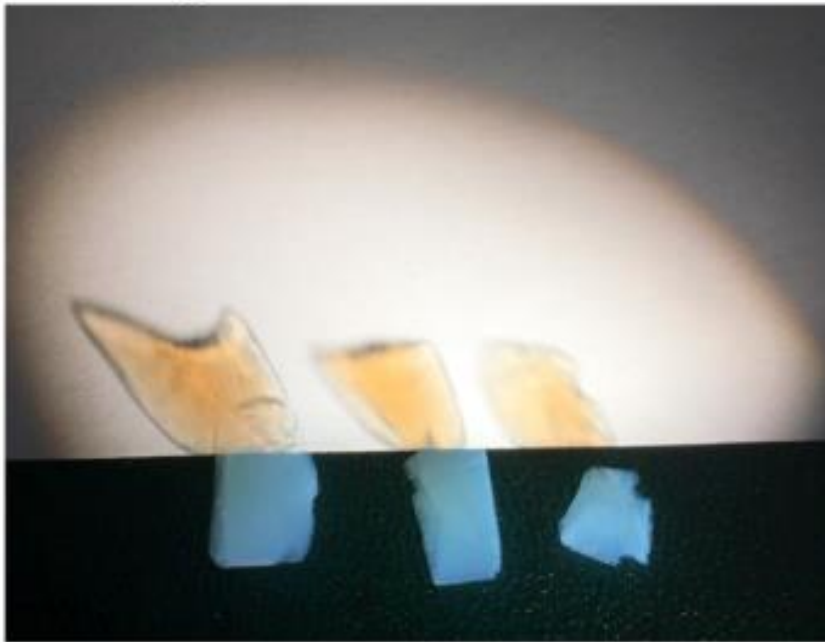
Other properties of aerogels



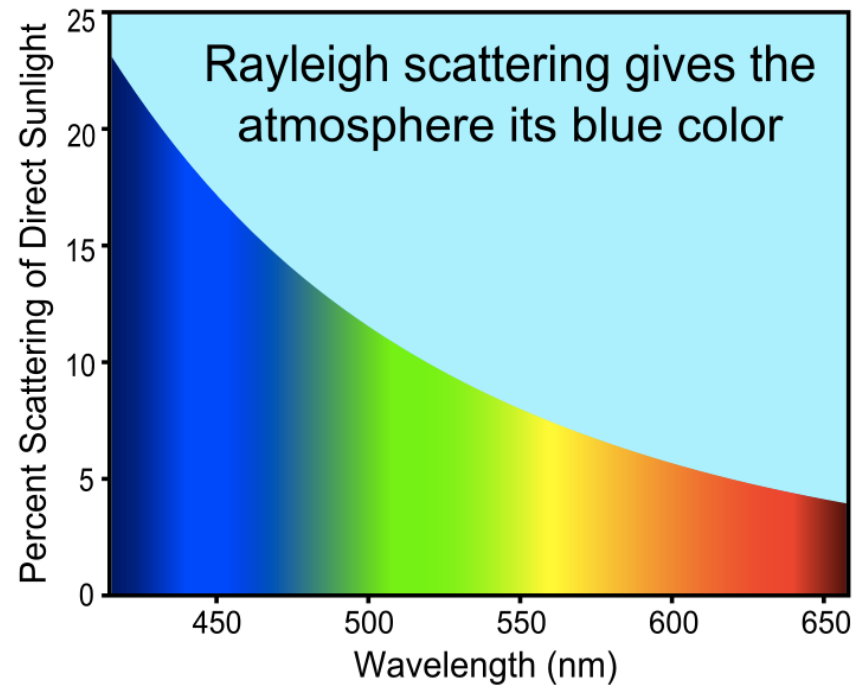
Other properties of aerogels

Why are some aerogels blue?

Rayleigh scattering through 3
 0.032 g cm^{-3} small monoliths



Rayleigh scattering is the elastic scattering of light by particles much smaller than the wavelength of light



Tiny particles or bubbles that scatter light.

In Rayleigh scattering an object looks blue in reflection and orange-red in transmission, because shorter wavelength (blue) light is scattered more.

Other properties of aerogels

Superelasticity / Shape memory effect

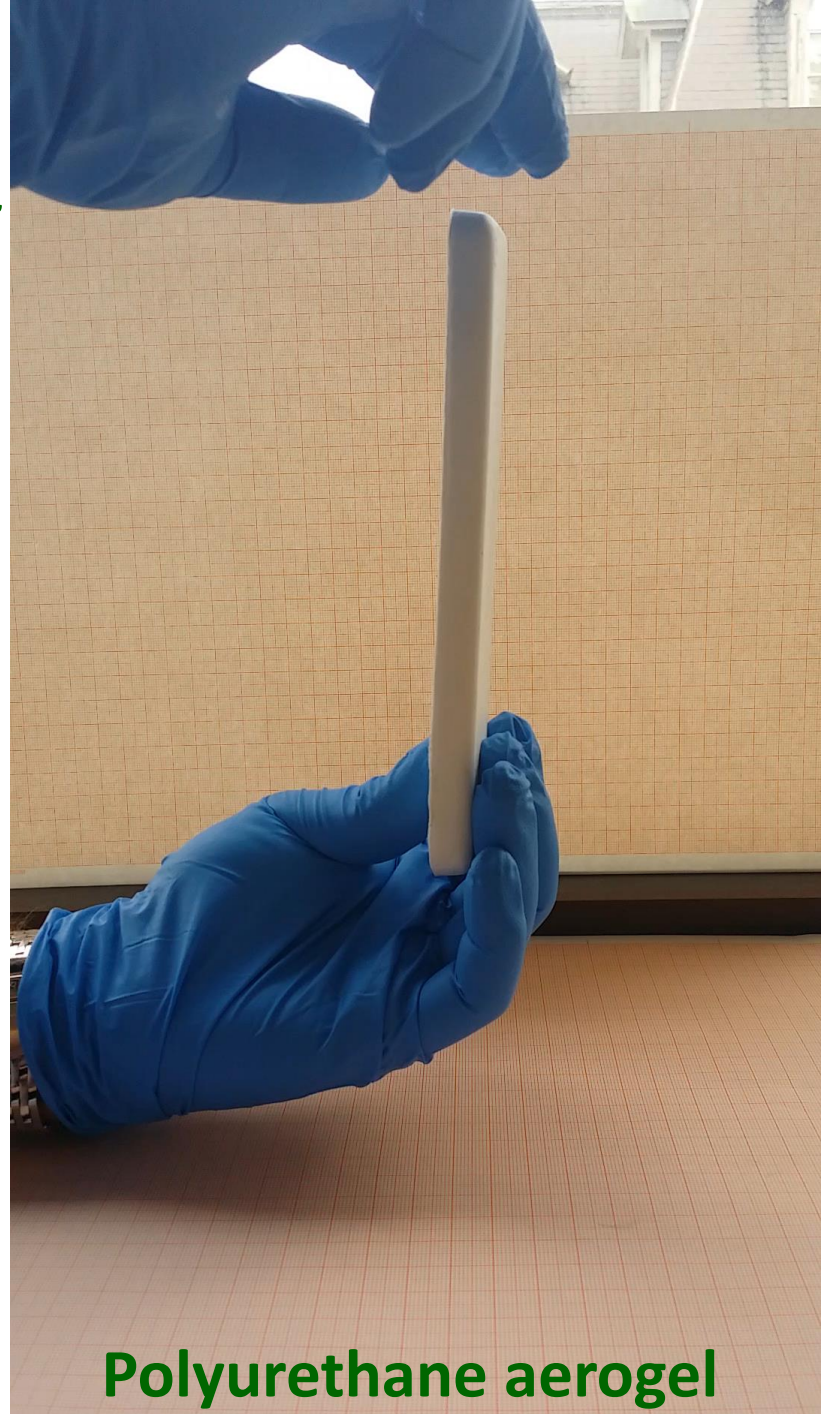
Shape Memory Effect (SME)

The property of a material to “remember” and return to a permanent shape when triggered with an appropriate stimulus (e.g., a change in temperature).

A necessary condition for the SME is:

Superelasticity

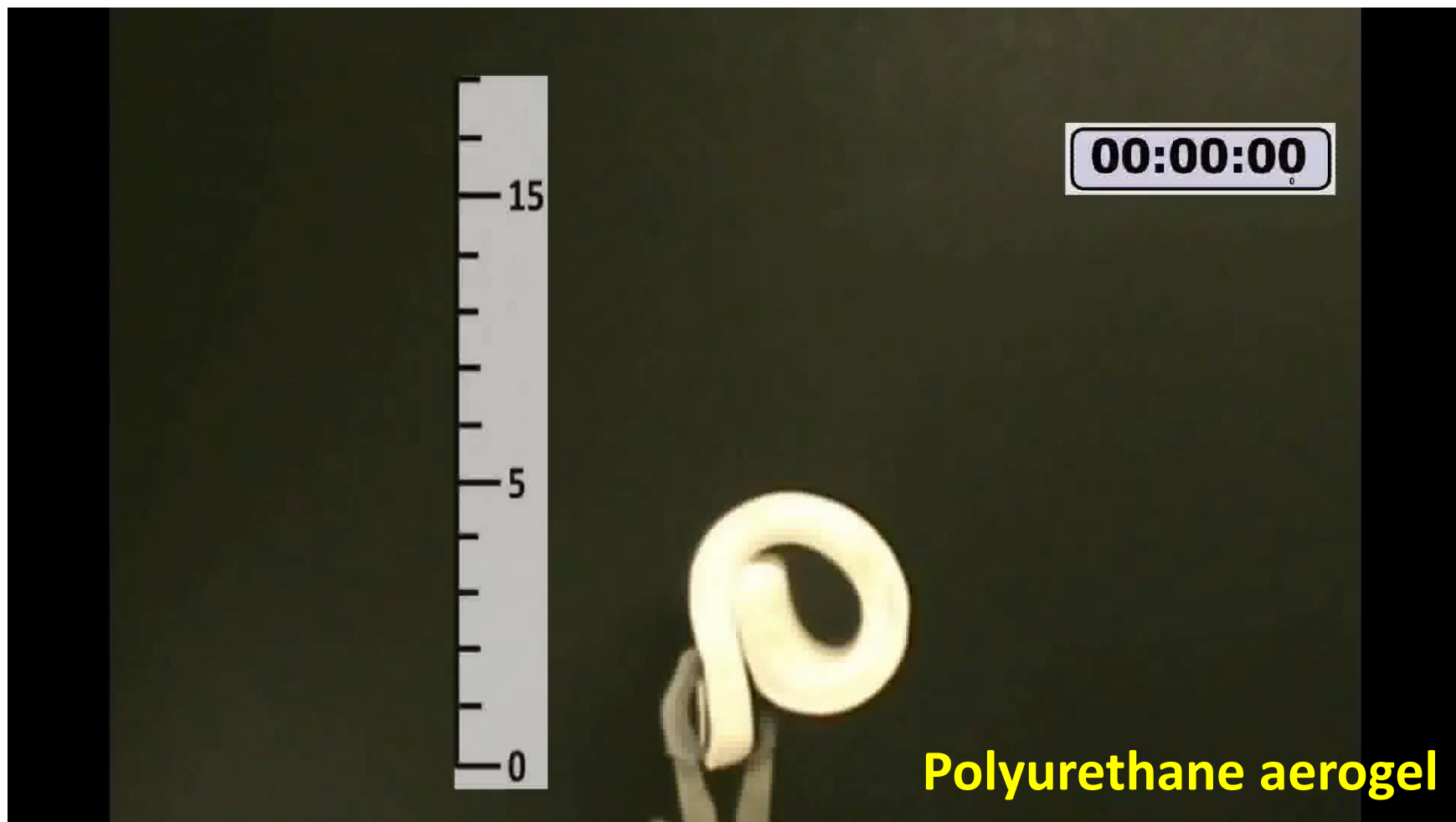
The property of a material to recover its shape after an extreme deformation.



Polyurethane aerogel

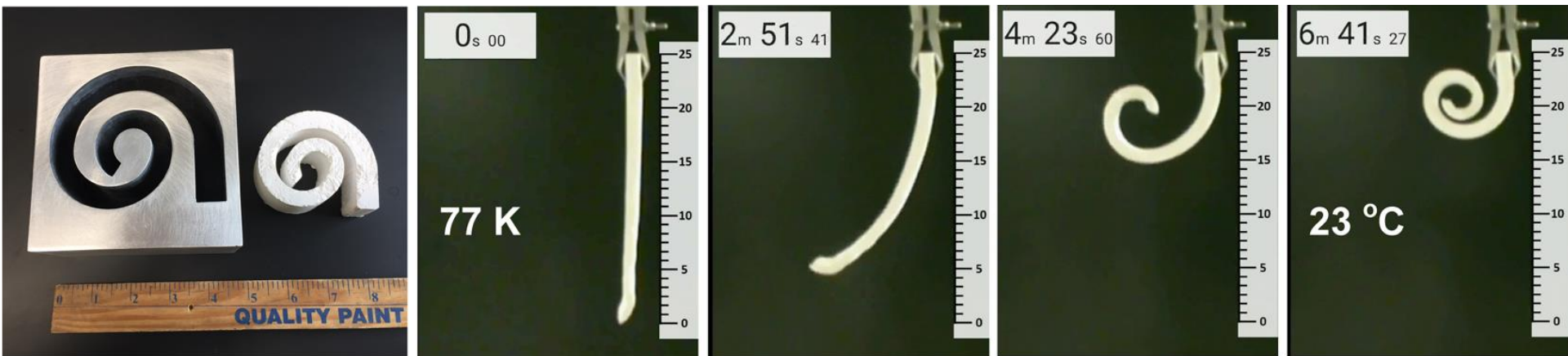
Other properties of aerogels

Superelasticity / Shape memory effect



Other properties of aerogels

Superelasticity / Shape memory effect



Polyurethane aerogel

a deployable panel that was folded,
cooled and then left to thaw

Other properties of aerogels

Superelasticity / Shape memory effect

mimicking the
complicated
muscle
coordination of a
human hand
grabbing a pen

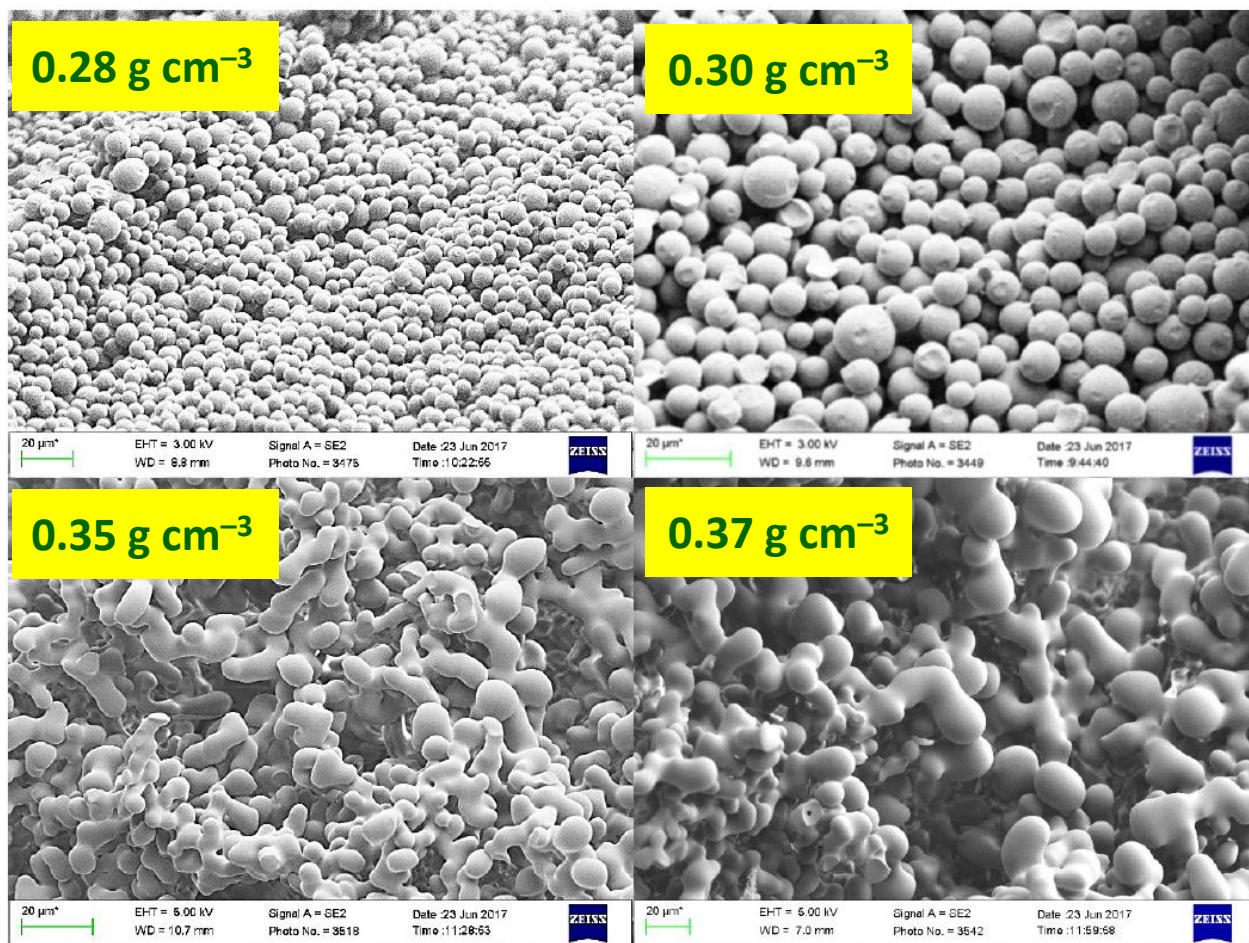


Aerogel properties

Aerogel properties depend on:

(a) the chemical composition

(b) the nanostructure



Aerogel properties

Aerogel properties depend on:

- (a) the chemical composition
- (b) the nanostructure

Factors affecting the nanostructure:

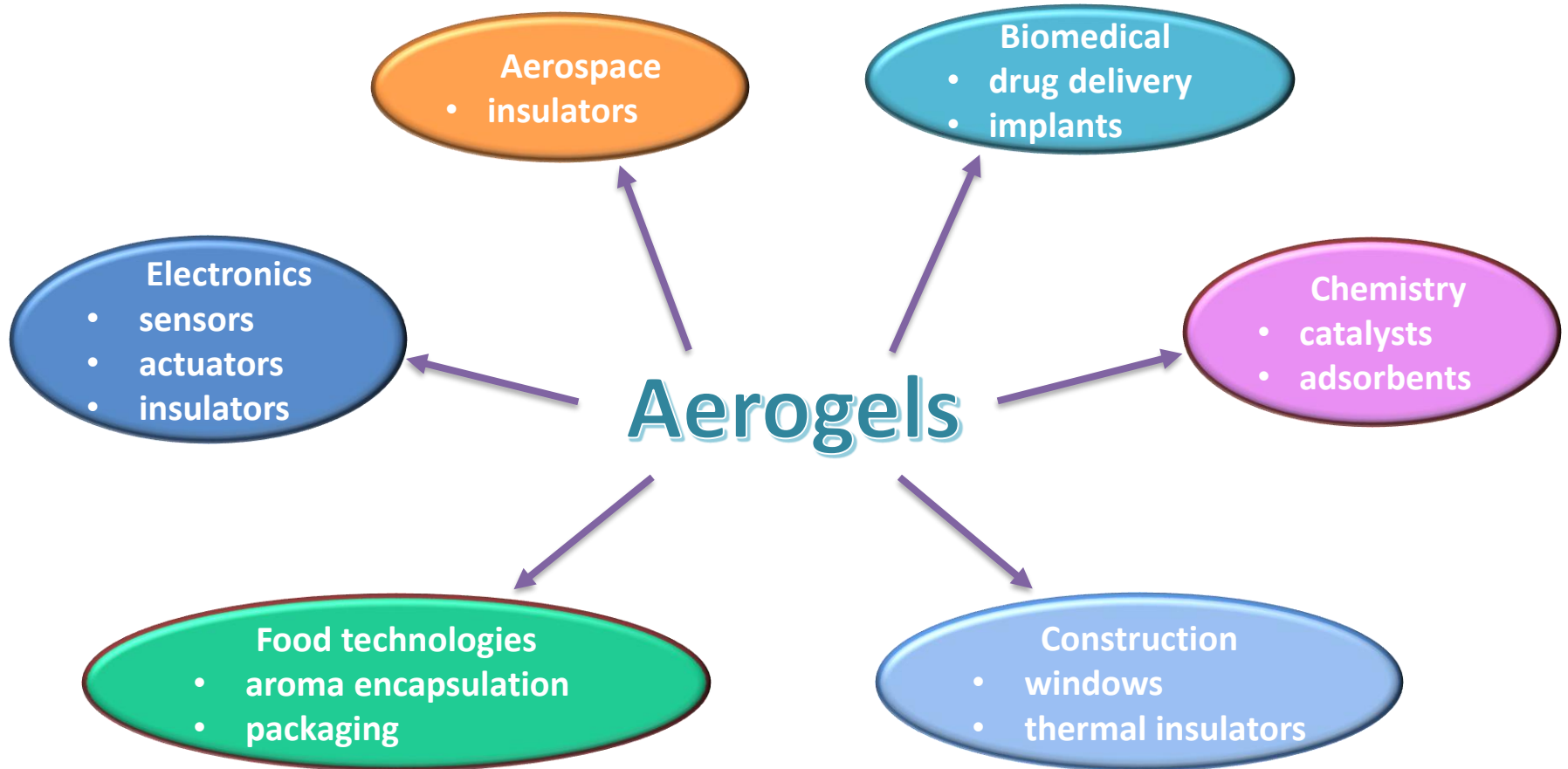
- (a) gelation kinetics
- (b) solubility of the polymer (high solubility delays phase separation and leads to large particles or dense materials)

We can we control these factors by:

- (a) changing the monomers
- (b) changing the catalyst
- (c) changing the solvent
- (d) changing the temperature
- (e) varying the concentration of the monomers and/or the catalyst

Design of experiments

Applications of aerogels





AERoGELS

COST ACTION CA18125

environment | medicine | biotech | industry | academia

Advanced Engineering and Research of aeroGels for Environment and Life Sciences

- <https://cost-aerogels.eu/>
- <https://www.cost.eu/actions/CA18125/>





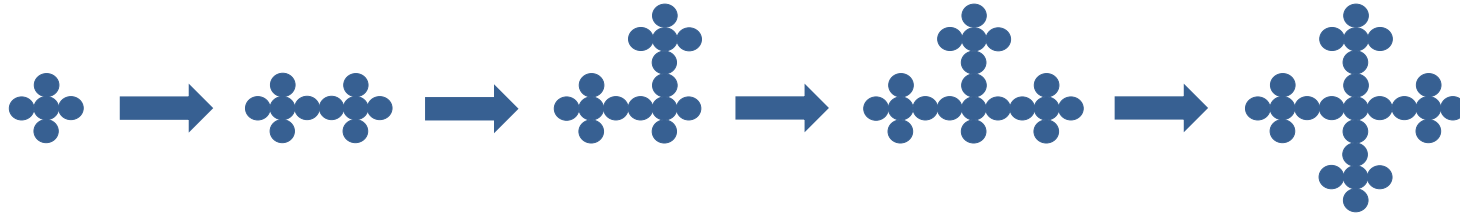
2nd International Conference on Aerogels for Biomedical and Environmental Applications

29 June – 1 July 2022

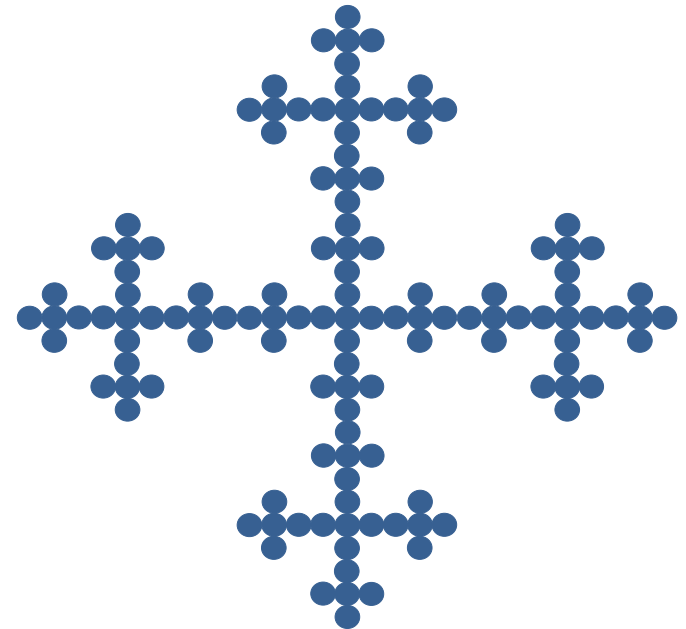
Athens, Greece



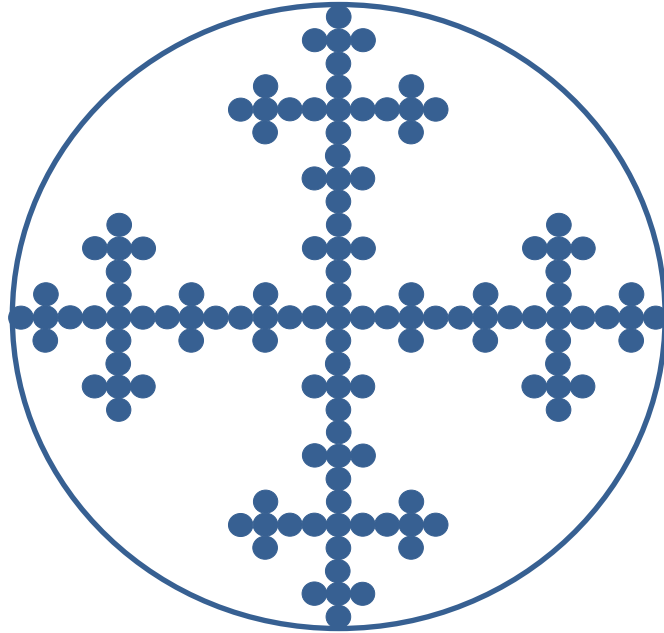
Formation of aerogels



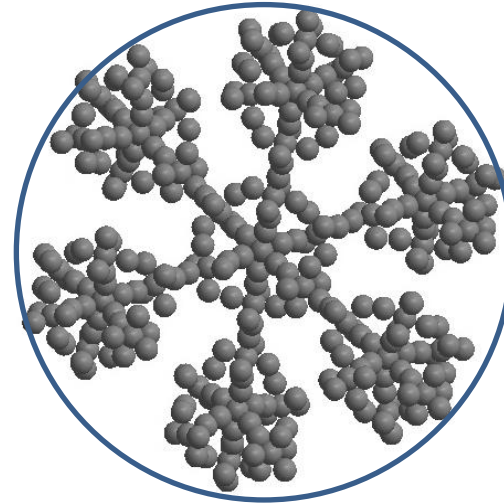
Self-repeating patterns ...
... fractals



Formation of aerogels



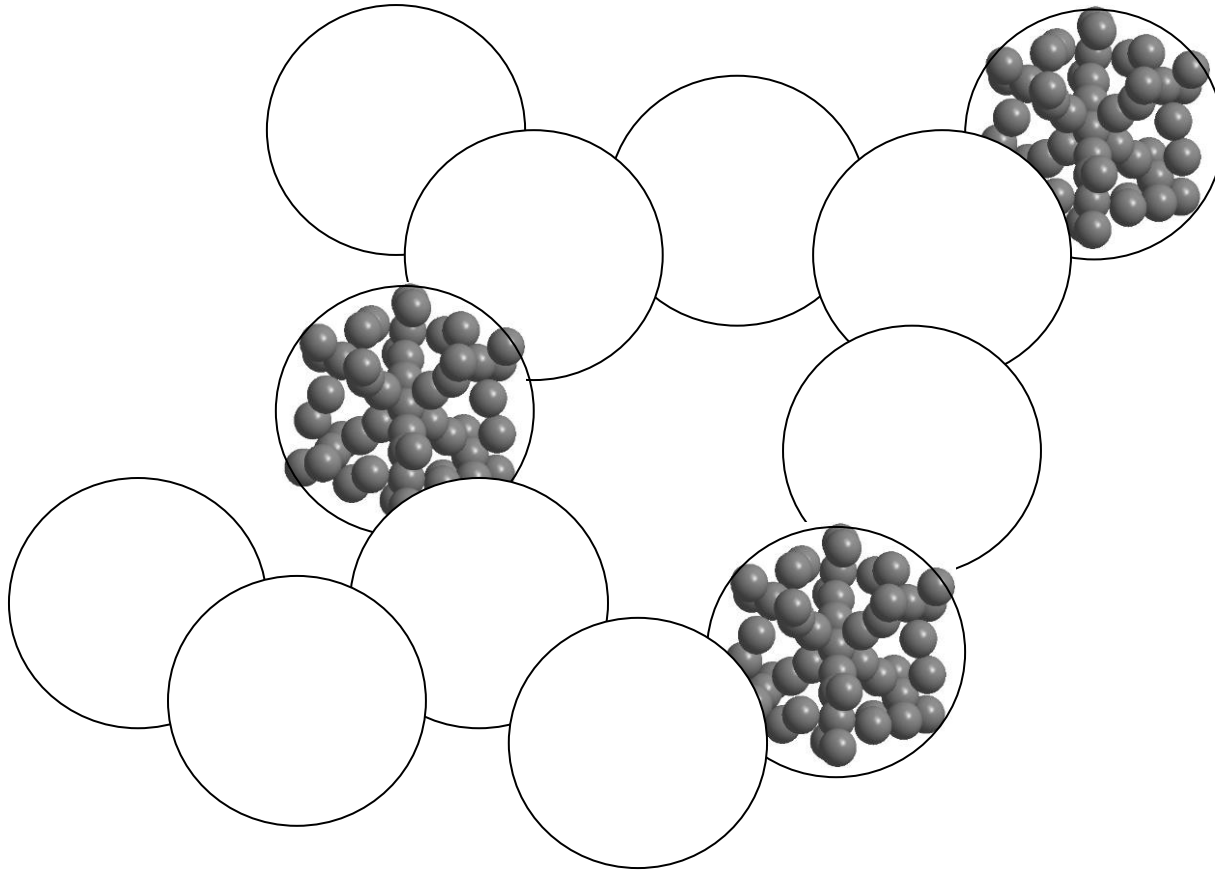
This is a particle with
primary particles (●) inside...
... in 2D



This is a particle with
primary particles (●) inside...
... in 3D

particles with an internal structure

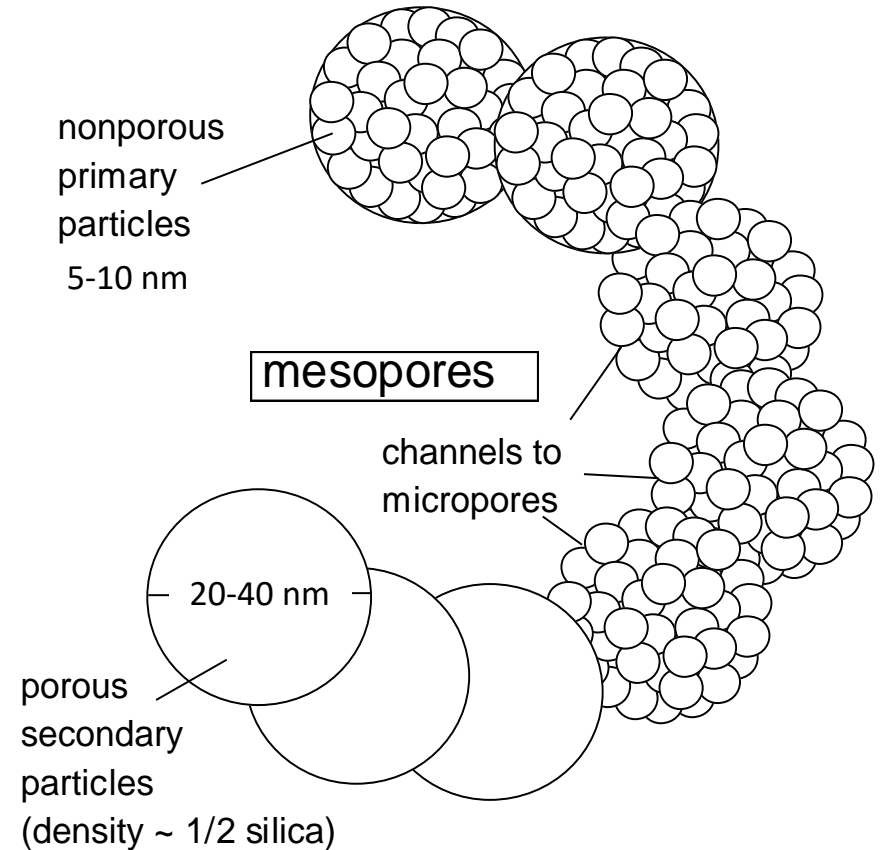
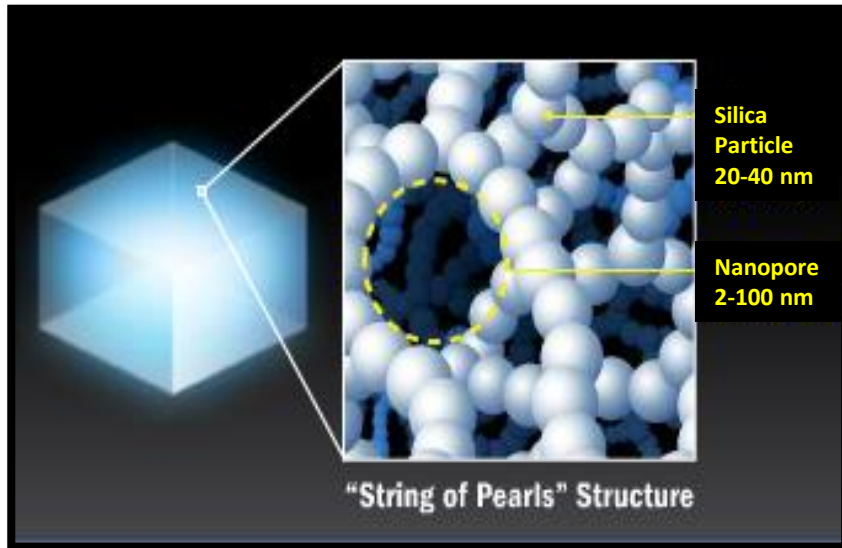
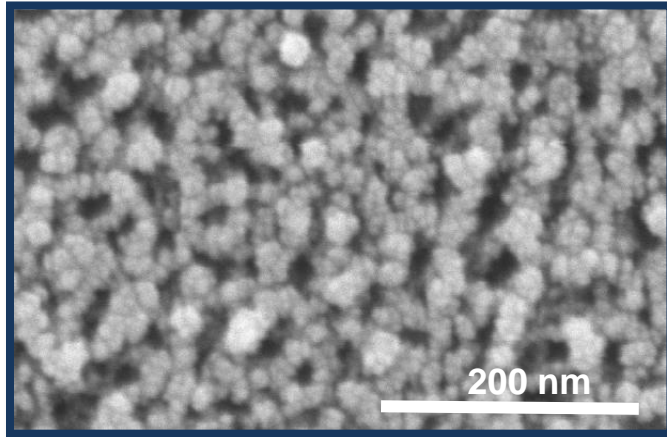
Formation of aerogels



secondary particles form porous networks

Aerogels

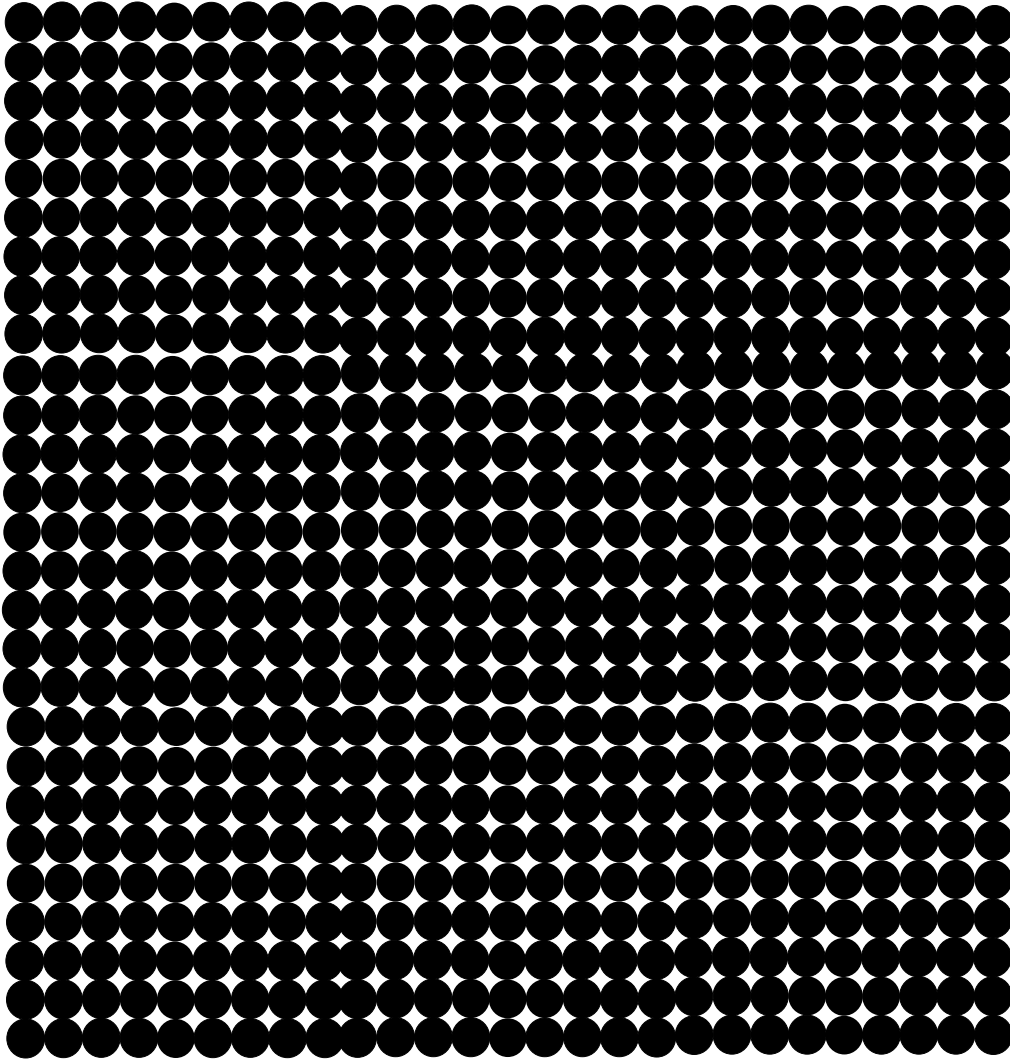
a typical silica aerogel microscopically



<http://science.howstuffworks.com/aerogel1.htm>

Aerogels – mass vs size

Let's consider a box full of black balls...



Obviously, there is lots of empty space.....

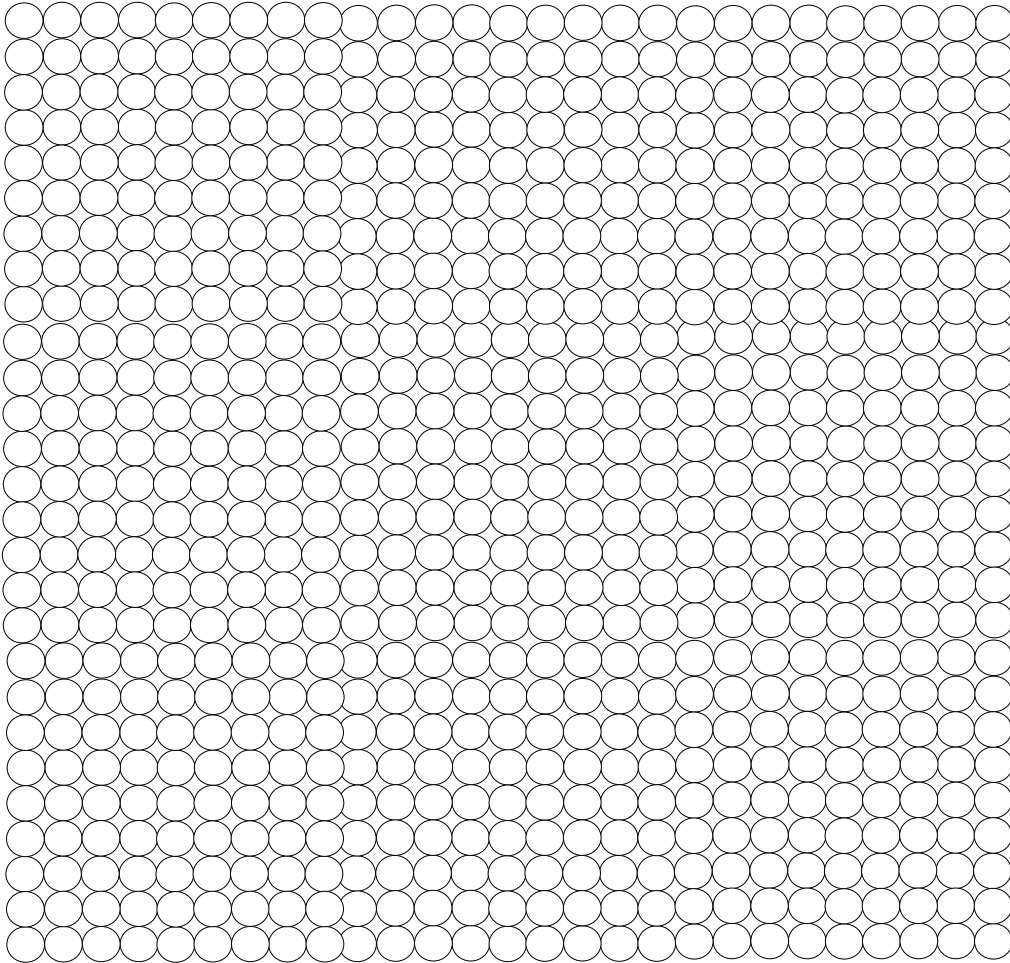
How much?

Well, this packing is called **cubic** and....

Empty space ~ 25% v/v

Aerogels – mass vs size

Now, let's fill the box with white balls....

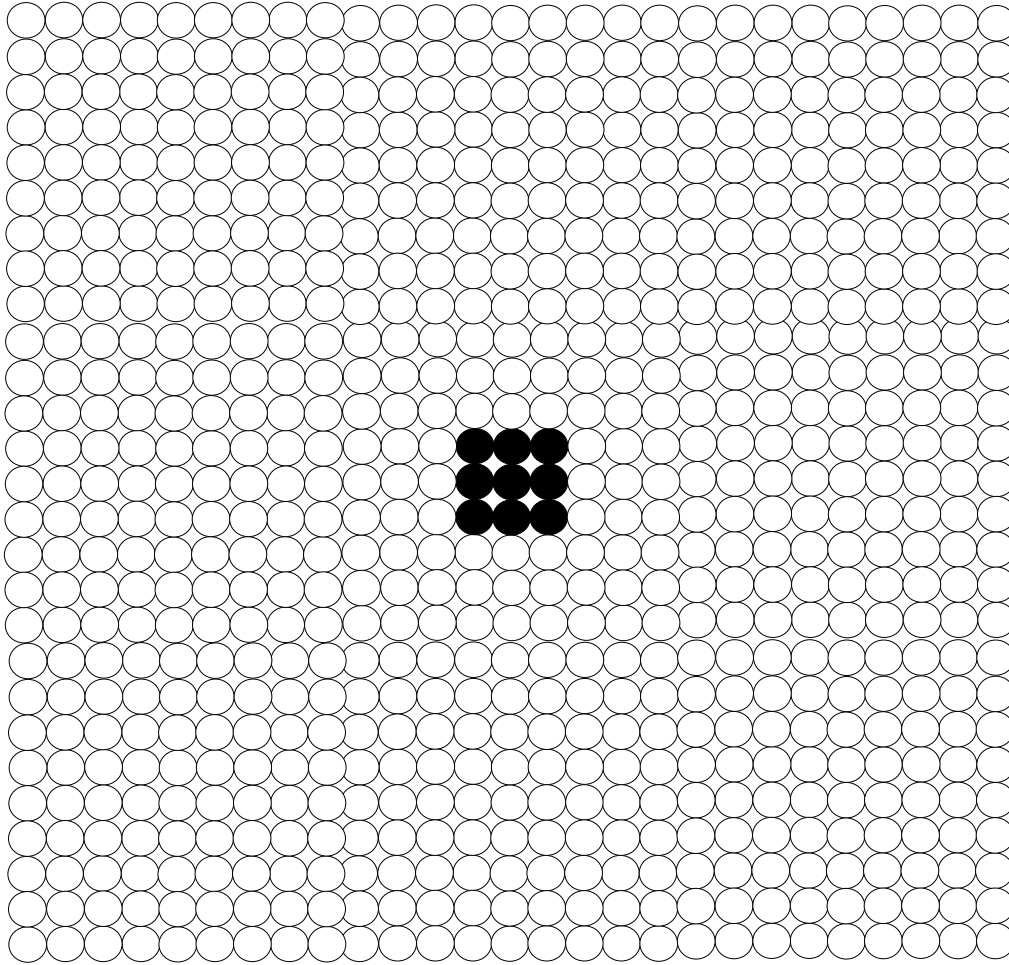


Obviously the empty space between the balls does not change.....

Empty space ~ 25% v/v

Aerogels – mass vs size

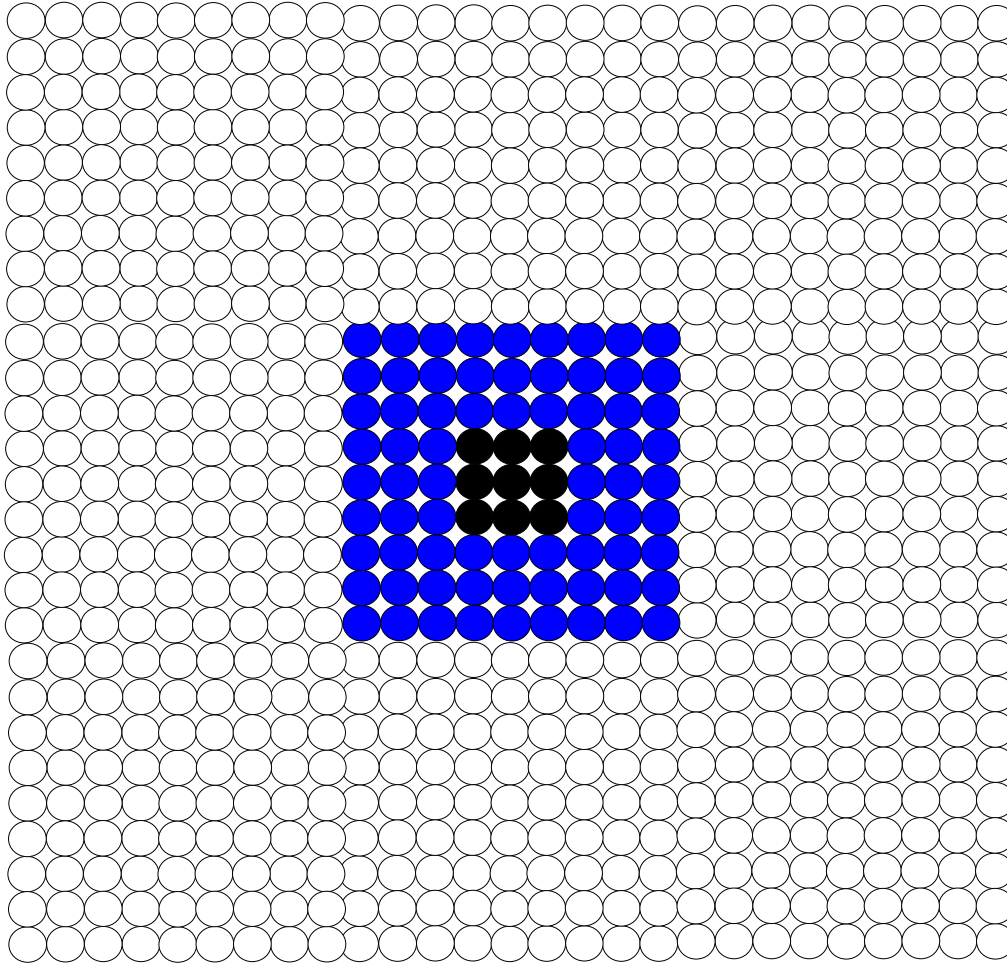
Now, let's select some balls and paint them again black....



That's nine balls....

Aerogels – mass vs size

Next, let's triple the size of our selection...



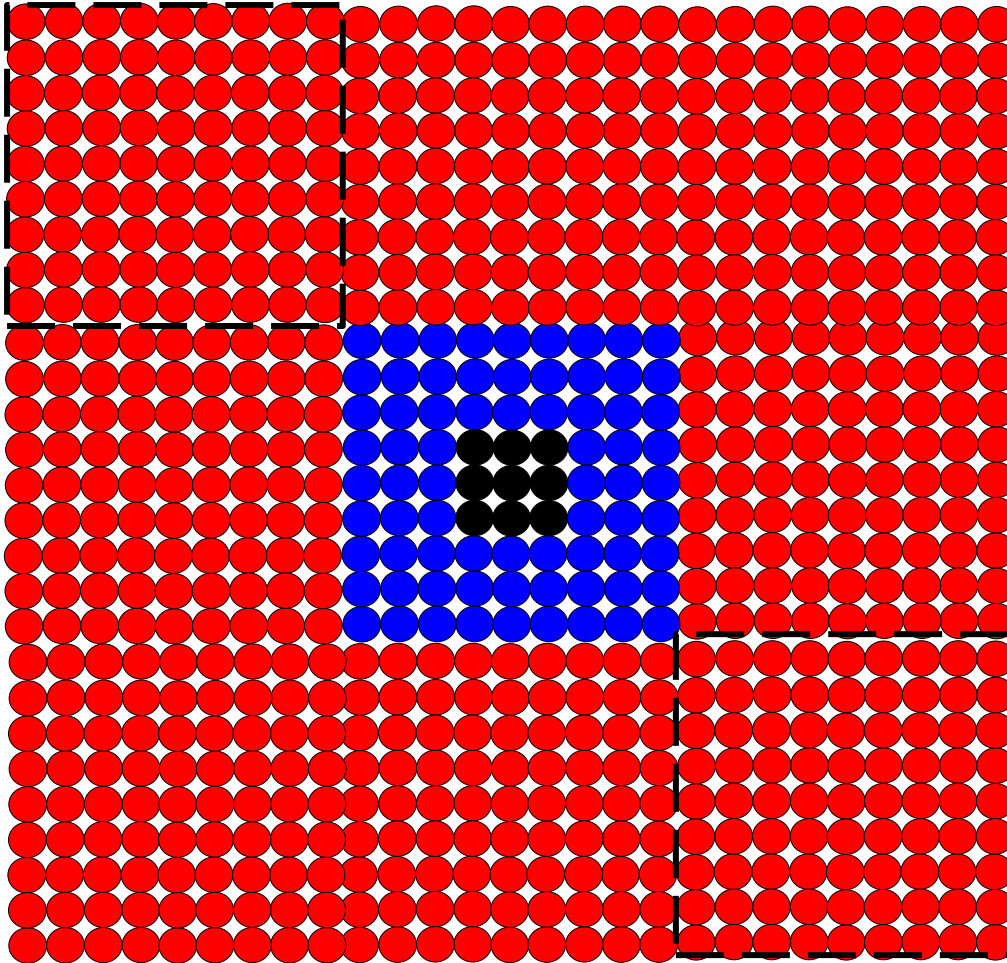
Size has gone up 3x

Mass has gone up 9x

$\text{Log(Mass)/Log(Size)} = 2$

Aerogels – mass vs size

Now, let's triple the size again....



Size has gone up 9x

Mass has gone up 81x

$$\text{Log(Mass)/Log(Size)} = 2$$

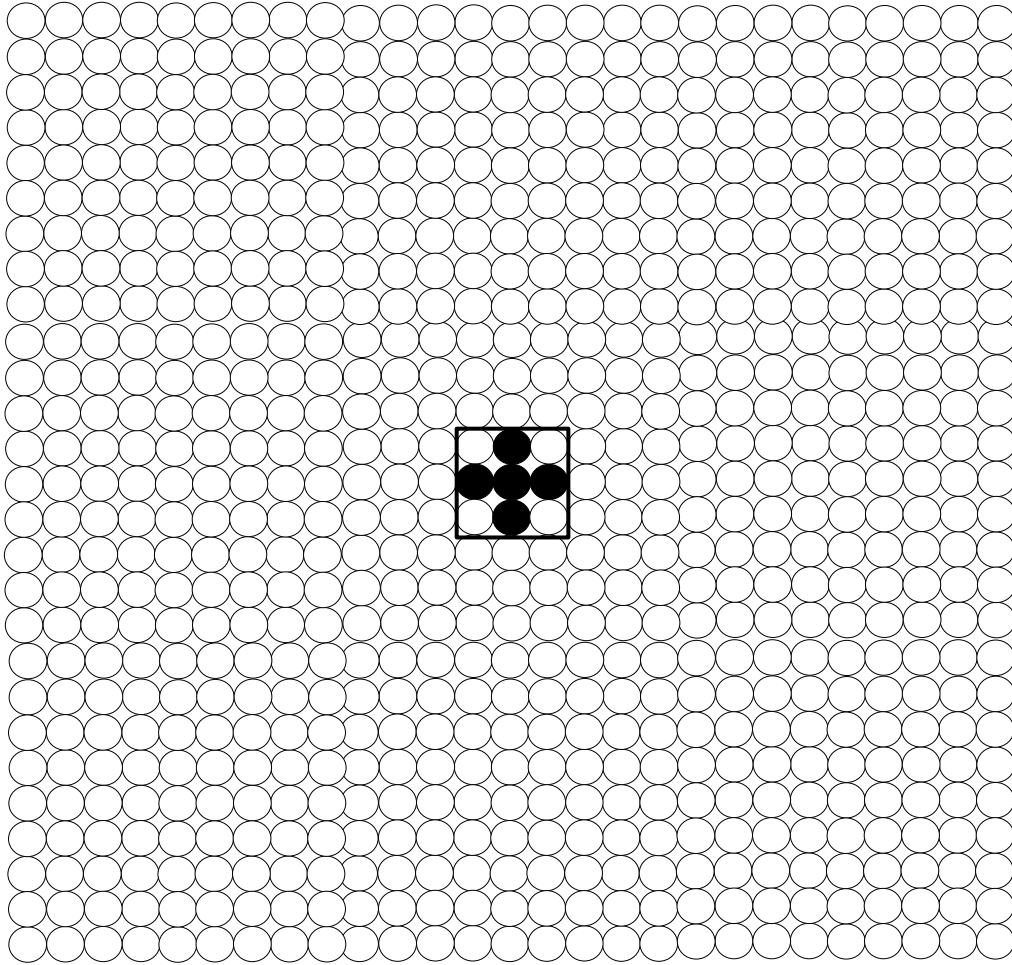
Note, if we had done this in 3-dimensions (3D),

$$\text{Log(Mass)/Log(Size)} = 3$$

Conversely, if: $\text{Mass} \sim \text{Size}^2$ in 2D or $\text{Mass} \sim \text{Size}^3$ in 3D,
then the object is densely packed

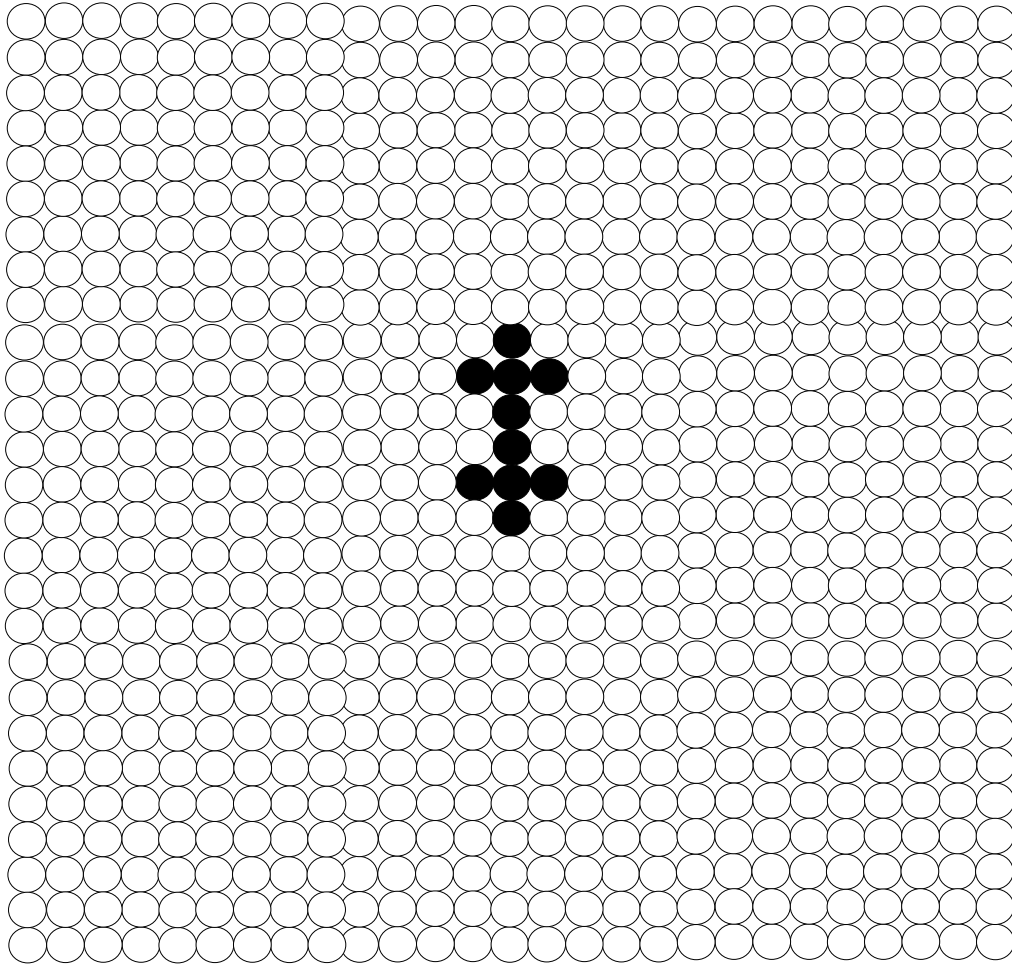
Aerogels – mass vs size

Now, let's change the pattern of our selection....



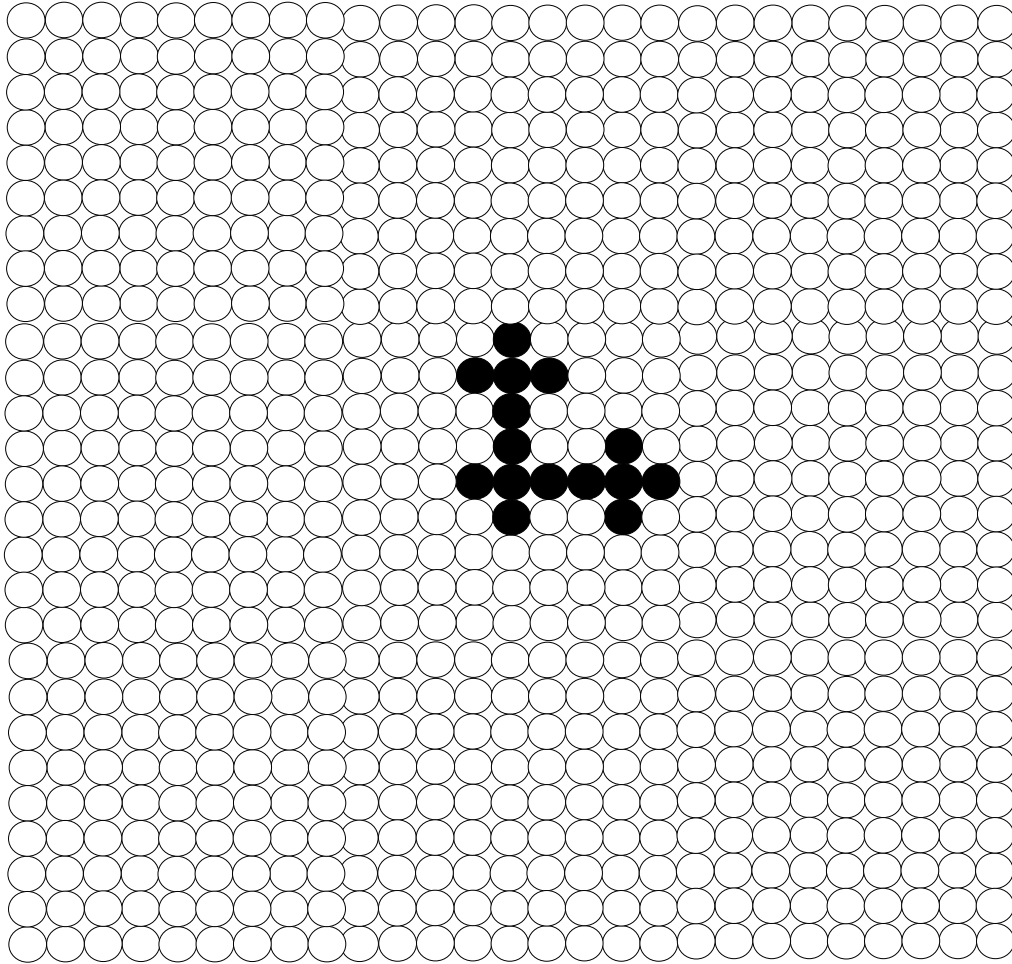
Aerogels – mass vs size

And, let's repeat it once....



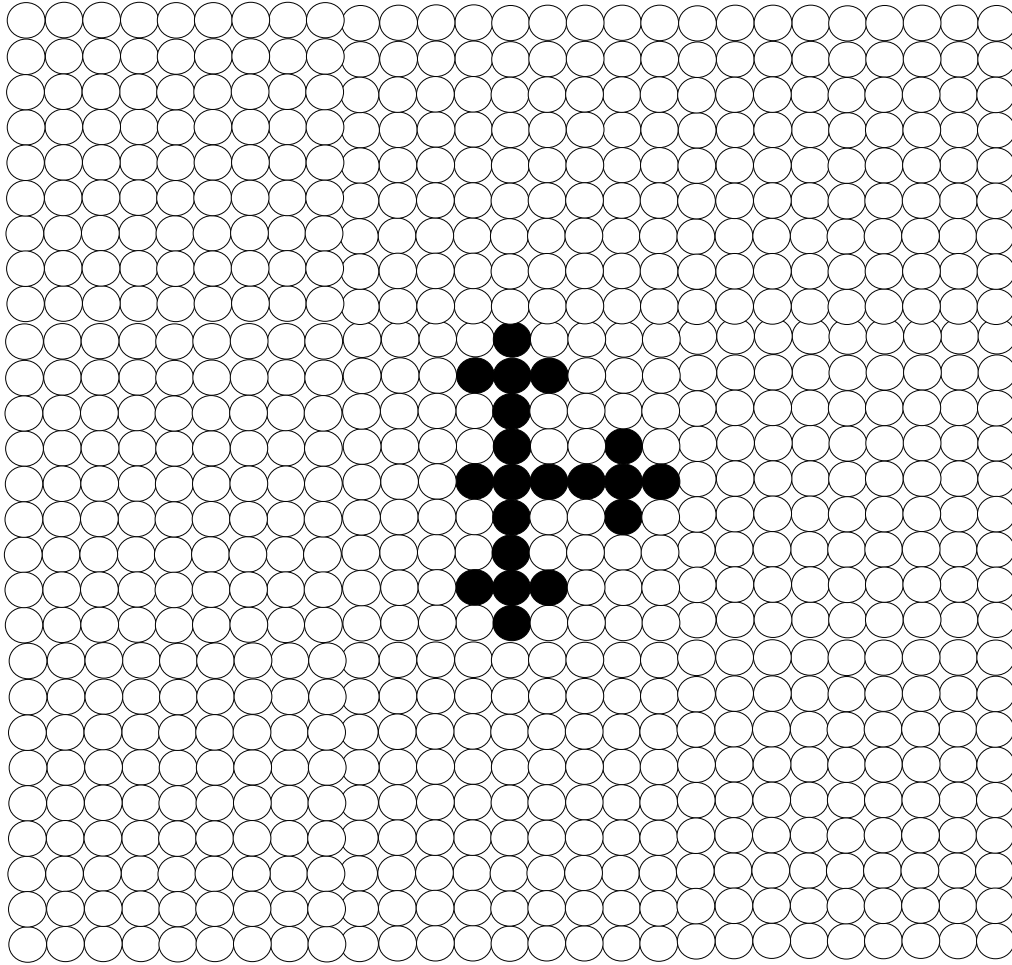
Aerogels – mass vs size

Twice....



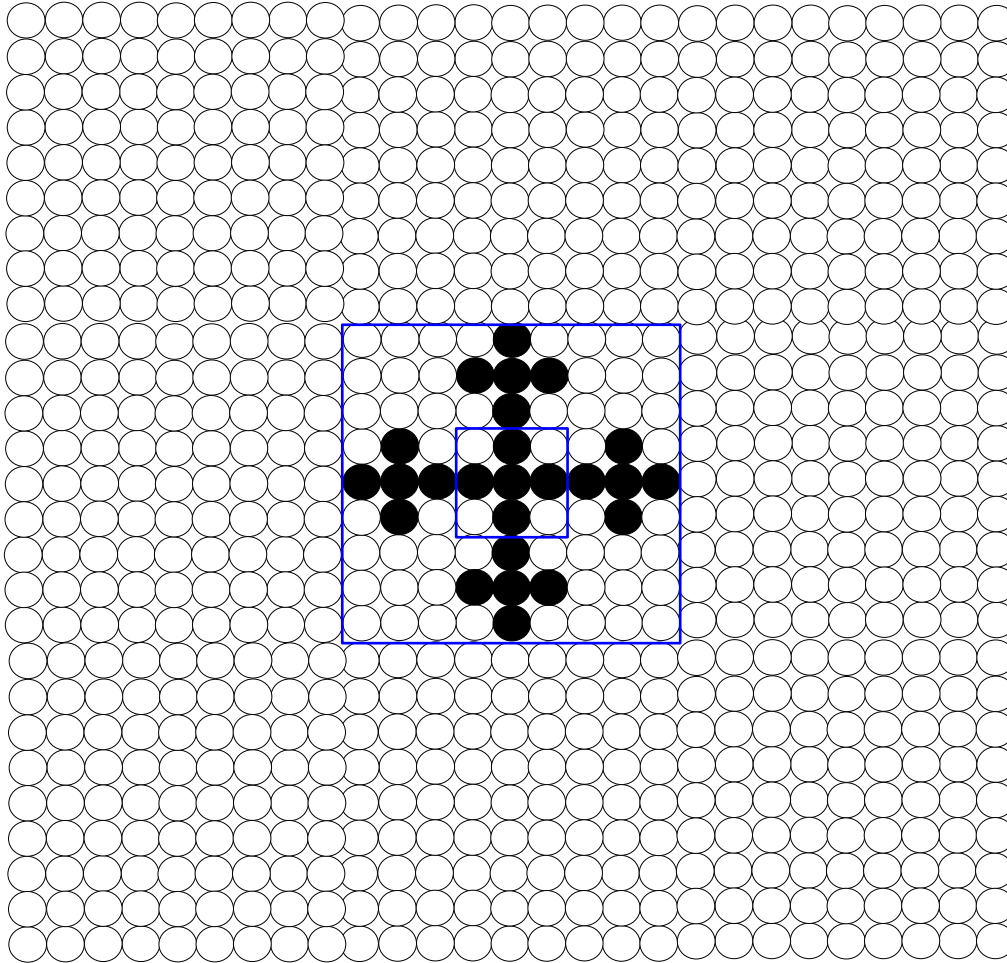
Aerogels – mass vs size

Three times....



Aerogels – mass vs size

And once more....



Size has gone up again 3x...

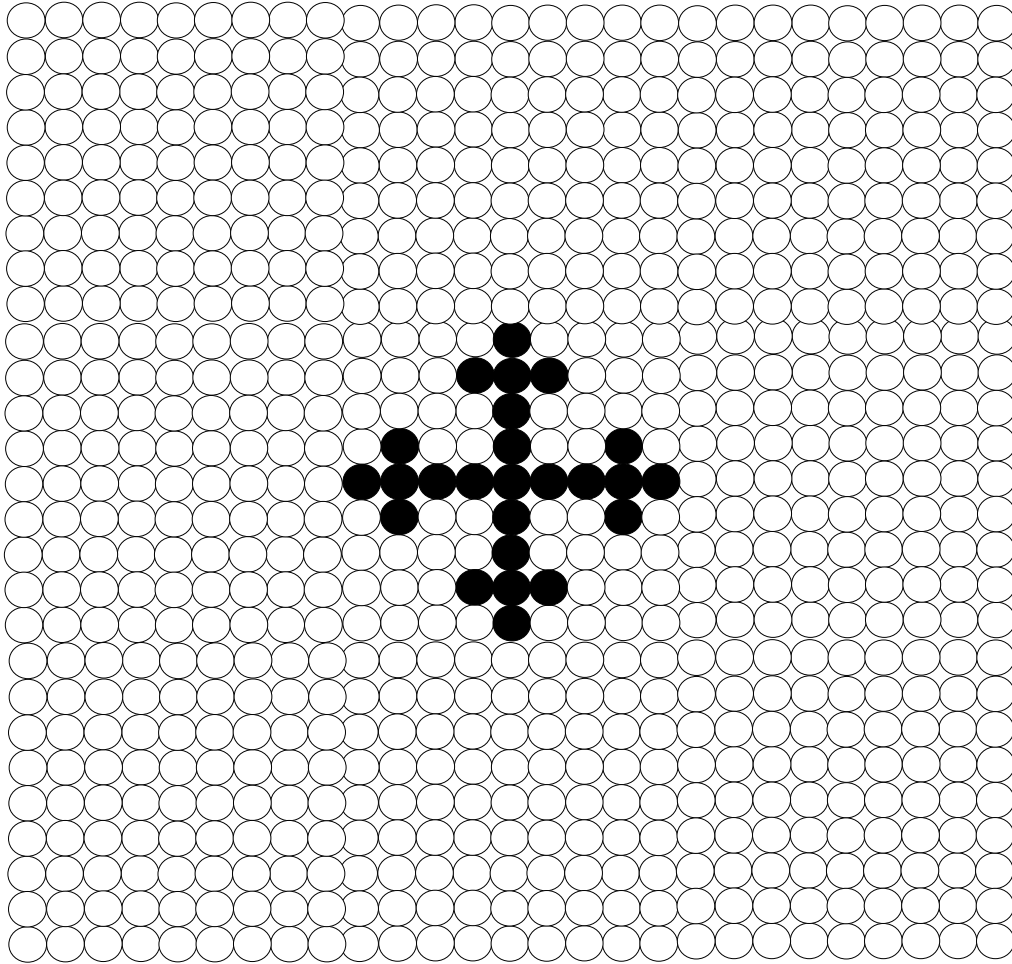
...but has lots of empty space

Mass has gone up only 5x

$\text{Log}(\text{mass})/\text{Log}(\text{size}) = 1.465$

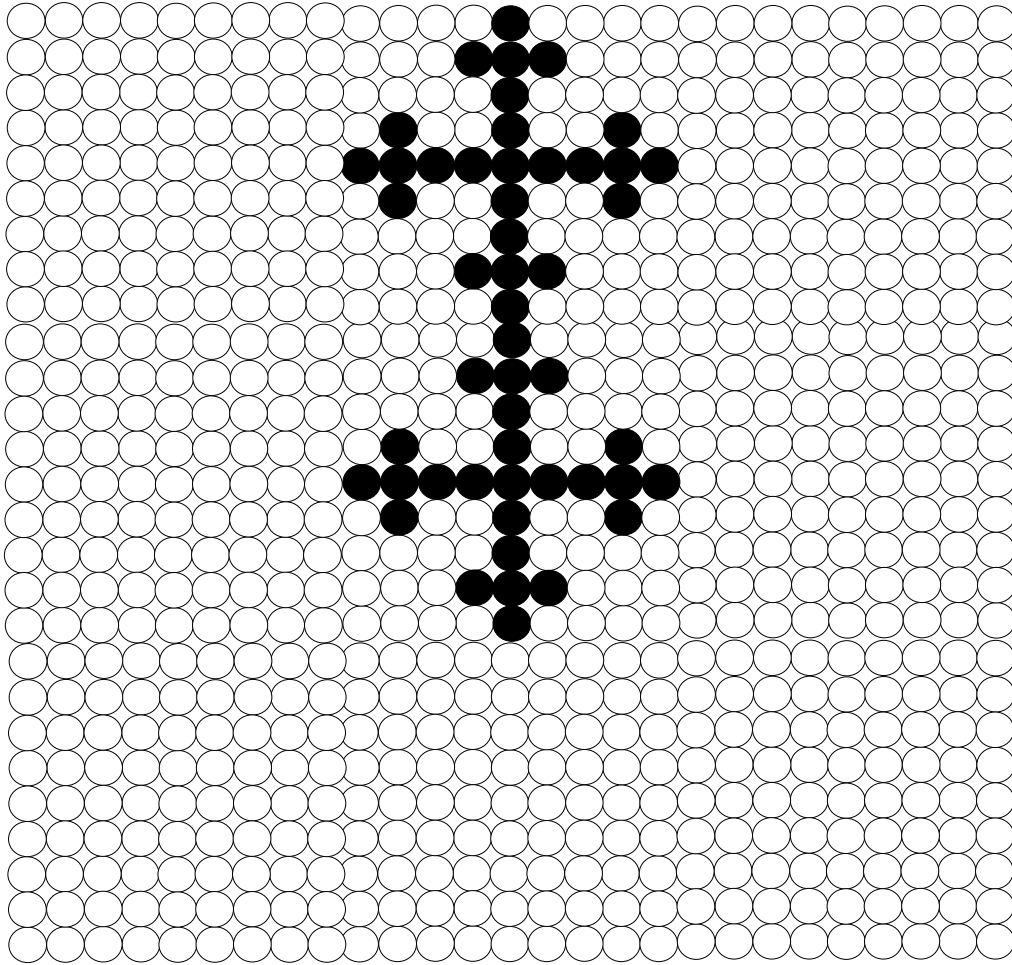
Aerogels – mass vs size

Let's repeat this pattern...



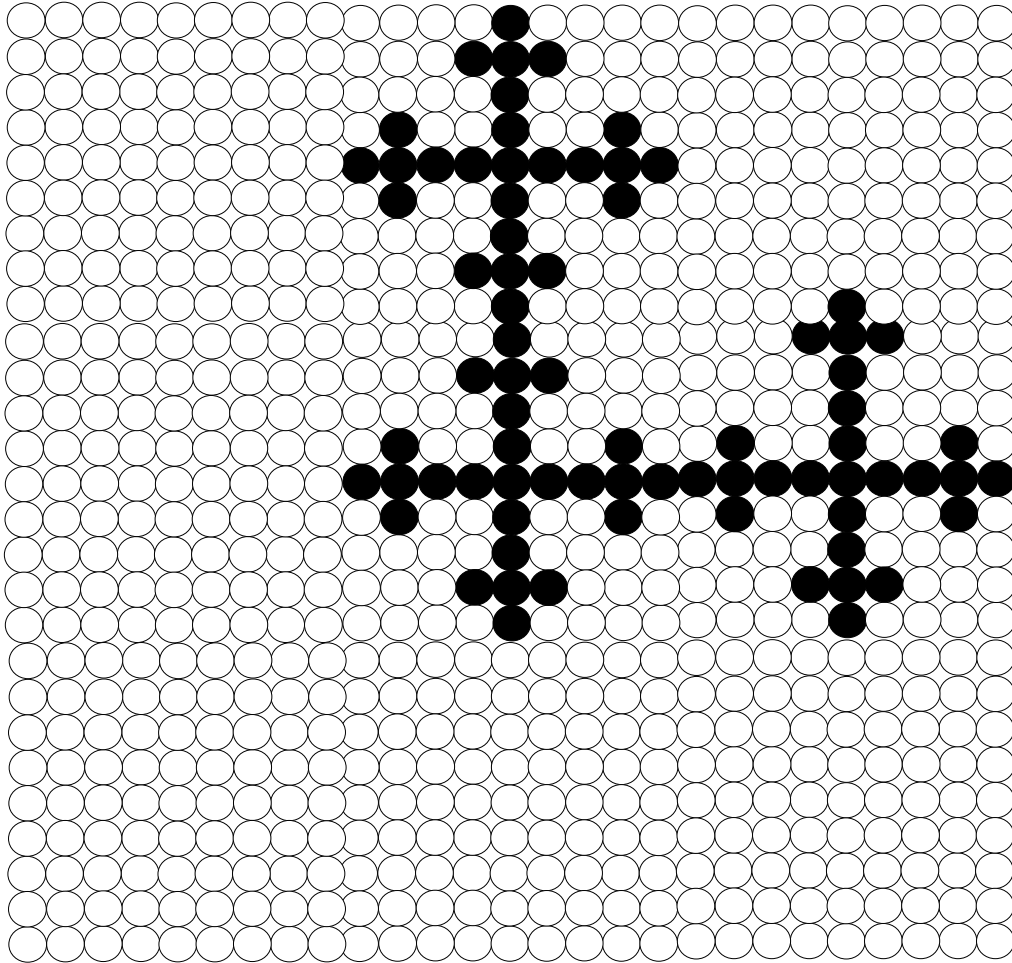
Aerogels – mass vs size

Once...



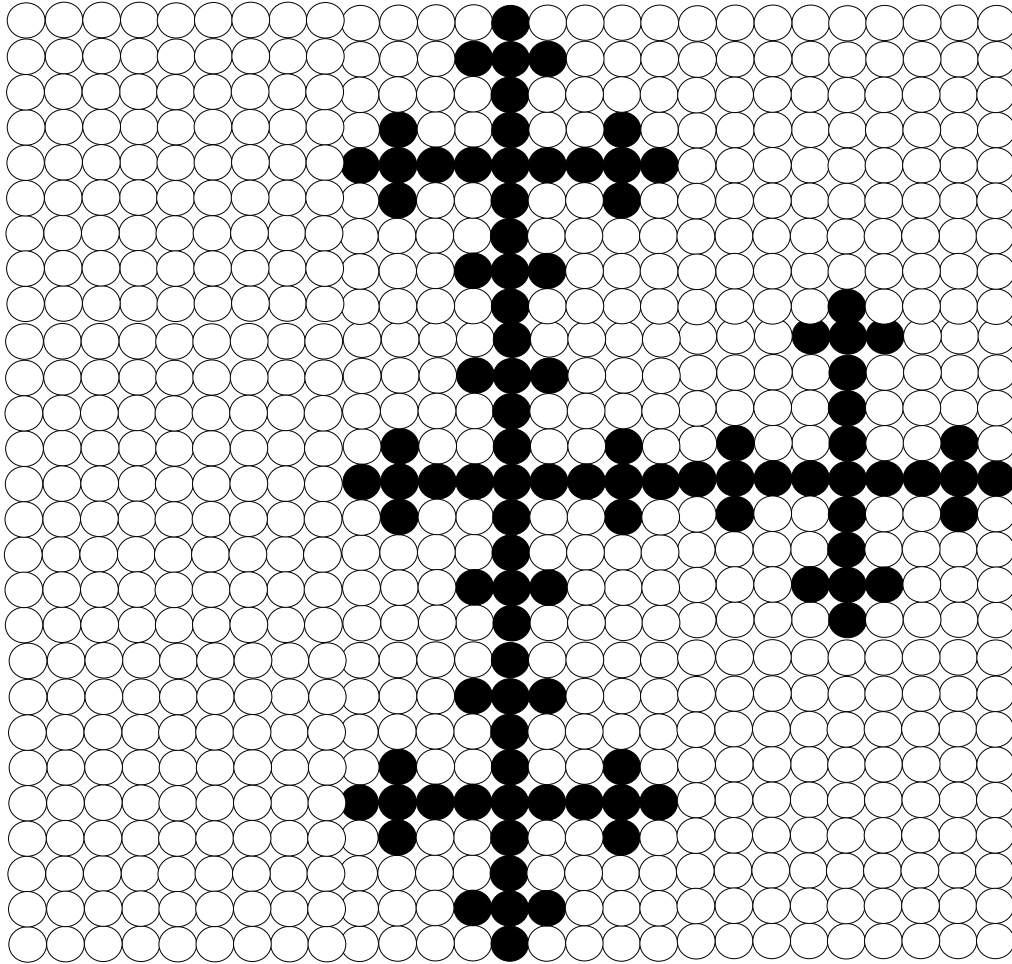
Aerogels – mass vs size

Twice...



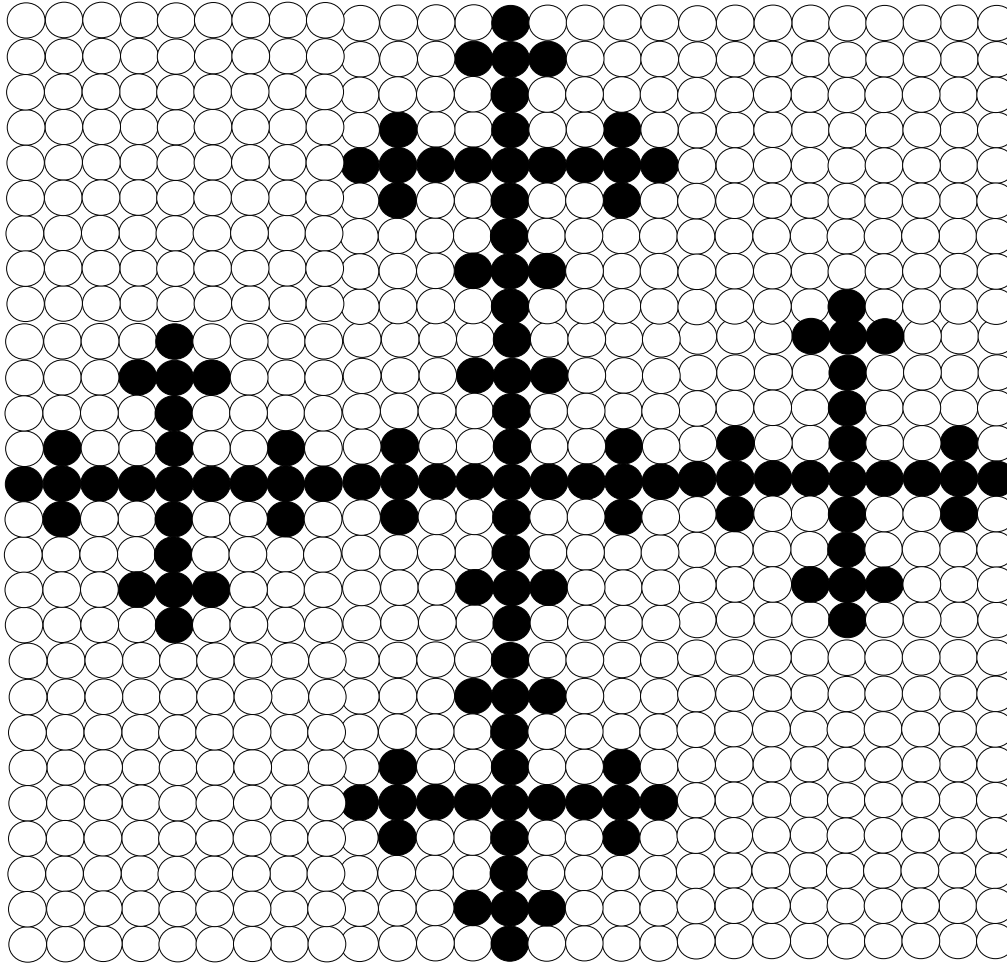
Aerogels – mass vs size

Three times...



Aerogels – mass vs size

Four times...



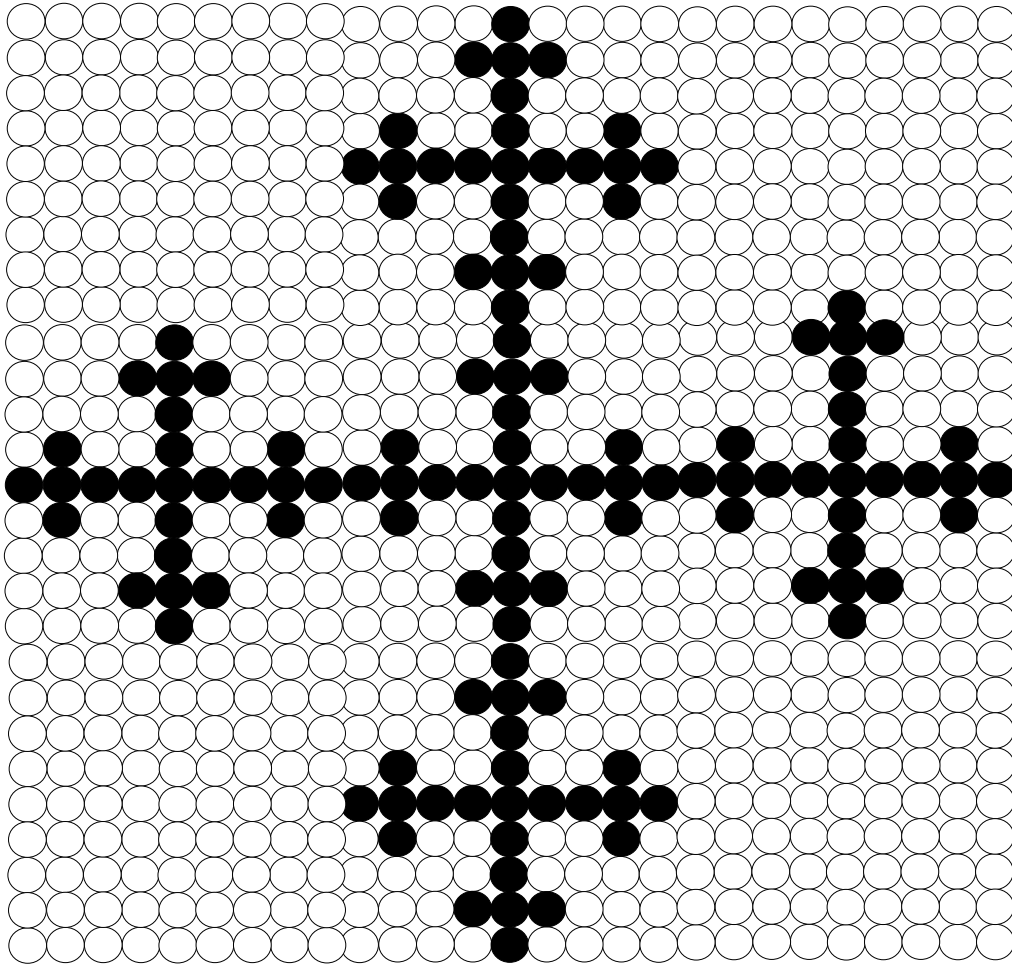
Size has gone up 9x...

Mass has gone up 25x

$$\text{Log}(\text{mass})/\text{Log}(\text{size}) = 1.465$$

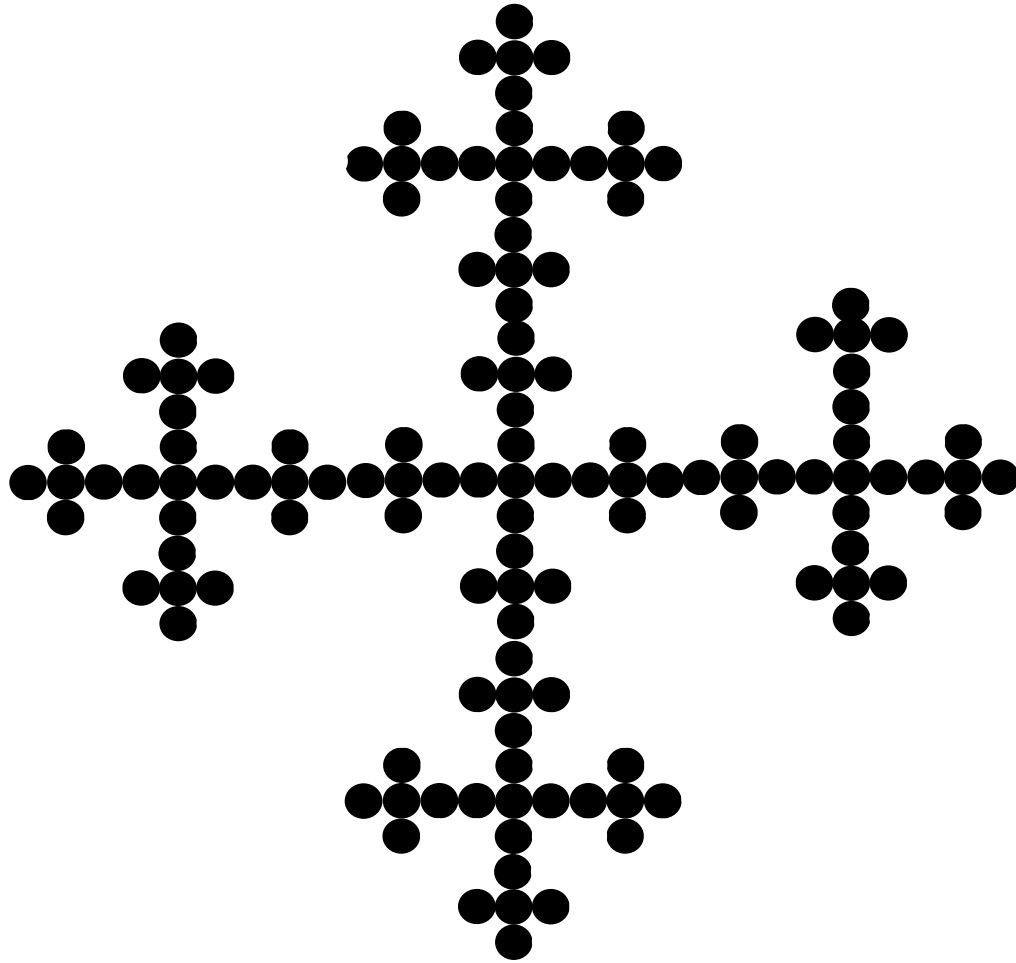
Aerogels – mass vs size

Now, let's remove the white balls...



Aerogels – mass vs size

What remains is ...

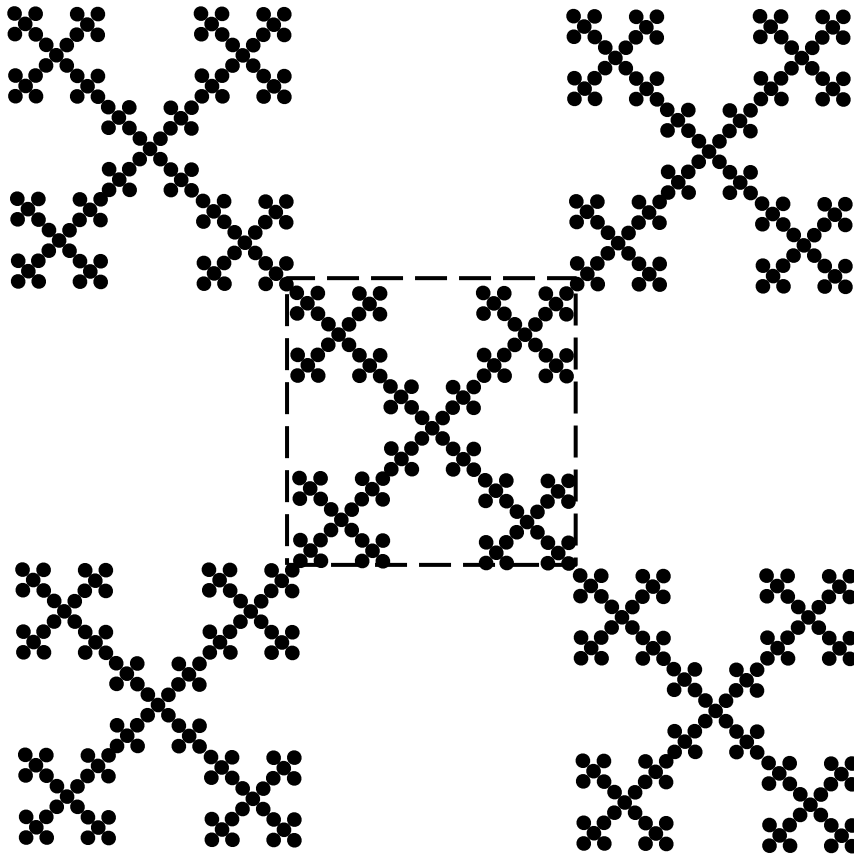


... a self-repeating pattern...

...a fractal

Aerogels – mass vs size

What if we increase the size again?



Size has gone up 27x...

Mass has gone up 125x

$\text{Log}(\text{mass})/\text{Log}(\text{size}) = 1.465$

Therefore, **in mass fractals:**

Mass \sim Size^{D_f}

where

D_f \neq 2 (or 3 in 3D)

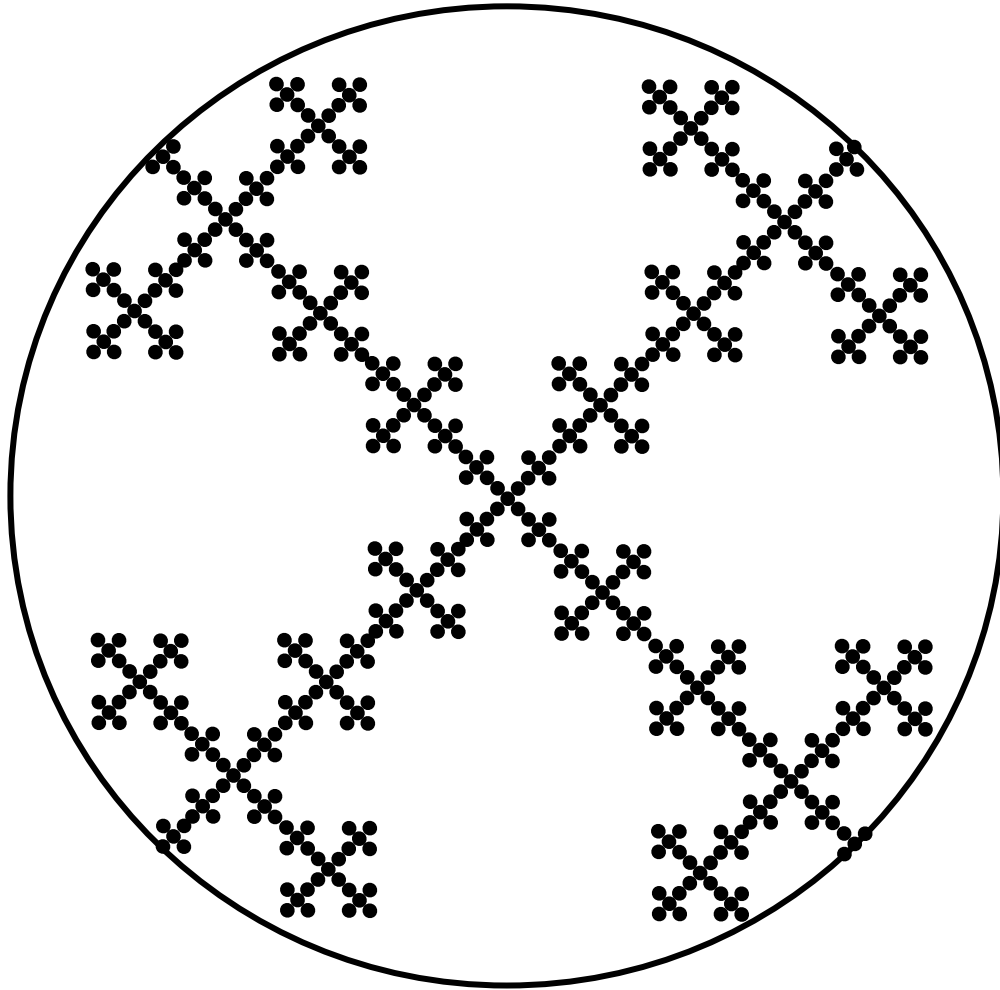
D_f: fractal dimension

Vicsek's deterministic fractal

(Vicsek, T. Fractal Growth Phenomena 2nd Ed., Singapore: World Scientific, 1992)

Aerogels – mass vs size

Now, let's imagine particles with that internal structure...



We call those particles:

Secondary particles

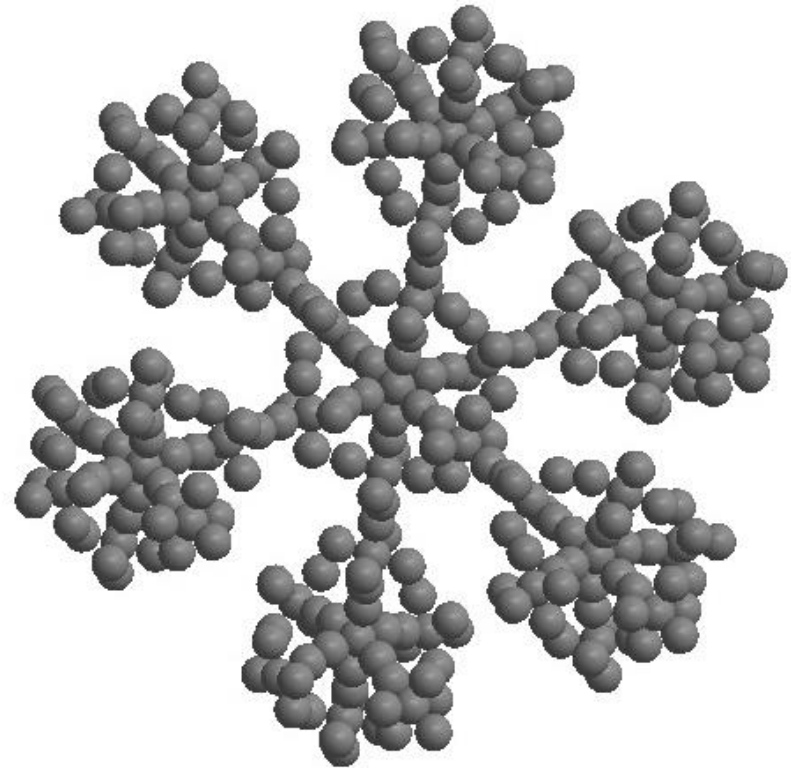
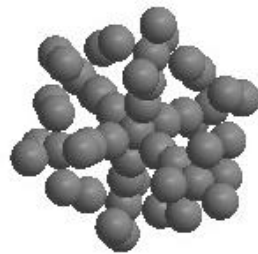
And the little particles inside

Primary particles

Aerogels – mass vs size

...or even better, let's see those secondary particles in 3D:

$$D_f = 2.0$$



1st generation

2nd generation

3rd generation

67%

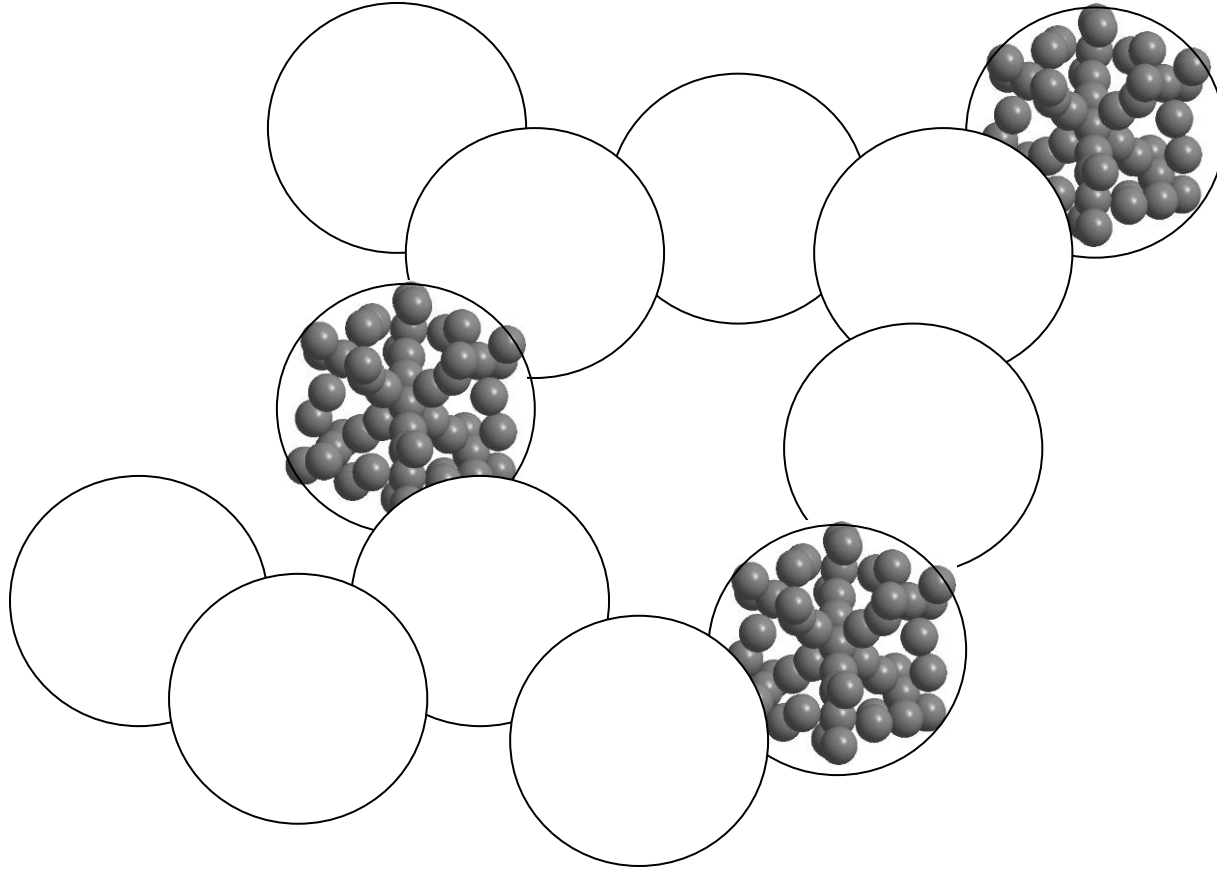
89%

96% empty space %

$$\% \text{ empty space} = 100 \times (1 - (R/R_o)^{D_f-3})$$

Aerogels

Secondary particles form porous networks...



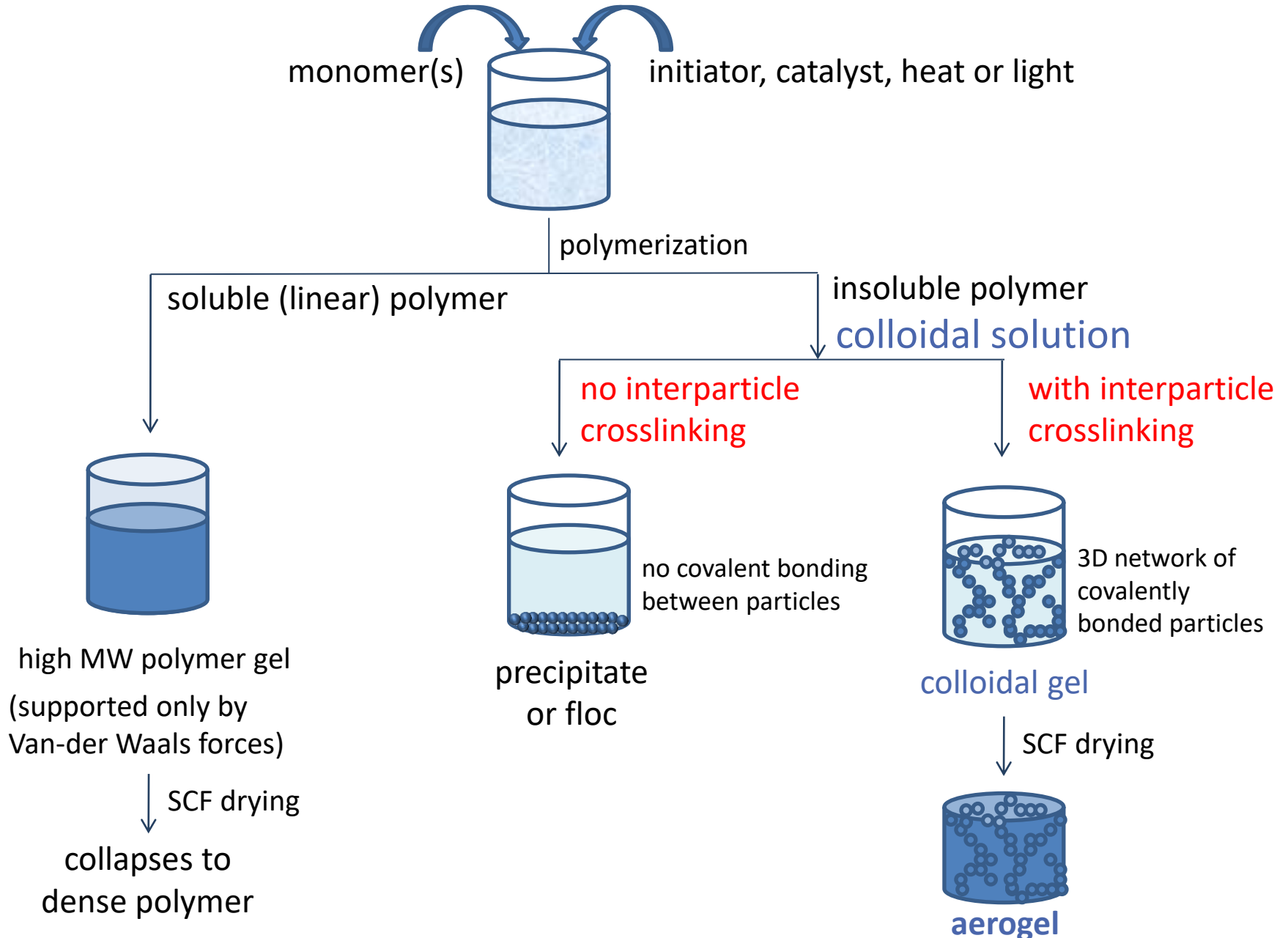
...and now, the question is how you make and how you characterize those networks in terms of chemical make up, connectivity, porosity and macroscopic properties....?

Synthesis of fractal nanoporous structures

Sol-Gel Chemistry

- by physical cooling
- by chemical cooling

Chemical cooling and synthesis of aerogels



Critical Point Dryers



10 L

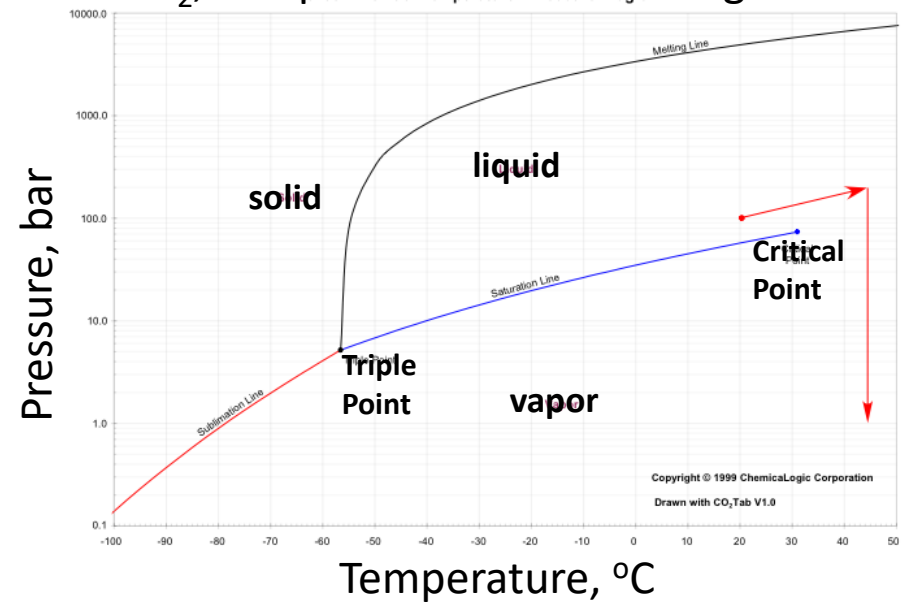


1 L

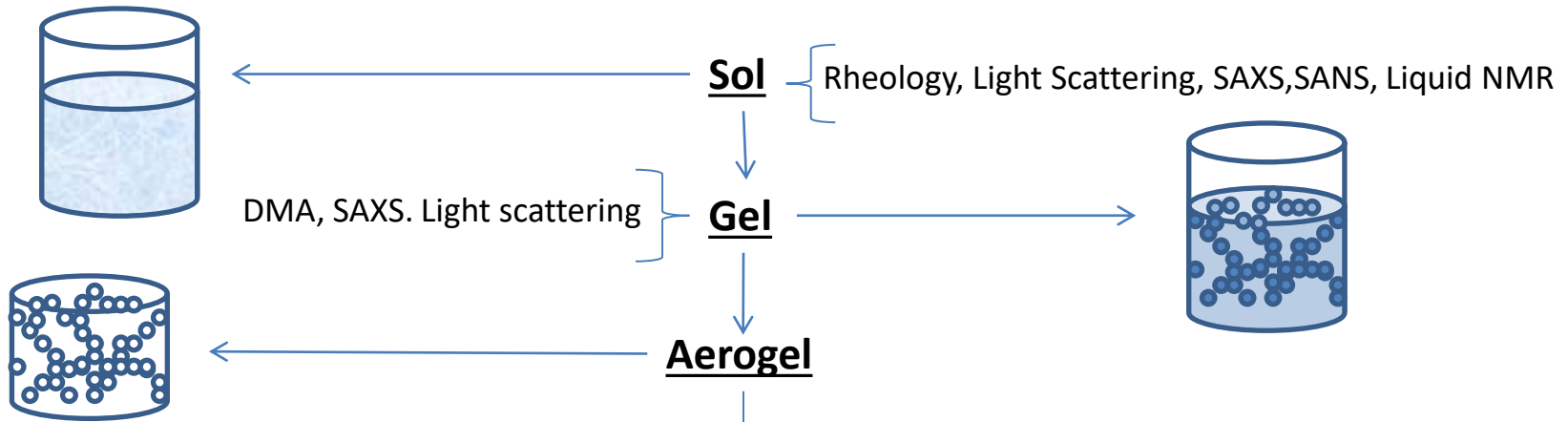


0.1 L

CO₂, Temperature-Pressure Diagram



Characterization Methods along Aerogel Synthesis



Skeletal Framework

Porous Structure

Molecular

Nano

Bulk

1 Å ----- 100 nm ----- >1 mm

N₂-sorption to 300 nm
Hg Intrusion 3 nm - 1 mm

Chemical: Solid-state NMR, IR, EXAFS

Structural: XRD

Other: DSC, TGA, GPC

Chemical: Mechanical Testing

Structural: TEM, SEM, SAXS, SANS

Mechanical Strength
Thermal Conductivity
Acoustic Impedance

Pores probed:

Micropores (<2 nm)

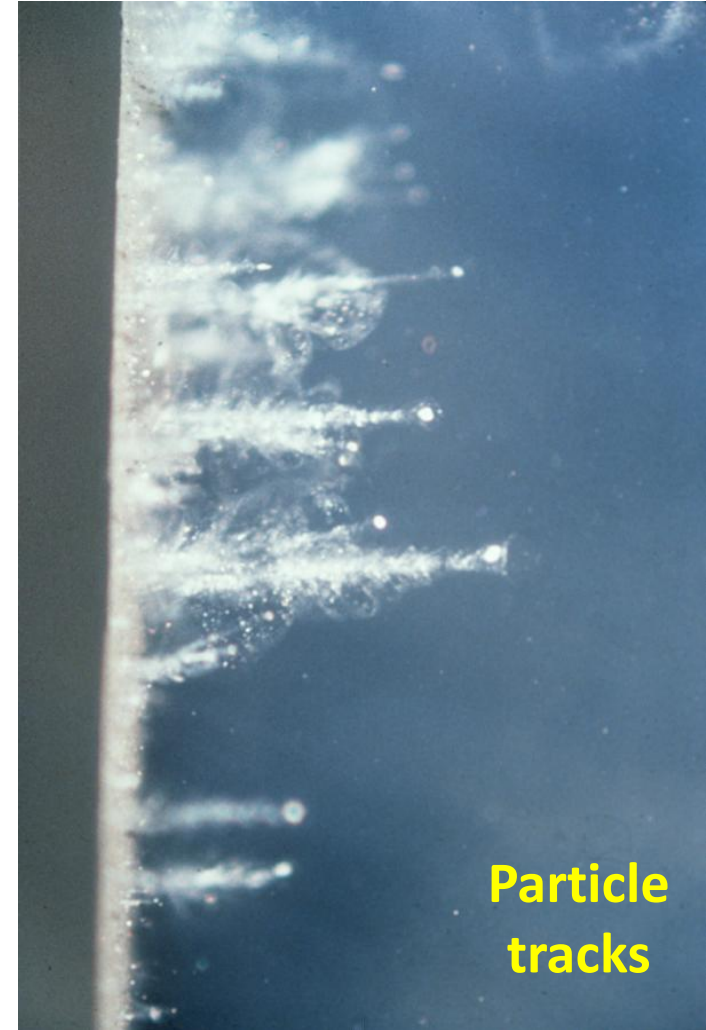
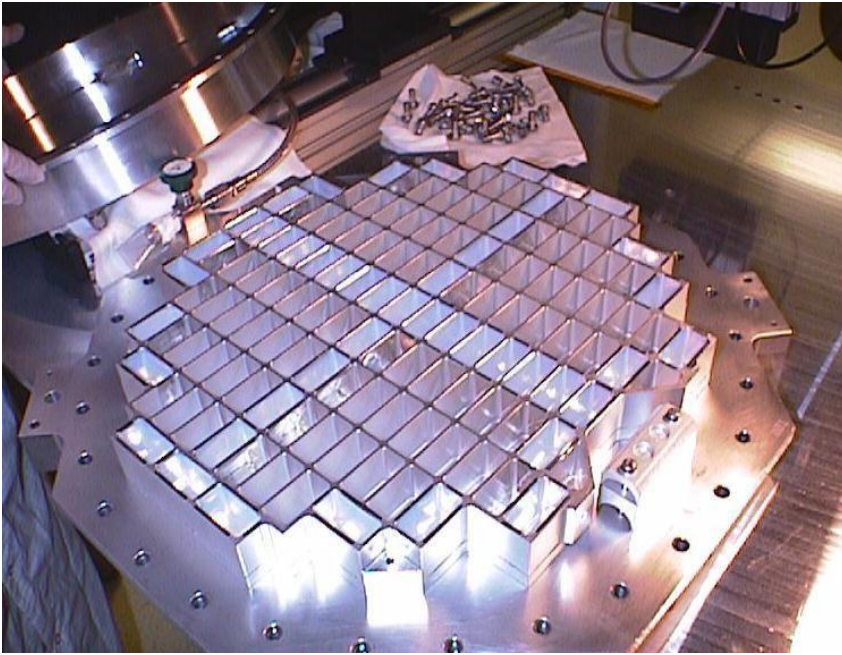
Mesopores (2-50 nm)

Macropores (>50 nm to ~1 mm)

Applications of aerogels

Stardust collector (Stardust program)

NASA used aerogels in a device that collects dust samples (including ancient stardust and comet particles) in space



Particle tracks

<https://www.jpl.nasa.gov/images/pia03188-dust-collector-with-aerogel>

<https://www.jpl.nasa.gov/images/pia03186-particle-tracks-in-aerogel>

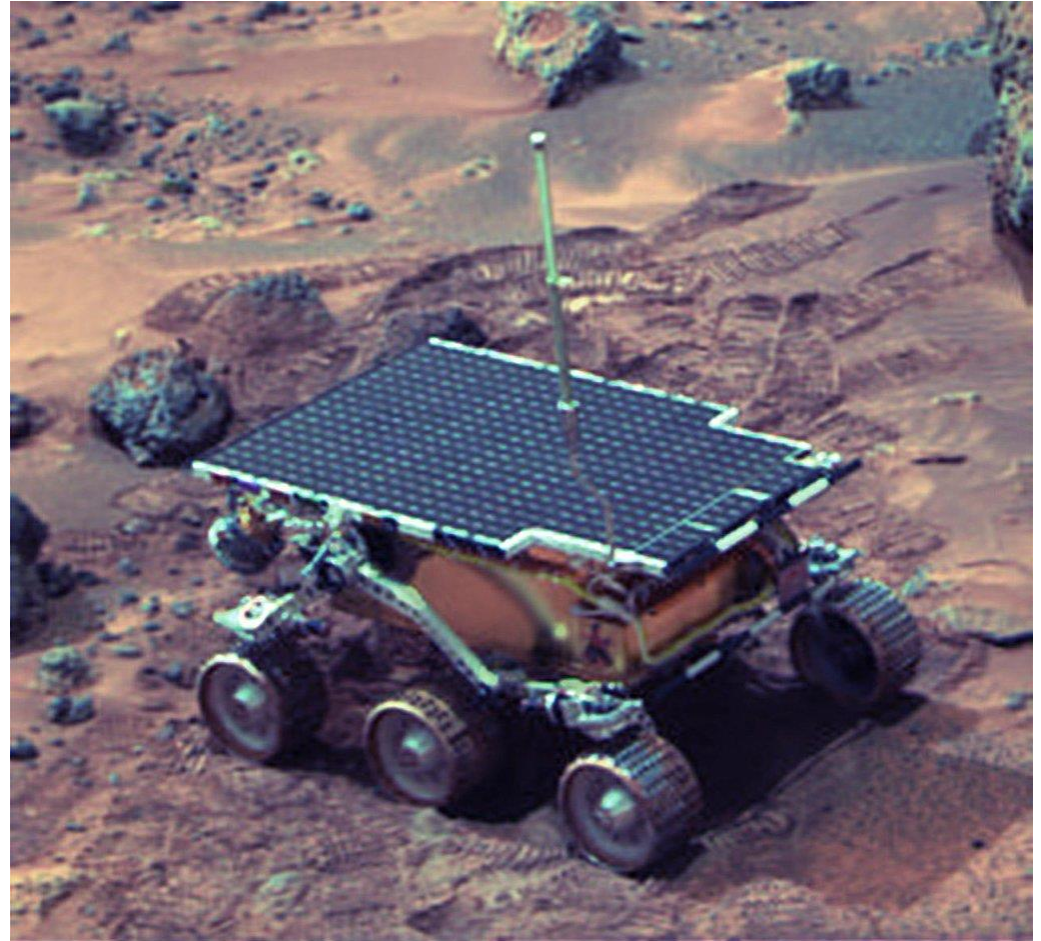
Applications of aerogels

For thermal insulation

Sojourner Rover – 1997

Spirit & Opportunity – 2004

Curiosity – 2012



Applications of aerogels

For thermal insulation in extremely harsh conditions



<https://spinoff.nasa.gov/spinoff2001/ch5.html>

PART 2

Silica aerogels



low-density highly porous solid

At best:

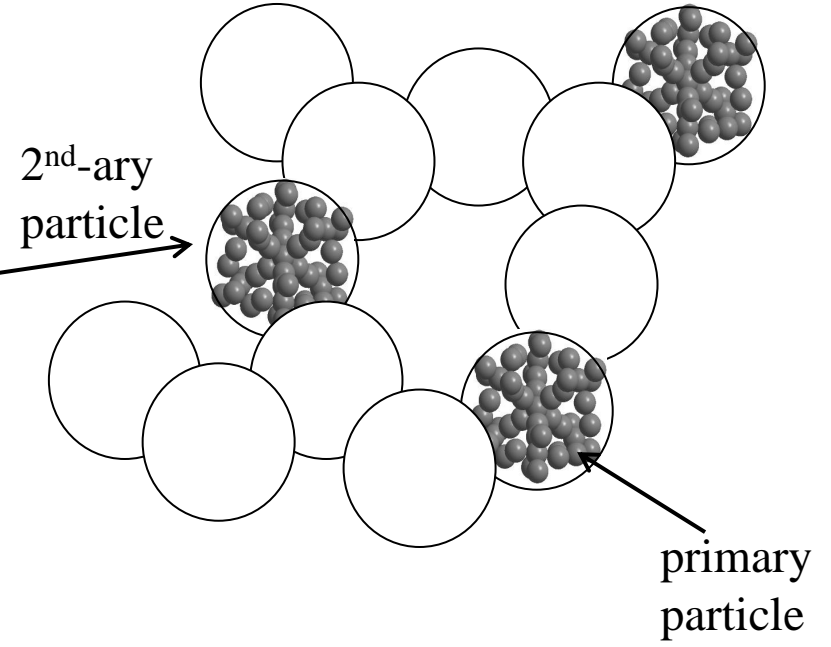
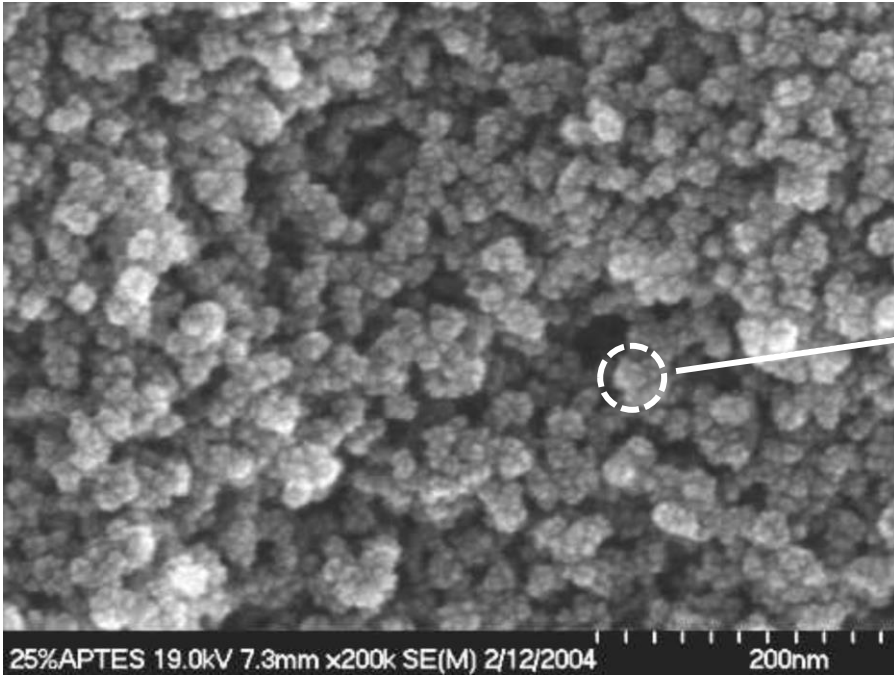
- 99.8% air
- 1000 times less dense than glass
- about 40 times better thermal insulators than the best fiberglass

However,

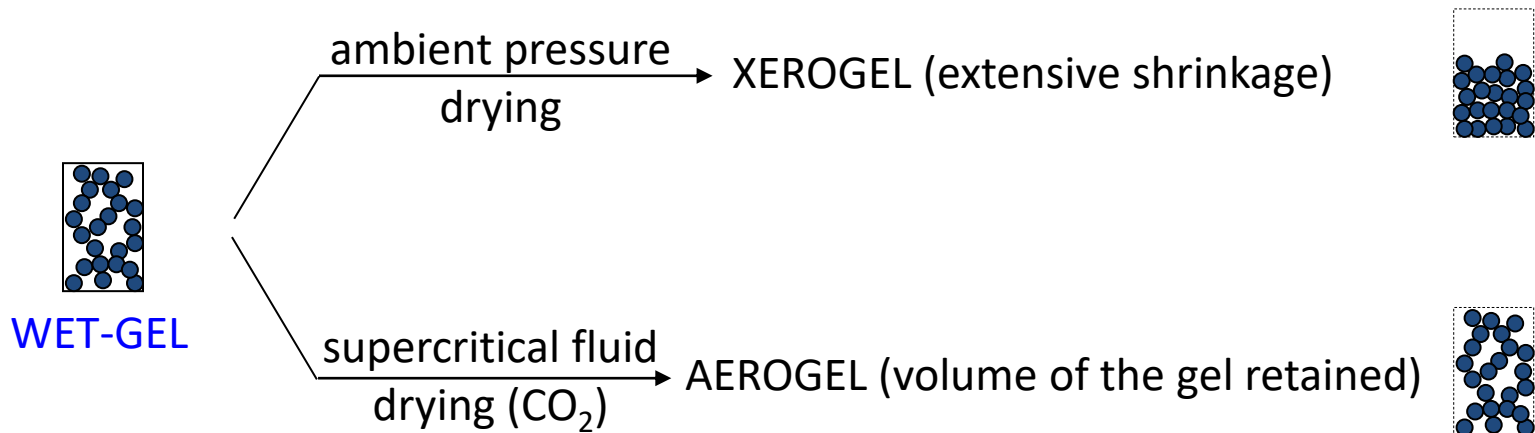
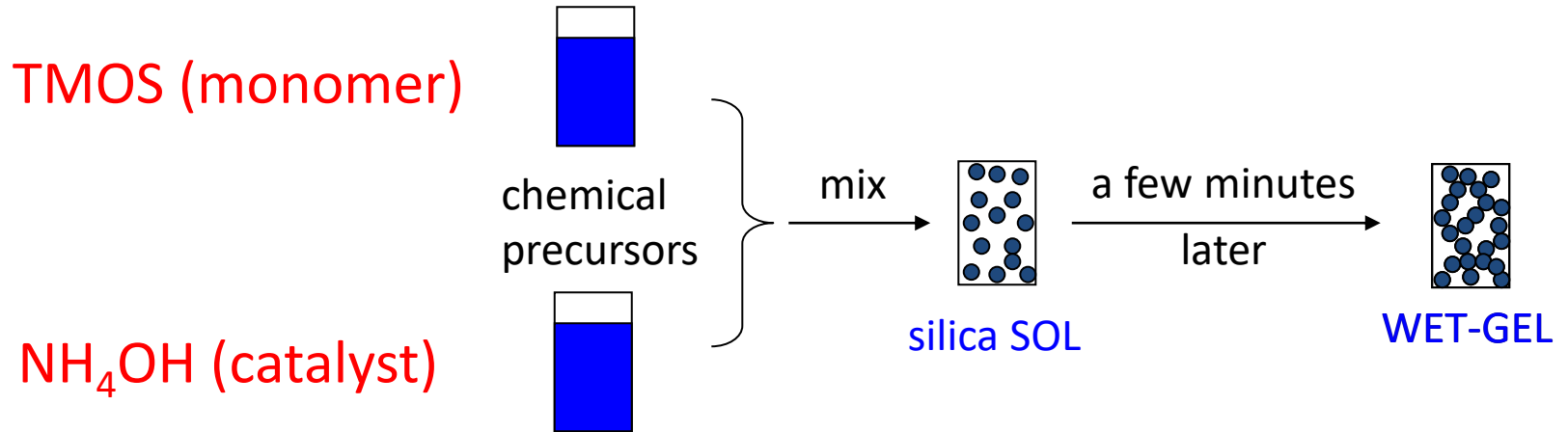
commercialization of pristine, monolithic silica aerogels has been slow, because they are:

- fragile;
- hygroscopic; and,
- require supercritical fluid (SCF) extraction

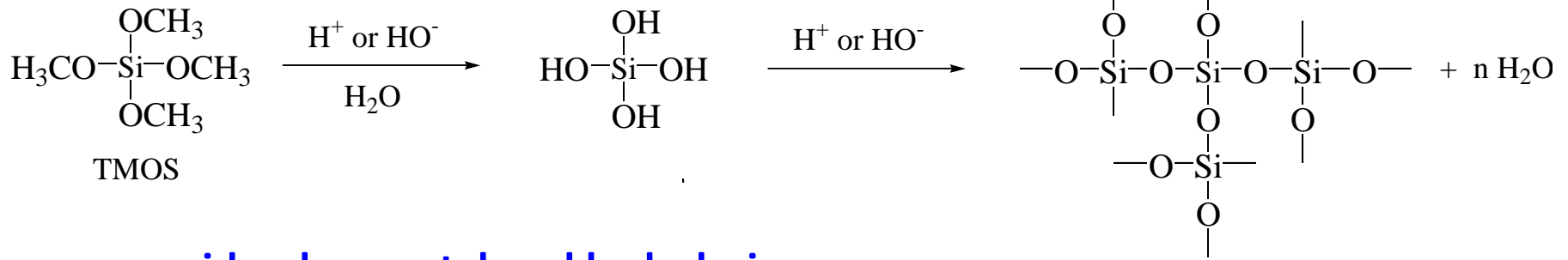
Silica aerogels



Preparation of silica aerogels



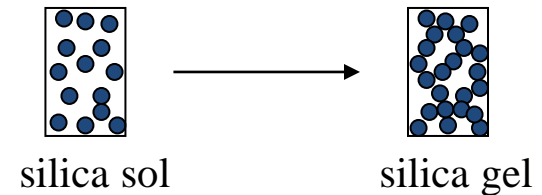
Preparation of silica aerogels



acid or base catalyzed hydrolysis

followed by:

in situ acid or base catalyzed condensation



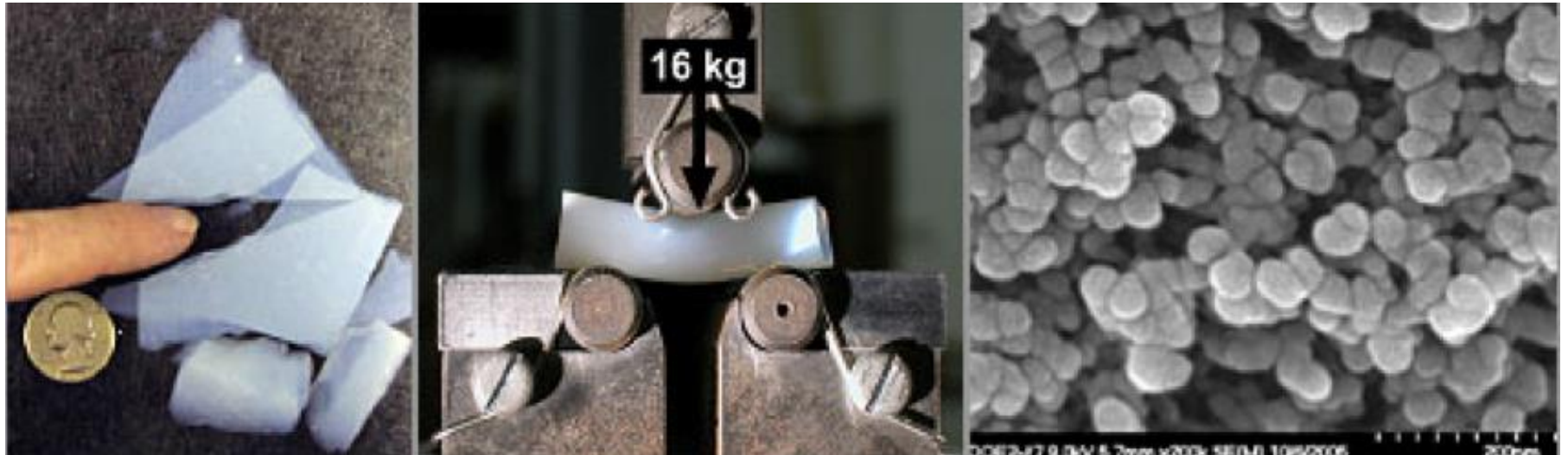
There have been two ways around the fragility issue...

.... both were invented around the same time,

.... in the early 2000s:

- Casting a sol (thereby a monolith) in a non-woven fibrous mat
(Aspen Aerogels: **Aerogel Blankets**)
- Casting a conformal polymer coating around the skeletal nanoparticles
(Missouri S&T: **Polymer-Crosslinked (X-) Aerogels**)

Polymer-Crosslinked (X-) Aerogels



A class of strong lightweight (*bulk*) materials with a minimal penalty in density (the 300:3 rule).

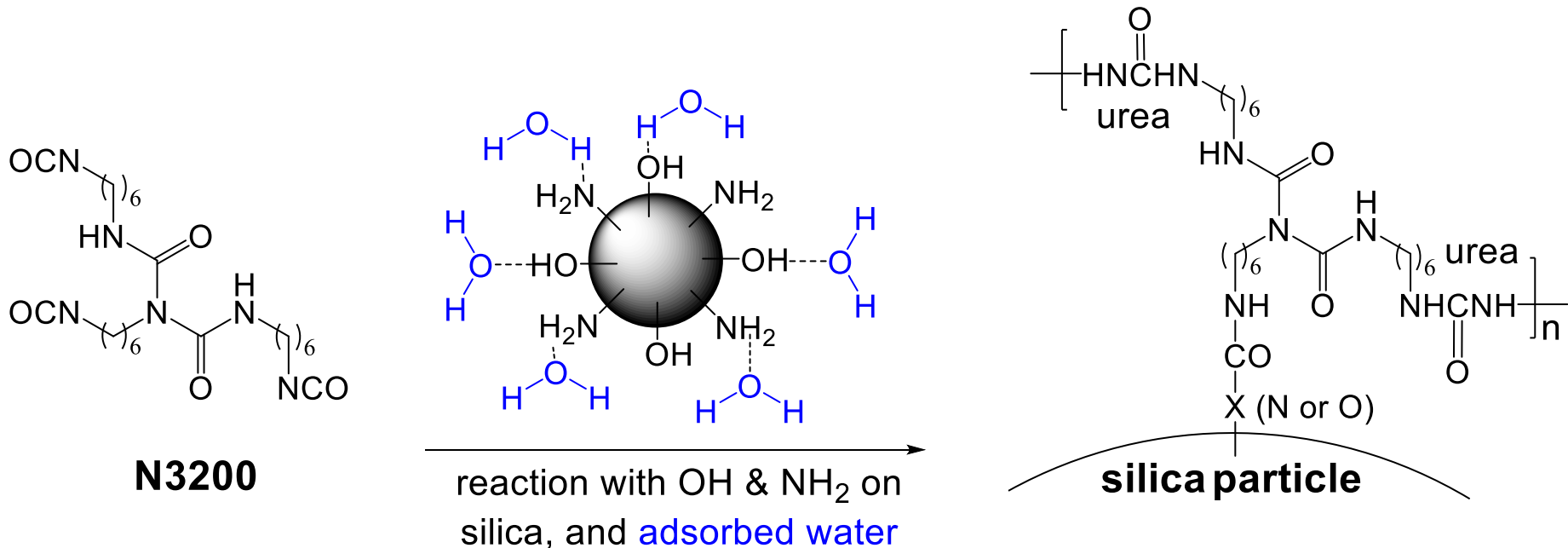
The mesoporous structure is maintained after cross-linking (right).

N. Leventis *et al.* *NanoLett.* **2002**, 2, 957-960

N. Leventis *et al.* *Acc. Chem. Res.* **2007**, 40, 874-884

N. Leventis *et al.* U.S. Patent 7,771,609 (**2010**)

The chemistry of crosslinking silica with a triisocyanate



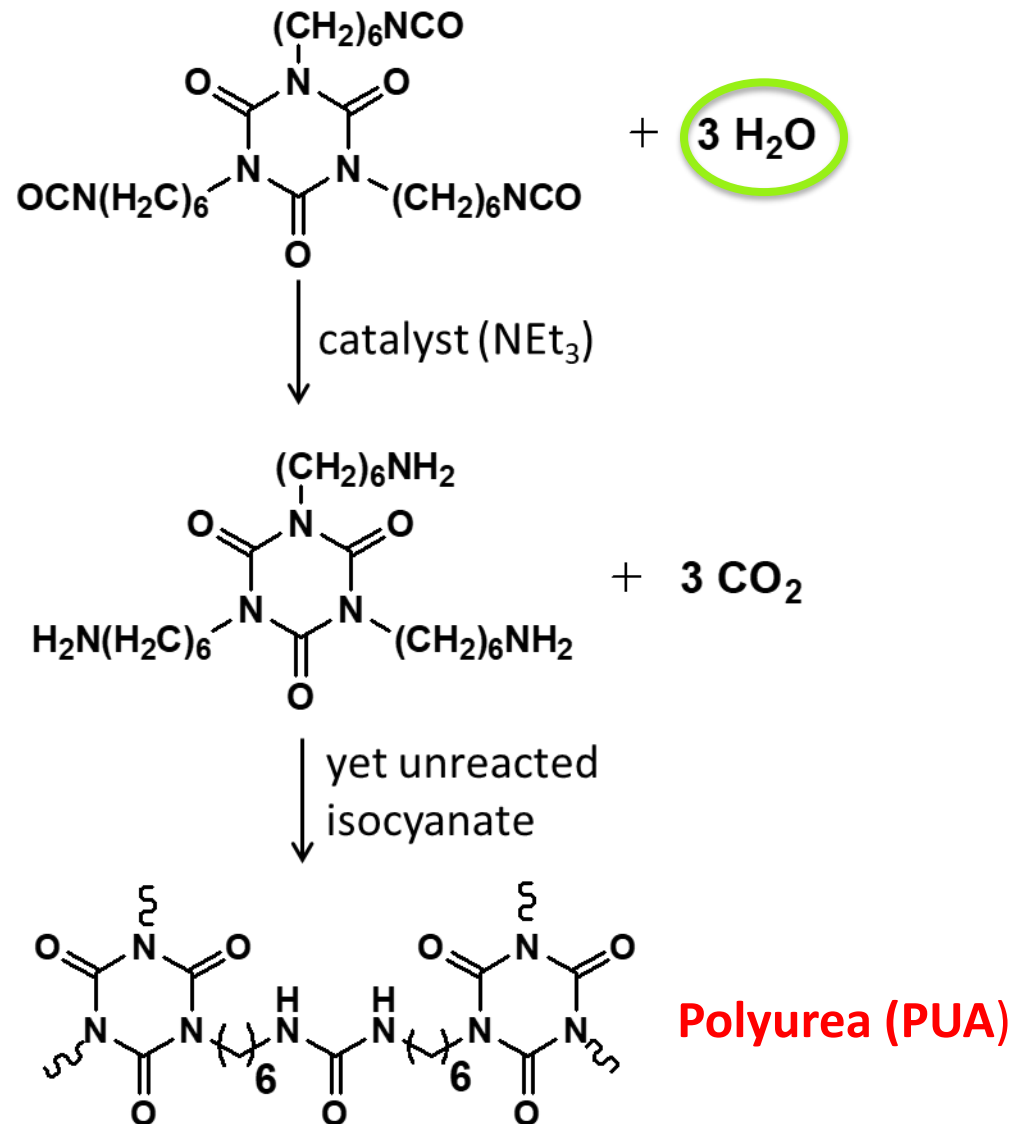
Multifunctional isocyanates react with surface silanol groups, amino groups and adsorbed water to form polyurethane / polyurea tethers bridging covalently the skeletal nanoparticles.

N. Leventis *et al.* *NanoLett.* **2002**, 2, 957-960

N. Leventis *et al.* *Acc. Chem. Res.* **2007**, 40, 874-884

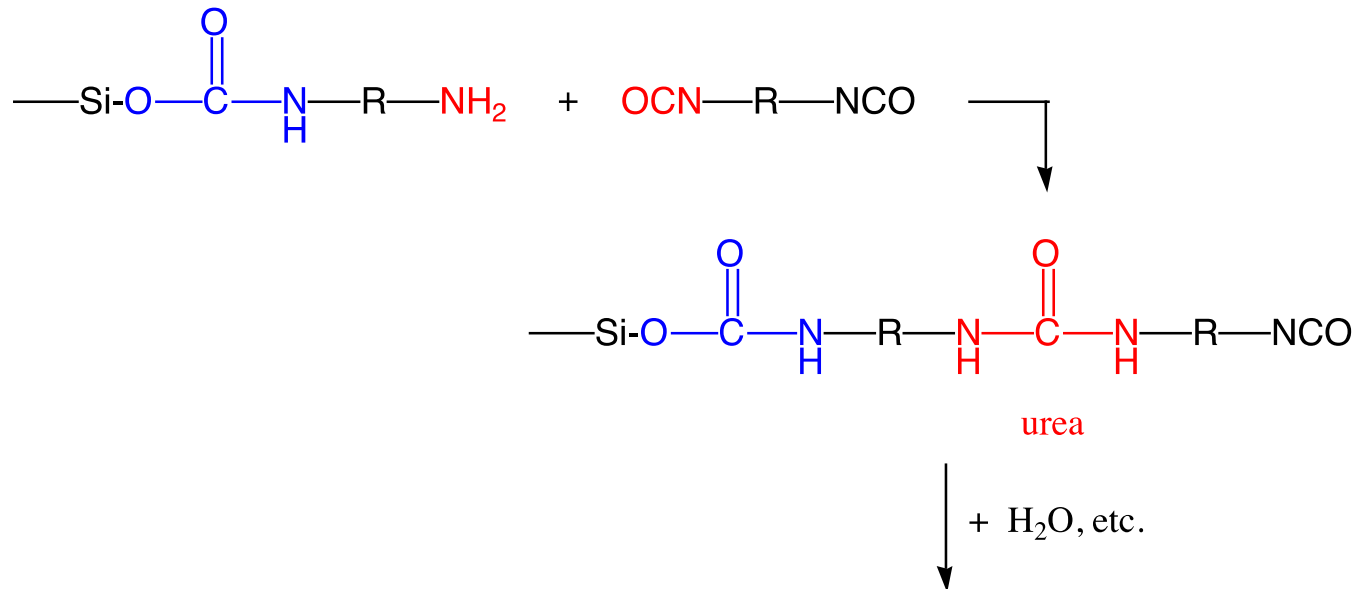
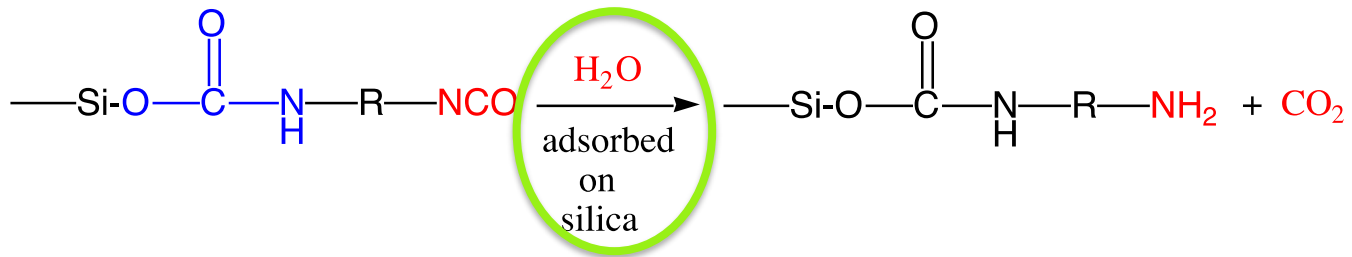
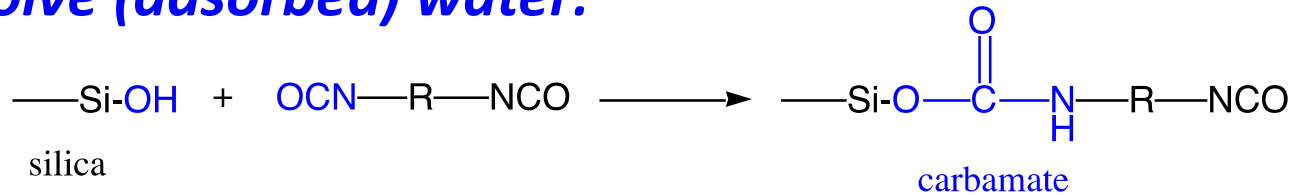
N. Leventis *et al.* U.S. Patent 7,771,609 (**2010**)

The chemistry of crosslinking silica with a triisocyanate



The chemistry of crosslinking silica with a triisocyanate

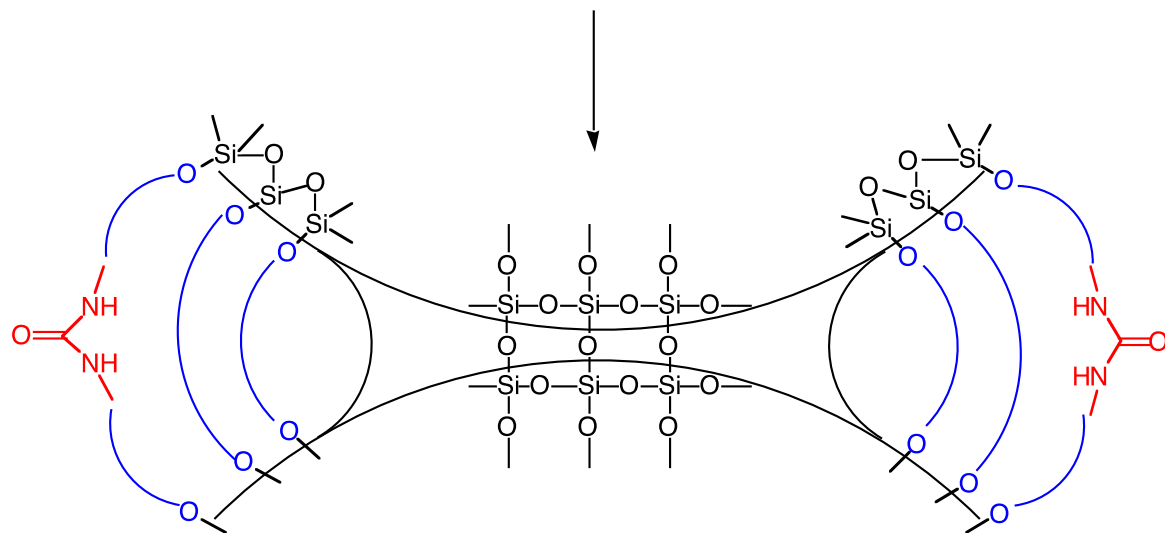
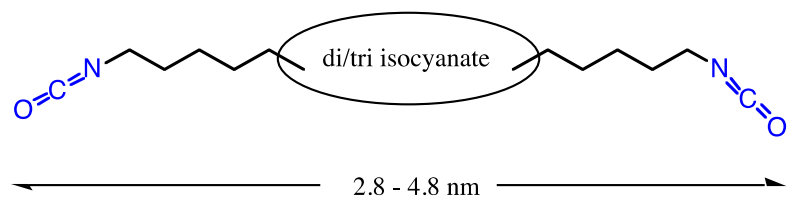
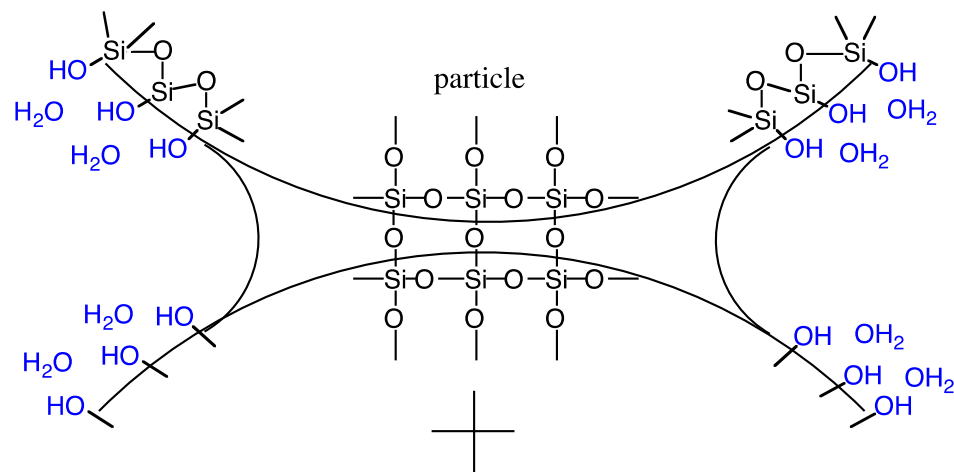
Therefore, the mechanism of crosslinking silica with isocyanates must involve (adsorbed) water:



The chemistry of crosslinking silica with a triisocyanate

Schematically

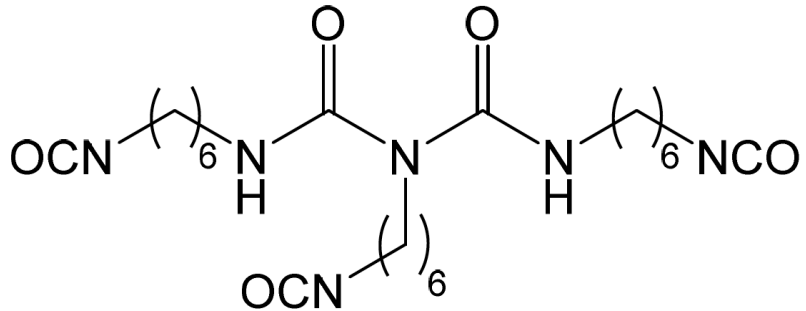
Aerogels have well-defined weak points: the interparticle necks



The crosslinking method reinforces those weak points:

The chemistry of crosslinking silica with a triisocyanate

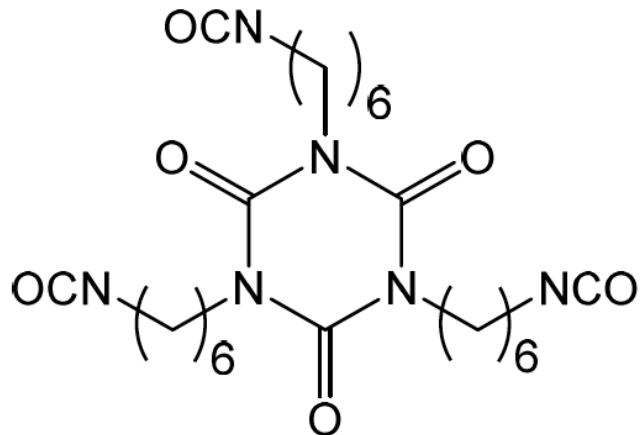
Most commonly used triisocyanates for crosslinking:



Desmodur N3200

Flexible / Aliphatic

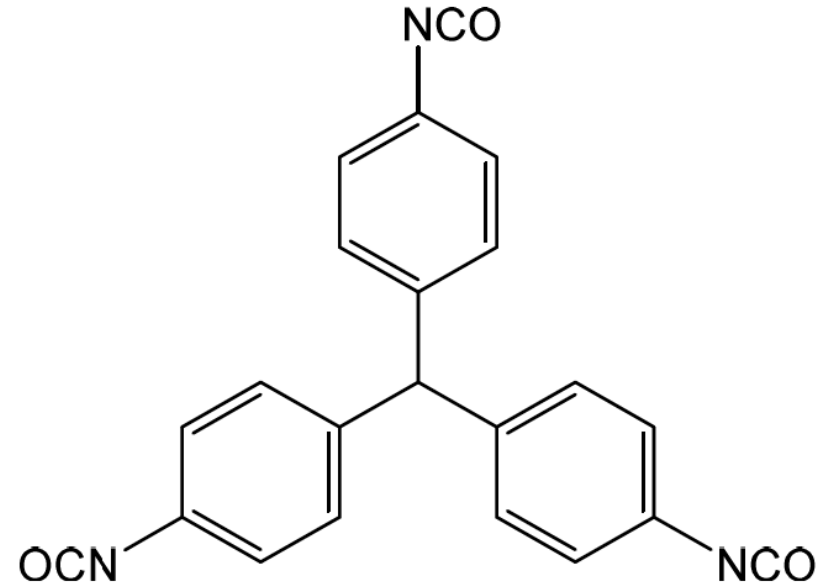
A biuret derivative of HDI



Desmodur N3300

Flexible / Aliphatic

Isocyanurate derivative of HDI

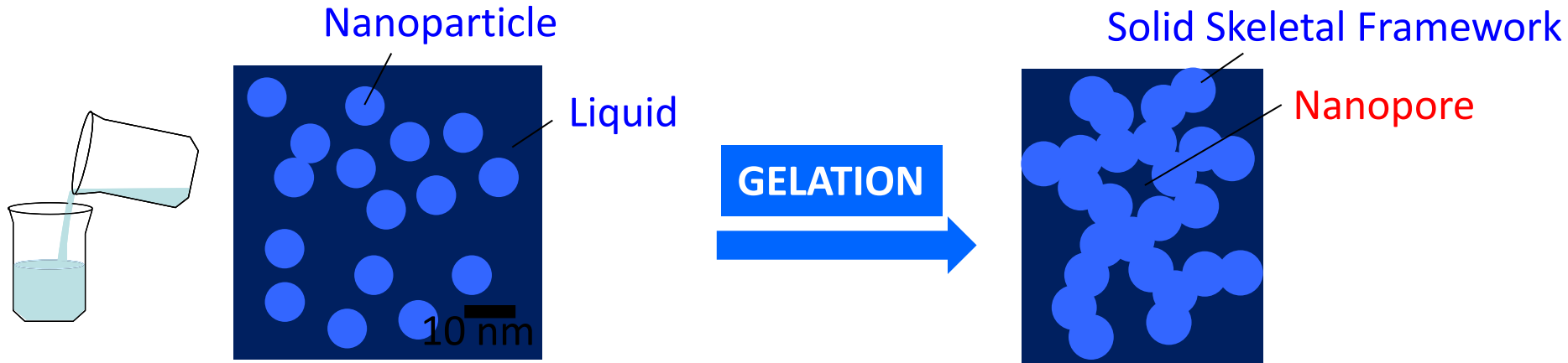


Desmodur RE (TIPM)

Rigid / Aromatic

Carbonizable

Polymer-Crosslinked (X-) Silica Aerogels



1. START BY PREPARING THE LIQUID PRECURSOR IN WHICH NANOPARTICLES WILL FORM (SOL)

2. THE SOL GELS

CROSSLINKING

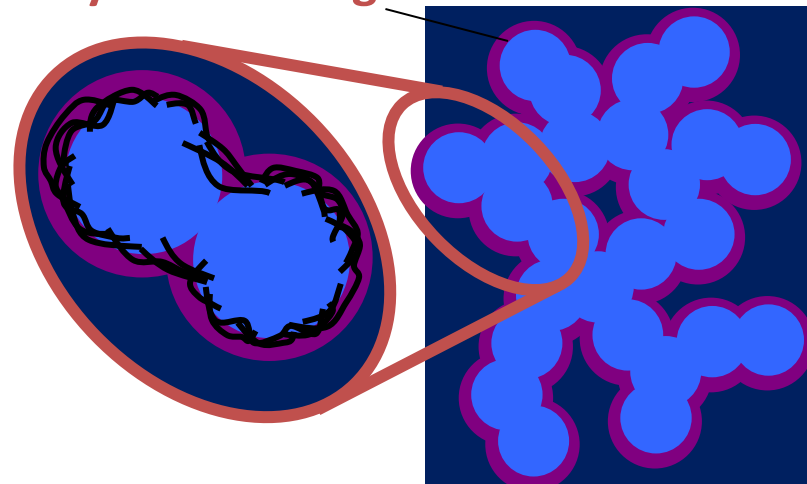
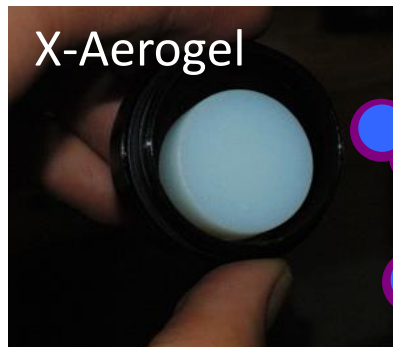
Polymer Coating

DRYING

3. A POLYMER SKIN FORMS

X-Aerogel

4. POLYMER CROSSLINKED (X-) AEROGEL



Polymer-Crosslinked (X-) Silica Aerogels

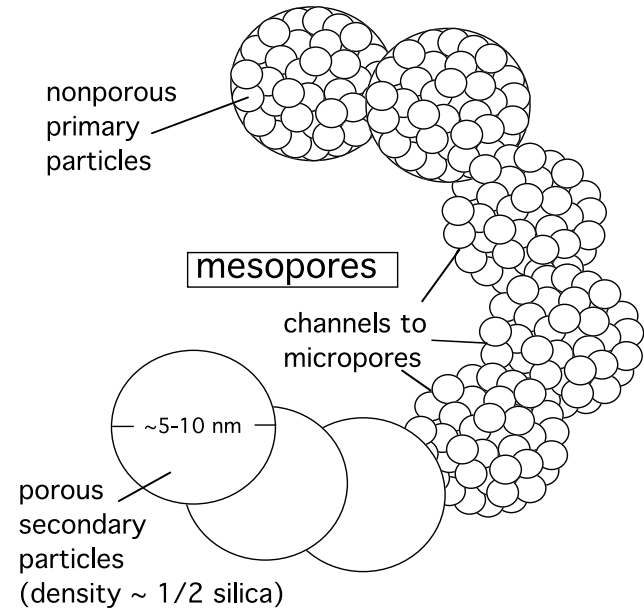
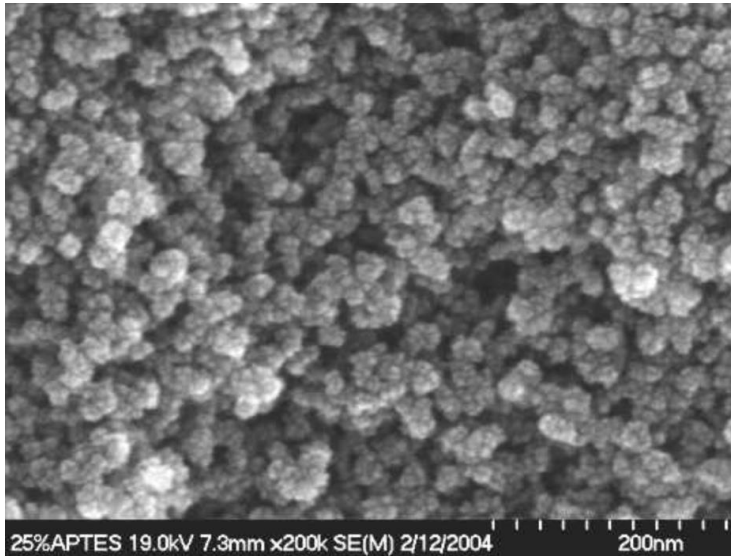
Polymer-crosslinked silica aerogels can be viewed as composites, in which the relative topology of silica and the crosslinker is defined at the nanoscopic scale rather than at the molecular level.

Polymer-Crosslinked (X-) Silica Aerogels

before
X-linking

$$\rho_b = 0.19 \text{ g/cc}$$

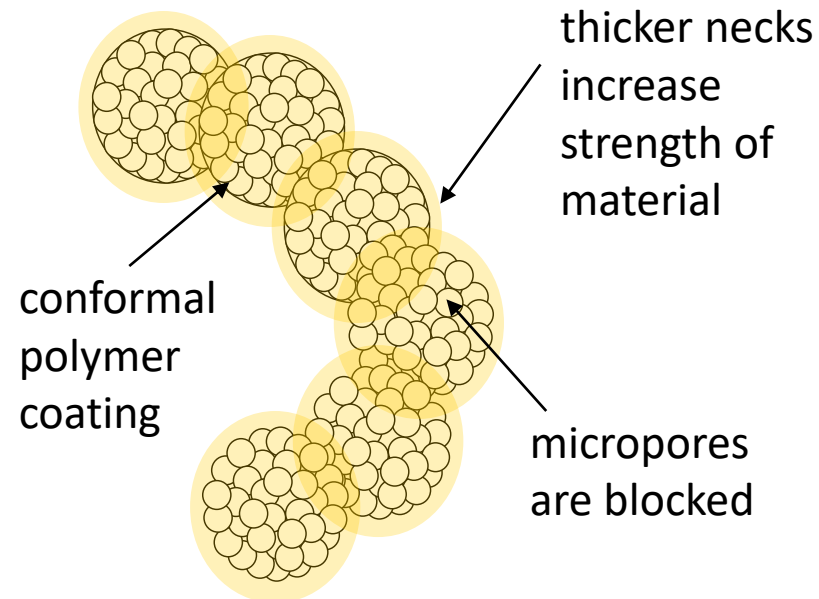
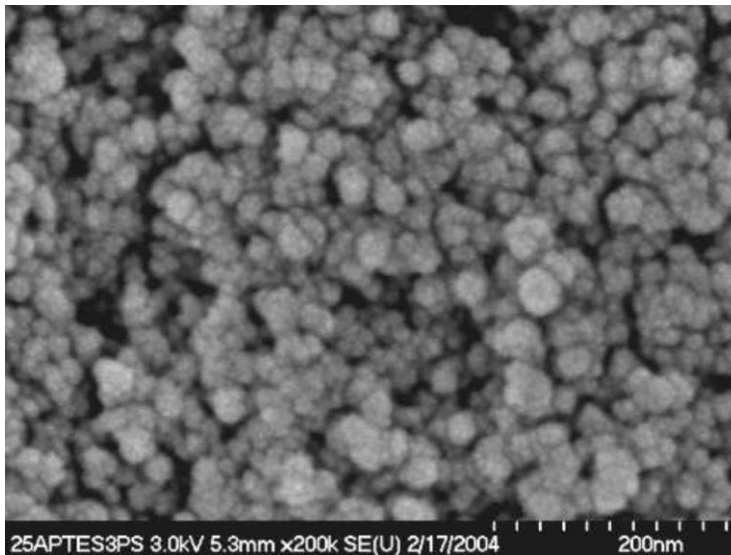
$$\Pi = 89 \% \text{ v/v}$$



after
X-linking

$$\rho_b = 0.48 \text{ g/cc}$$

$$\Pi = 65 \% \text{ v/v}$$



Polymer-Crosslinked (X-) Silica Aerogels

Solid-state NMR spectroscopy

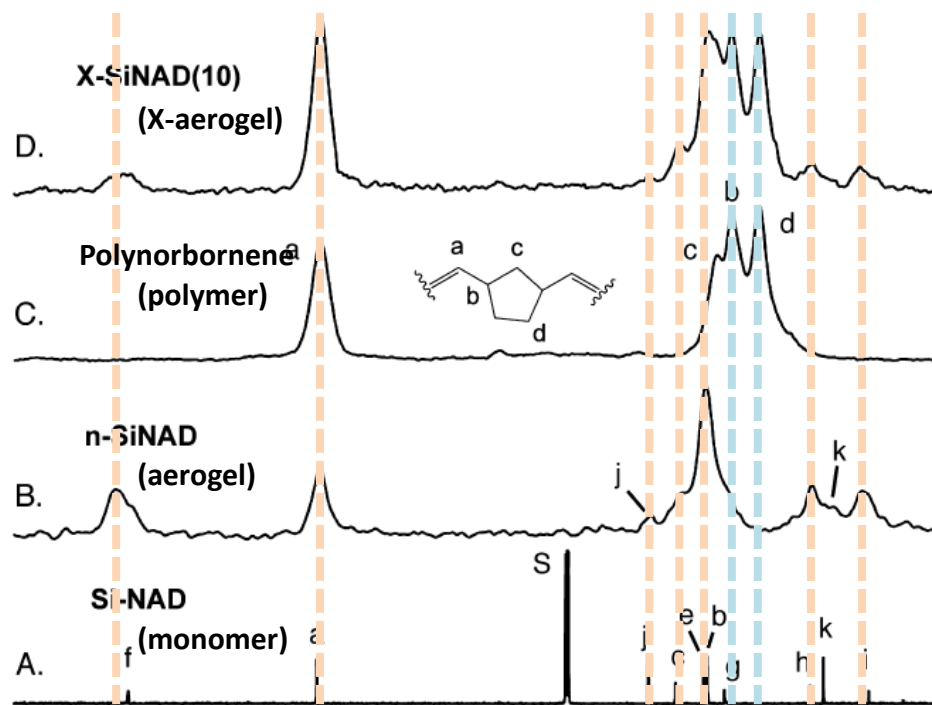


Figure 4. ^{13}C CPMAS NMR of solids samples, in comparison to the liquid ^{13}C NMR of Si-NAD (CDCl_3). Polynorbornene (frame C) was isolated from the cross-linking bath. For peak assignments, see structures in text.

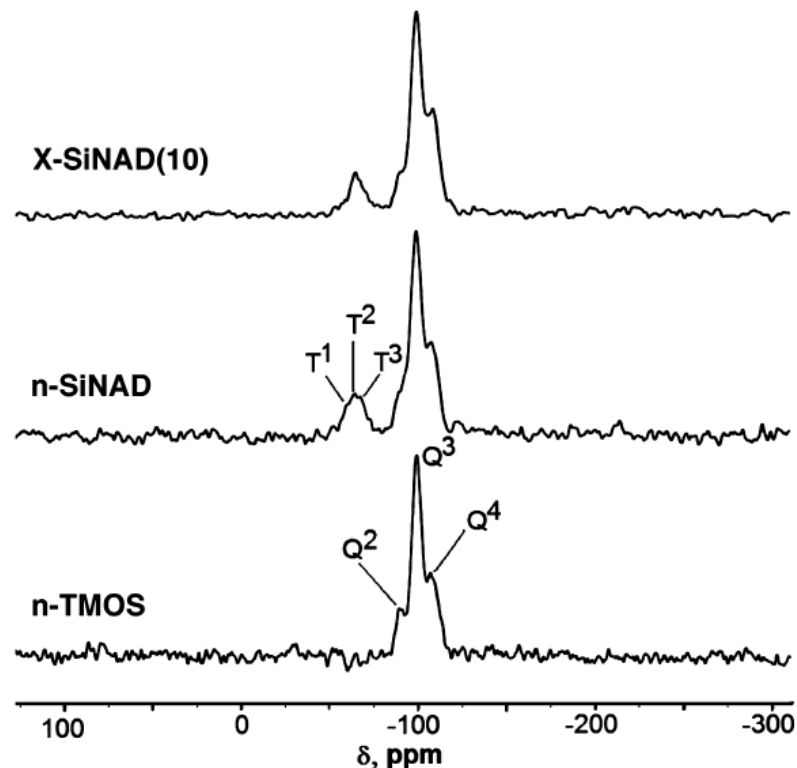


Figure 5. Solid ^{29}Si CPMAS NMR data.

Polymer-Crosslinked (X-) Silica Aerogels

Transmission Electron Microscopy (TEM) Scanning Electron Microscopy (SEM)

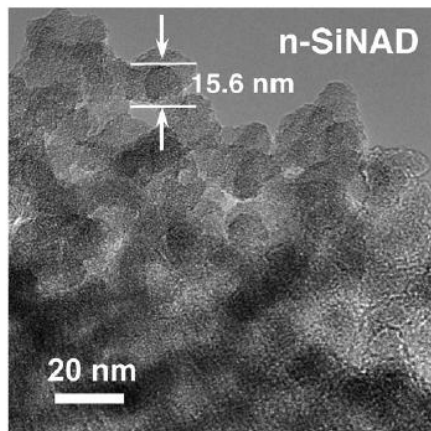
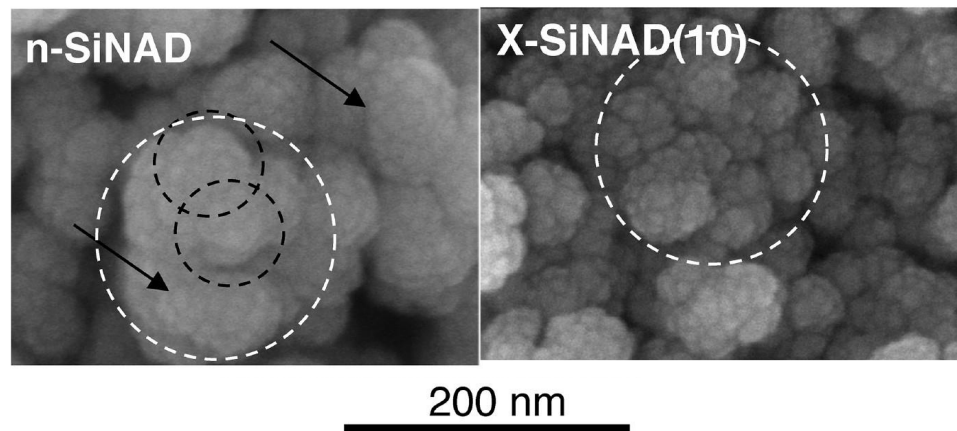


Figure 7. Transmission electron micrograph (TEM) of n-SiNAD. The primary particle diameter (15.6 nm) matches with that found using SAXS (15.4 nm; see Figure 6 and Table 2). For TEM of the X-SiNAD(xx) samples see Figure S.4 in Supporting Information.



In SEM, primary particles, as identified by both SAXS/SANS and TEM, are indicated with arrows. Dashed dark circles delineate secondary particles, as identified by SAXS/SANS. Dashed white circles delineate aggregates of secondary particles forming the network, as suggested by rheology.

Polymer-Crosslinked (X-) Silica Aerogels

Where is the polymer located?

Small Angle X-ray Scattering and Small Angle Neutron Scattering (SAXS and SANS))

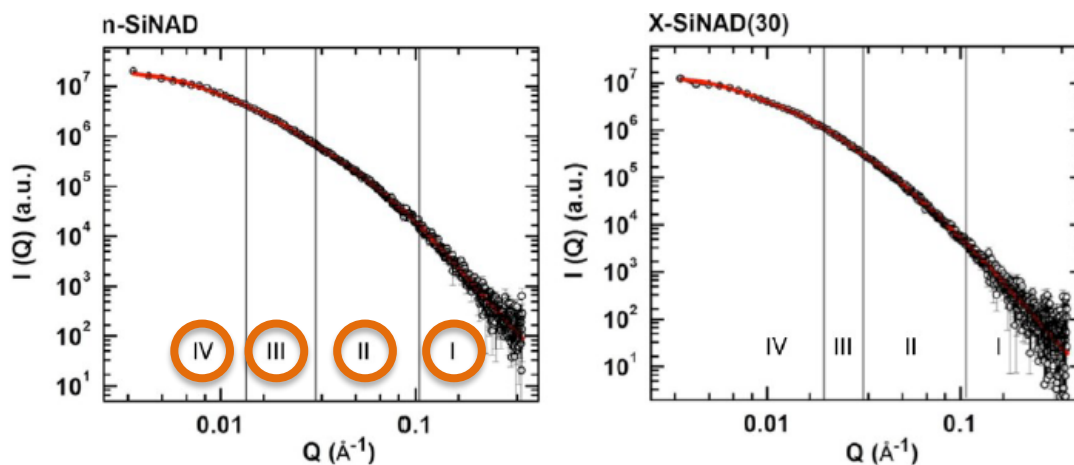
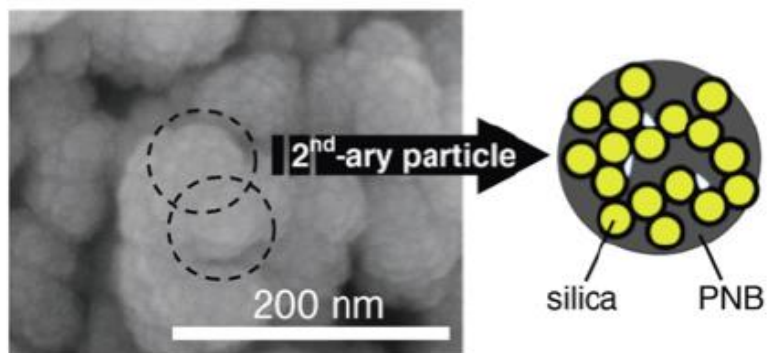


Figure 6. Small angle X-ray scattering (SAXS) data for aerogel samples. (Data are summarized in Table 2; for additional sample information, refer to Table 4.) Primary particle radii were extracted from Guinier Region II. Secondary particle radii from Region IV. Fractal dimensions of secondary particles from Region III. Fitting power-law Region I to modified Porod's law (eq 4) yielded the surface layer thickness of primary particles.



The X-aerogel technology has been expanded to:

other skeletal frameworks

oxides

polymers

biopolymers

other surface chemistries

amines

free radical initiators

monomers

other crosslinking polymers

polyacrylonitrile

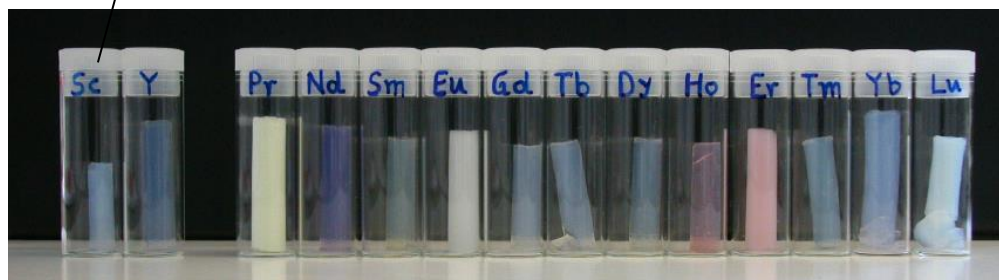
polynorbornene

Crosslinking of metal oxides with polyurea just like silica

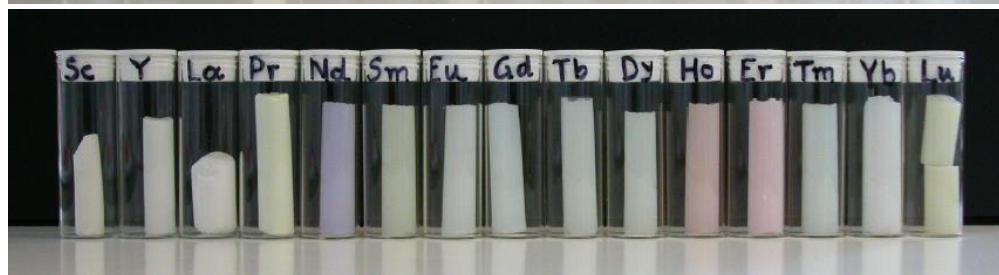
*over 30
other-than-silica
'metal oxide' aerogels
have been X-linked
with polyurea:*

A periodic table with several elements highlighted in blue and purple. The blue elements include Sc, Ti, V, Cr, Mn, Fe, Co, Ni, Cu, Zn, Ga, In, Sn, Pb, Bi, Po, At, and the entire lanthanide and actinide series. The purple elements include Al, Si, Ge, and Sn. A white bracket on the left side of the table groups the elements from Sc to Lu, with a line pointing to the 'Native aerogels' image below.

Native aerogels:

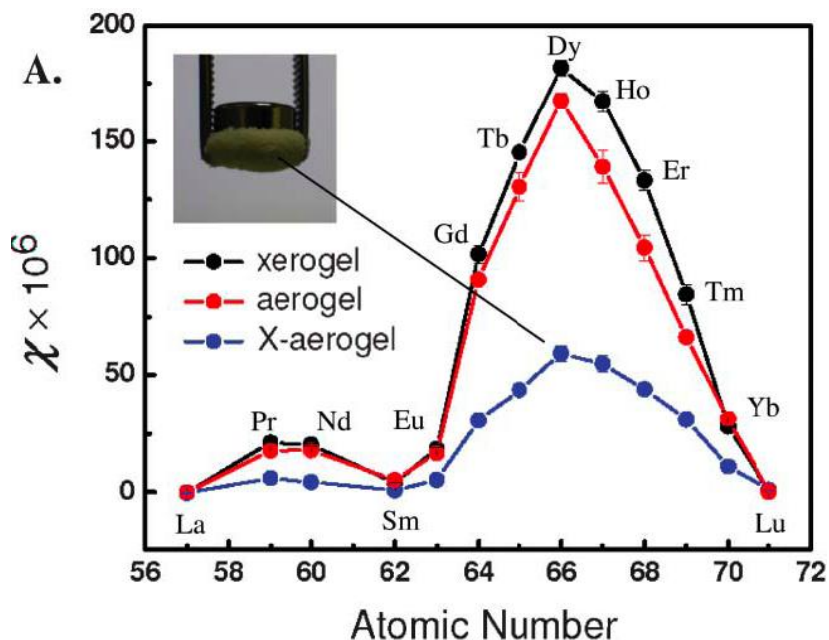


X-aerogels:

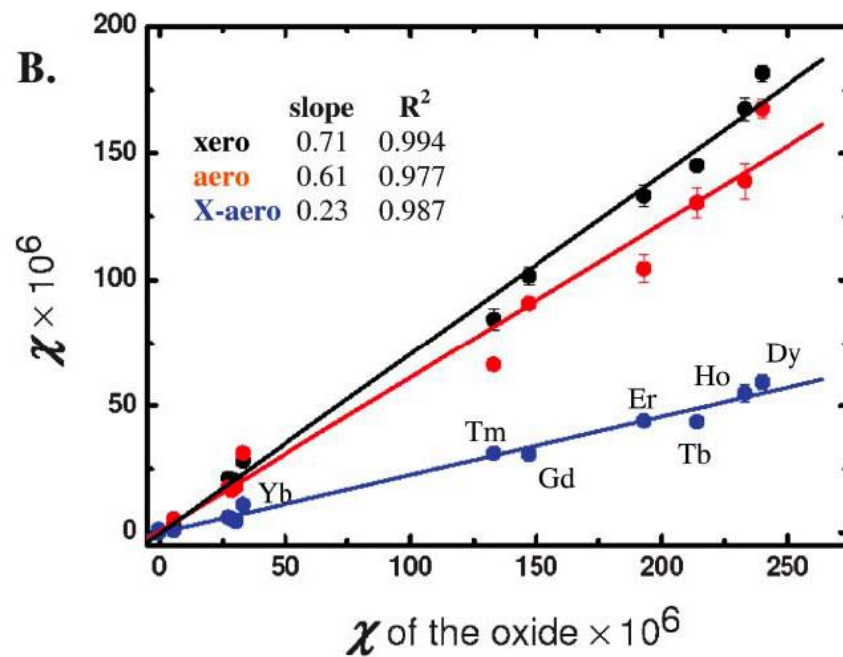


Crosslinking of metal oxides with polyurea just like silica

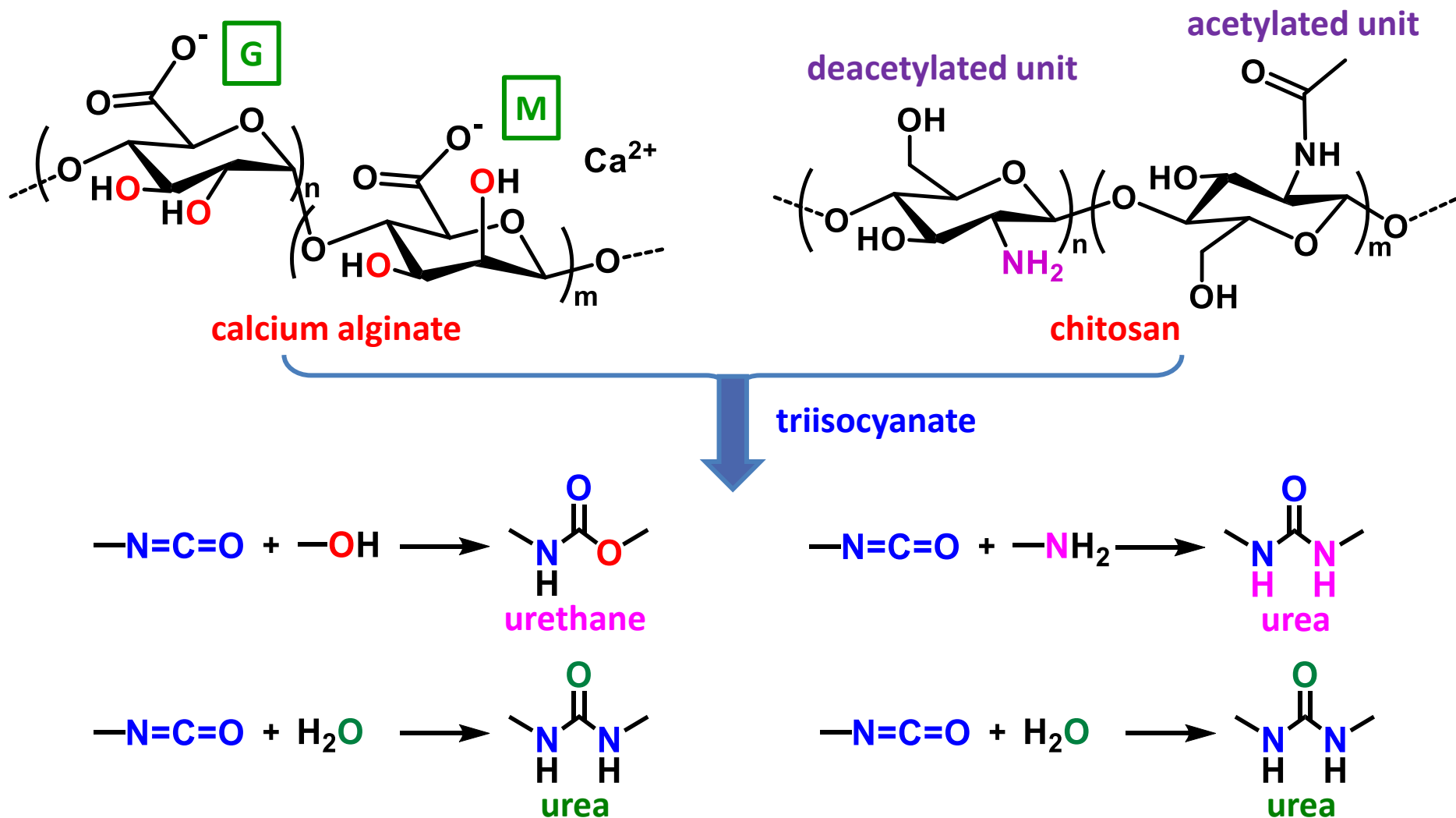
... some with interesting optical, electric and magnetic properties



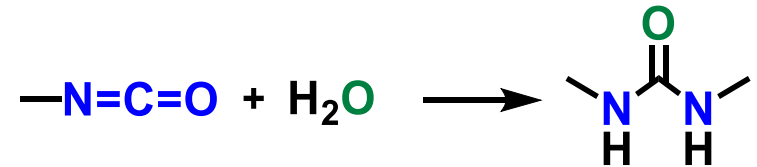
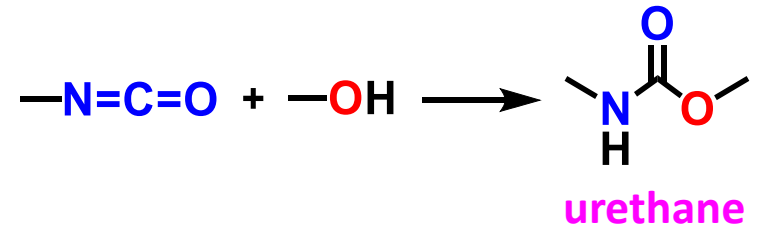
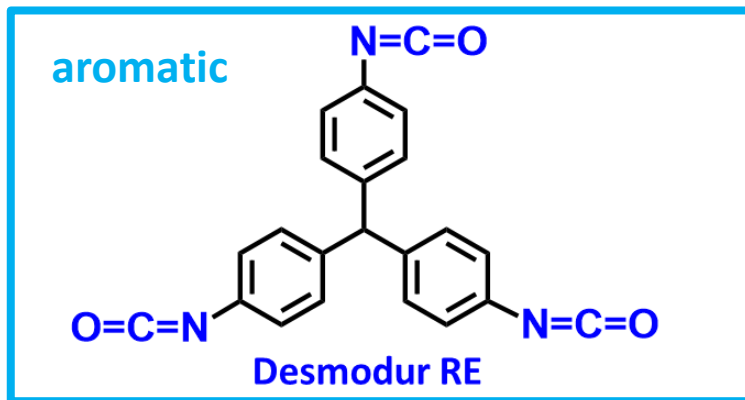
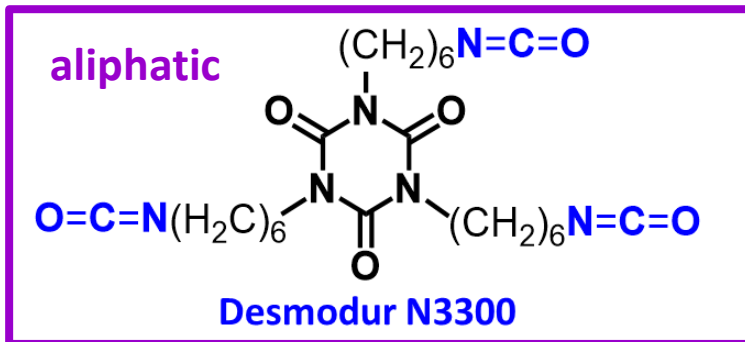
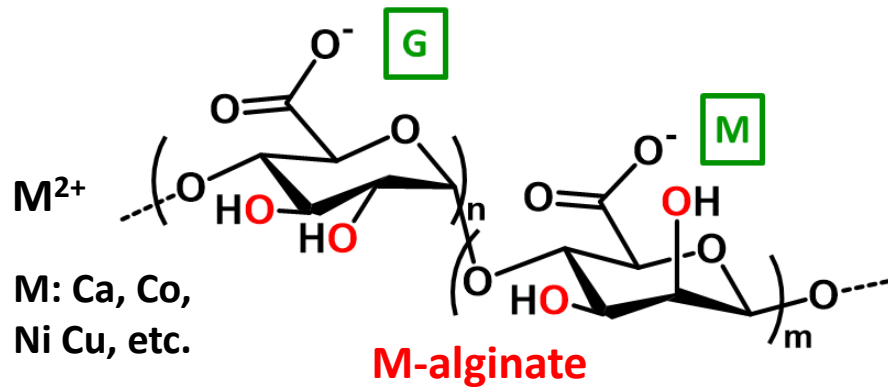
χ : gram magnetic susceptibility



Crosslinking of biopolymers with polyurea just like silica

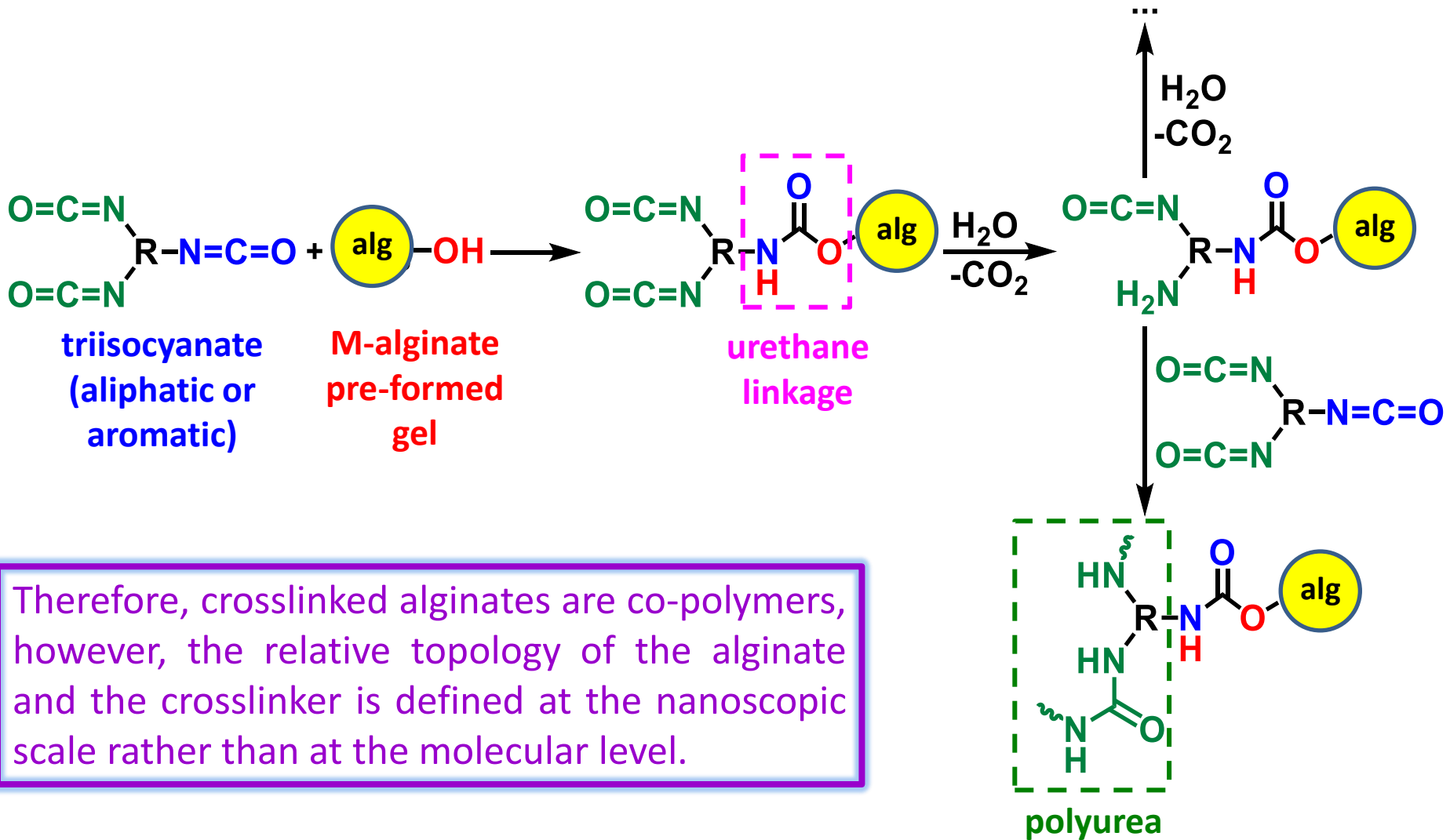


Crosslinking of M-alginate pre-formed gels with polyurea



urea
aliphatic
or
aromatic

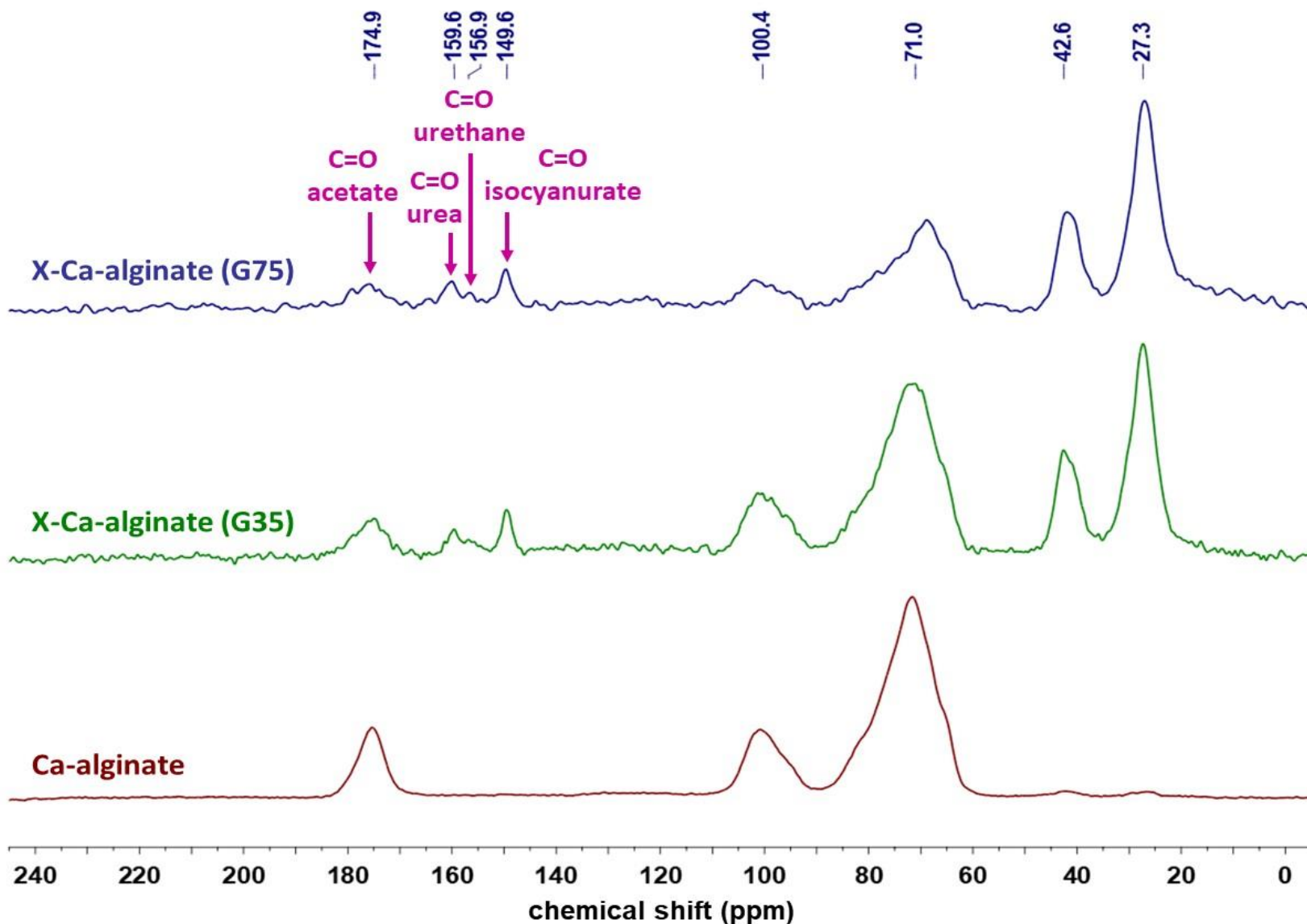
Crosslinking of M-alginate pre-formed gels with polyurea



Therefore, crosslinked alginates are co-polymers, however, the relative topology of the alginate and the crosslinker is defined at the nanoscopic scale rather than at the molecular level.

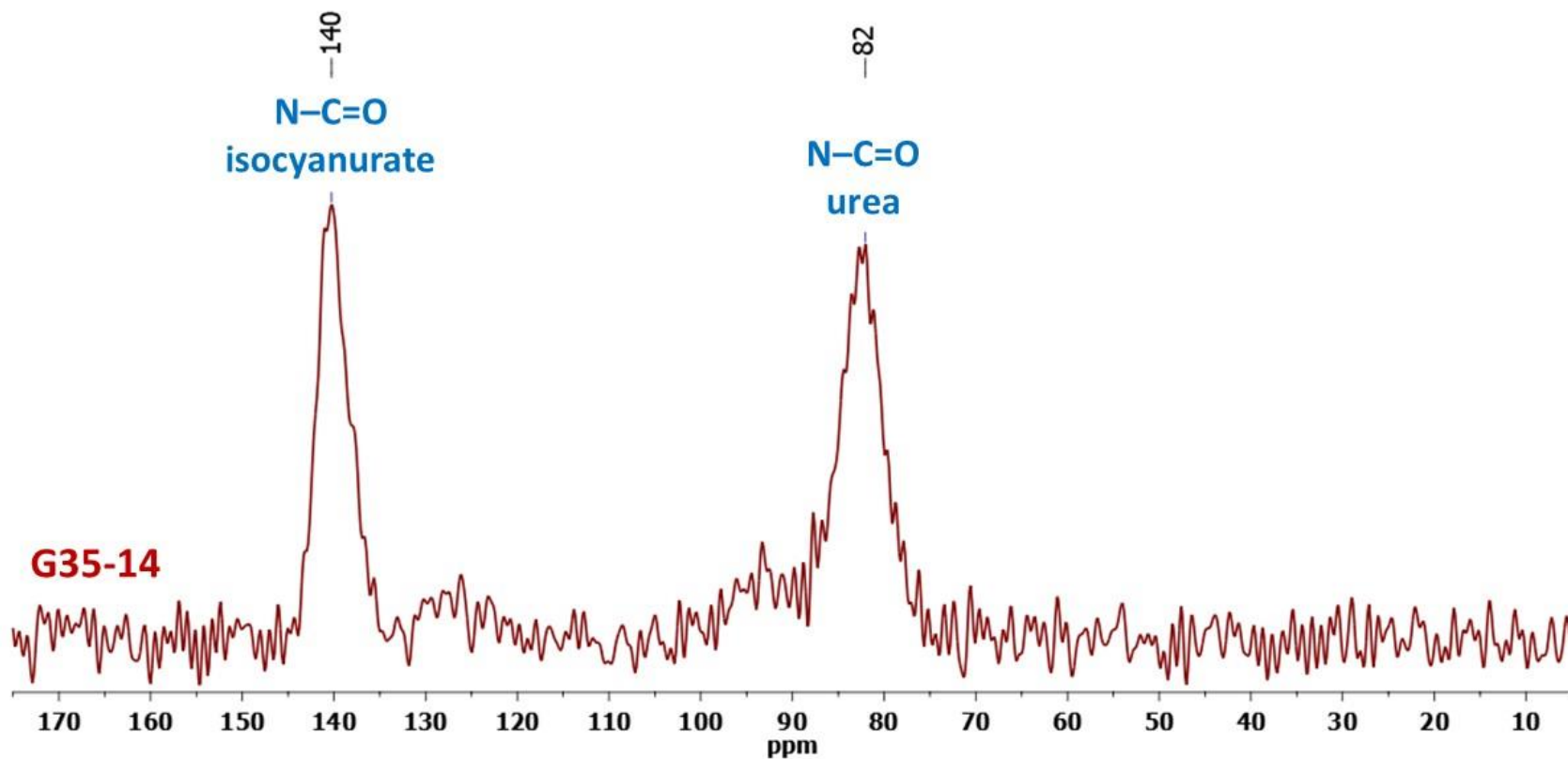
Chemical characterization of X-M-alginate aerogels

^{13}C CPMAS NMR



Chemical characterization of X-M-alginate aerogels

^{15}N CPMAS NMR

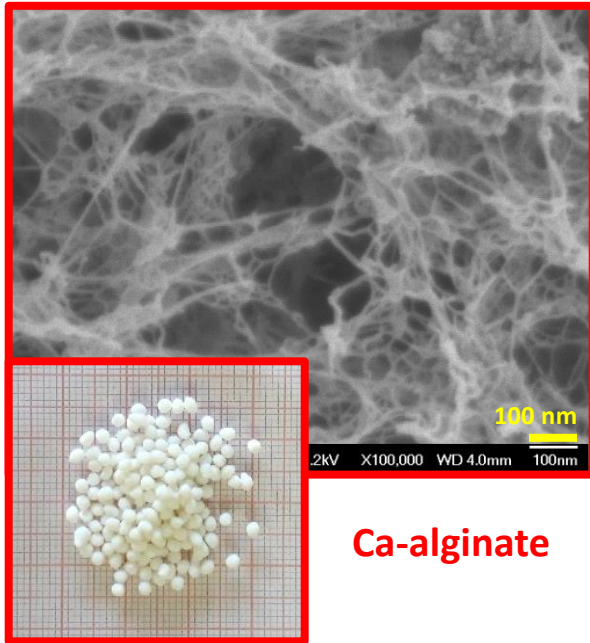


Selected material properties of X-M-alginate aerogels

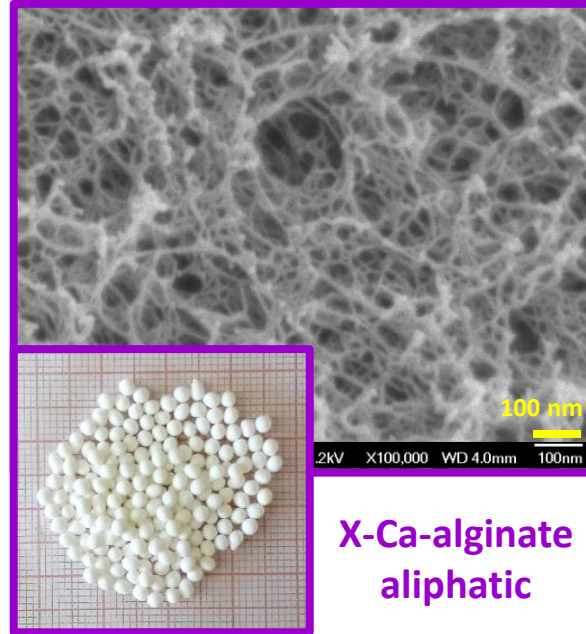
... vs. native M-alginate aerogels from the same Na-alginate concentration

- ➔ **Bulk density** is higher (0.06-0.18 g cm⁻³)
- ➔ **BET surface area** is lower (appr. 200-500 m² g⁻¹)
- ➔ **Porosity** is lower (89-96% v/v)
- ➔ **Young's modulus** is much higher (1.3-147 MPa)
(depends a lot on the G/M ratio of Na-alginate, and on [Na-alginate] and [triisocyanate])
- ➔ **Ultimate compressive strength** is much higher
as high as 700 MPa (at 0.18 g cm⁻³)
They are comparable to the best X-aerogels reported in the literature, e.g.,
X-silica (SiO₂-N3200): 190 MPa (at 0.48 g cm⁻³) and
X-vanadia (VO_x-N3200): 600 MPa (at 0.44 g cm⁻³)
- ➔ **Stability in natural waters (e.g., seawater)**

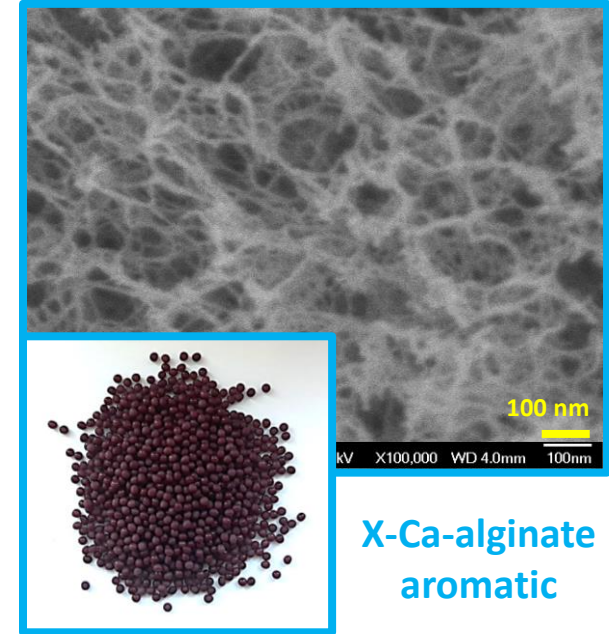
Morphology of X-Ca-alginate aerogels



Ca-alginate



X-Ca-alginate
aliphatic



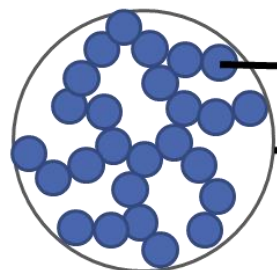
X-Ca-alginate
aromatic

- All samples, both native and crosslinked, are nanofibrous.
- Polyurea is confined on the skeletal network of the alginate.
- Therefore, the micromorphology remained the same.

Proposed nanoscale structure of Ca-alginate aerogels

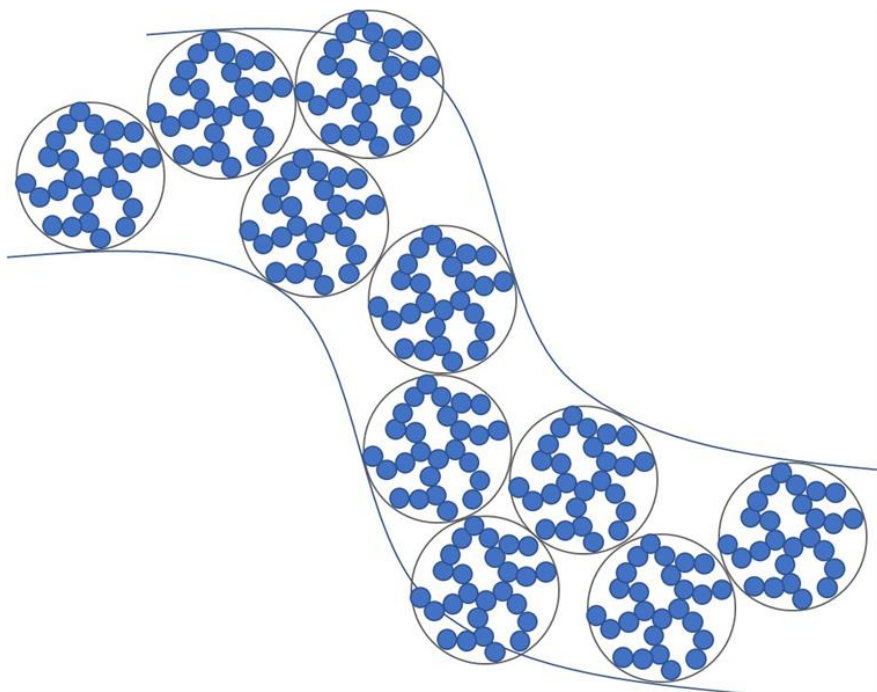
– via Small Angle Neutron Scattering (SANS)

Ca-alg



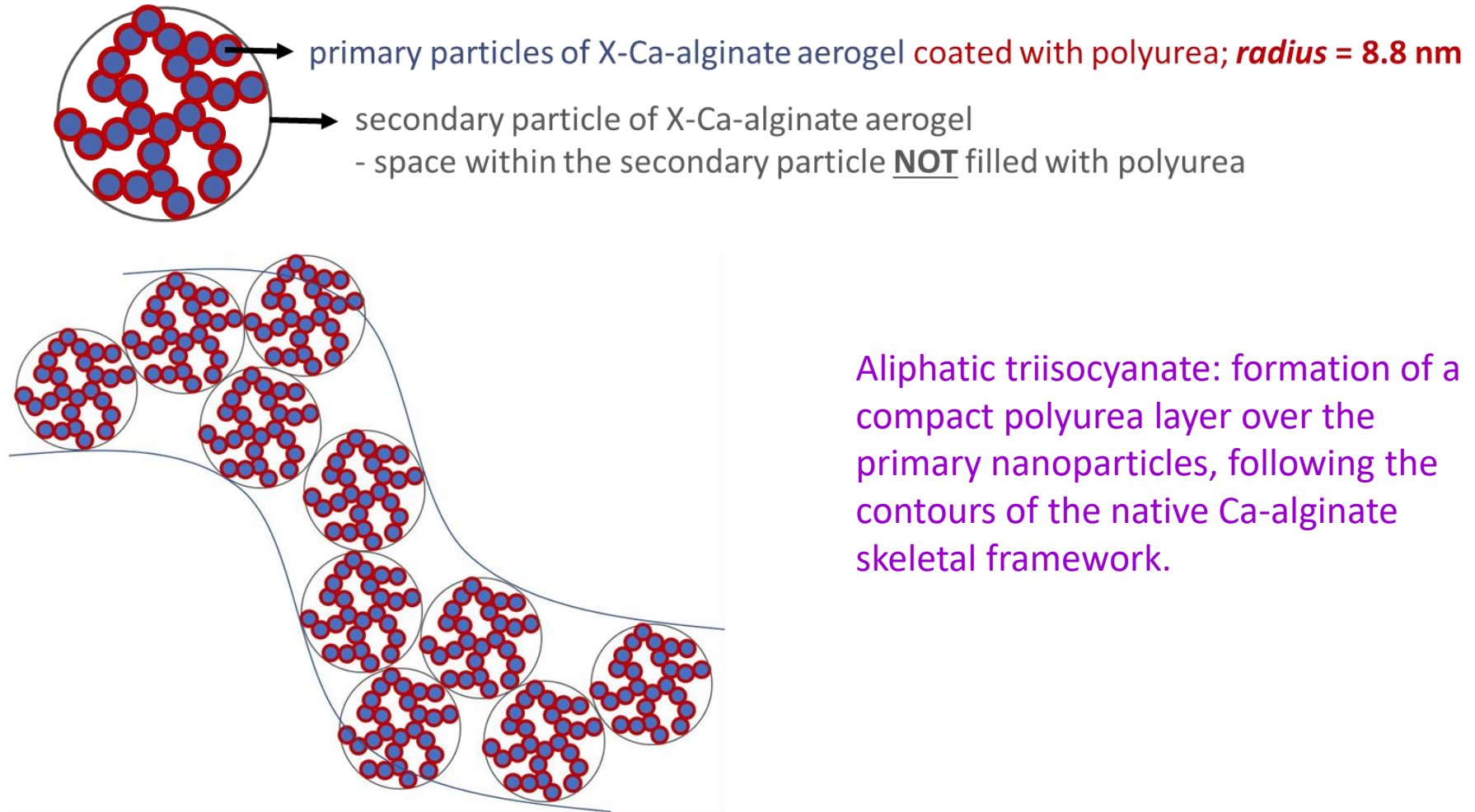
primary particle of Ca-alginate aerogel; *radius* = 8.3 nm

secondary particle of Ca-alginate aerogel



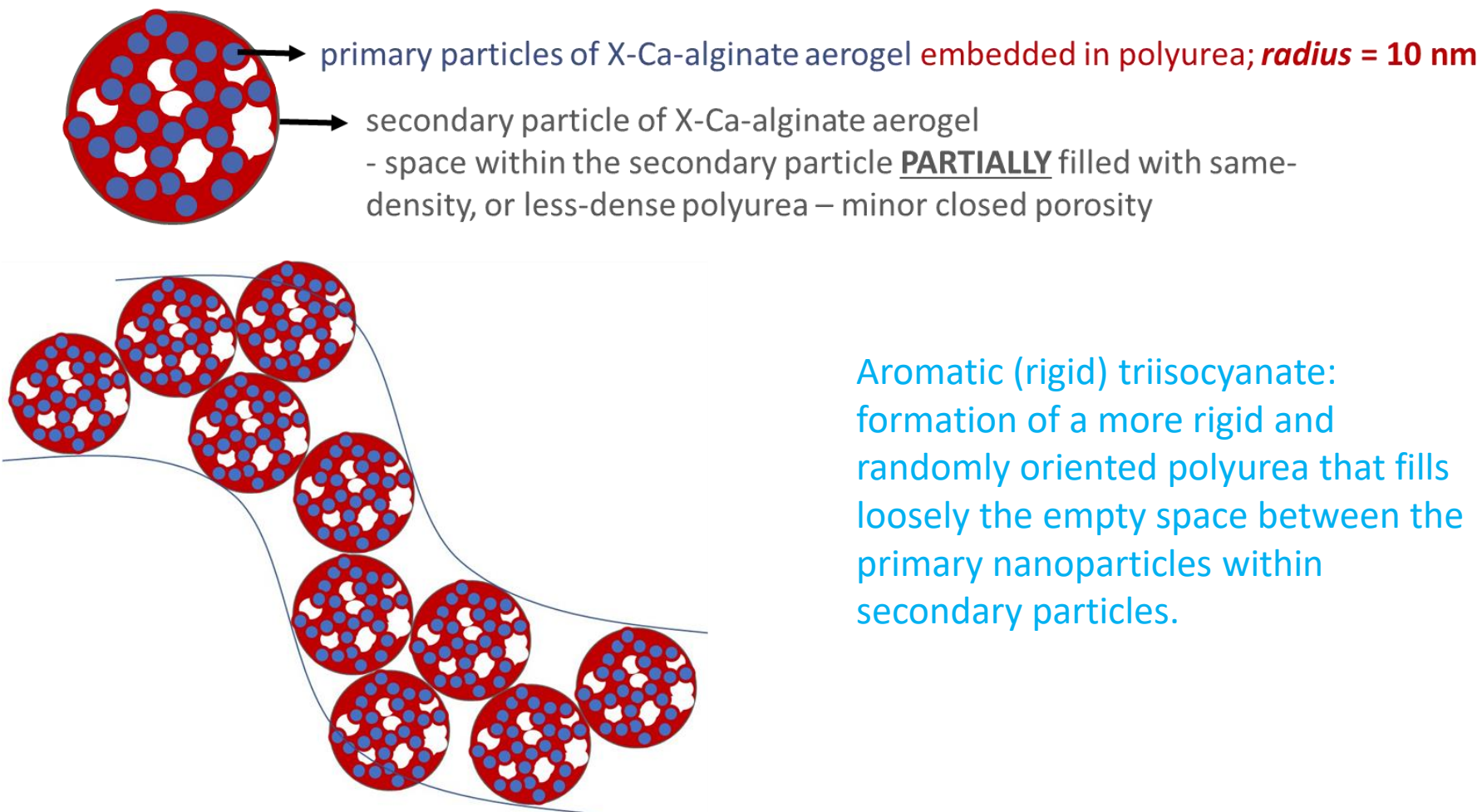
Proposed nanoscale structure of aliphatic X-Ca-alginate aerogels

– via SANS



Proposed nanoscale structure of aromatic X-Ca-alginate aerogels

– via SANS



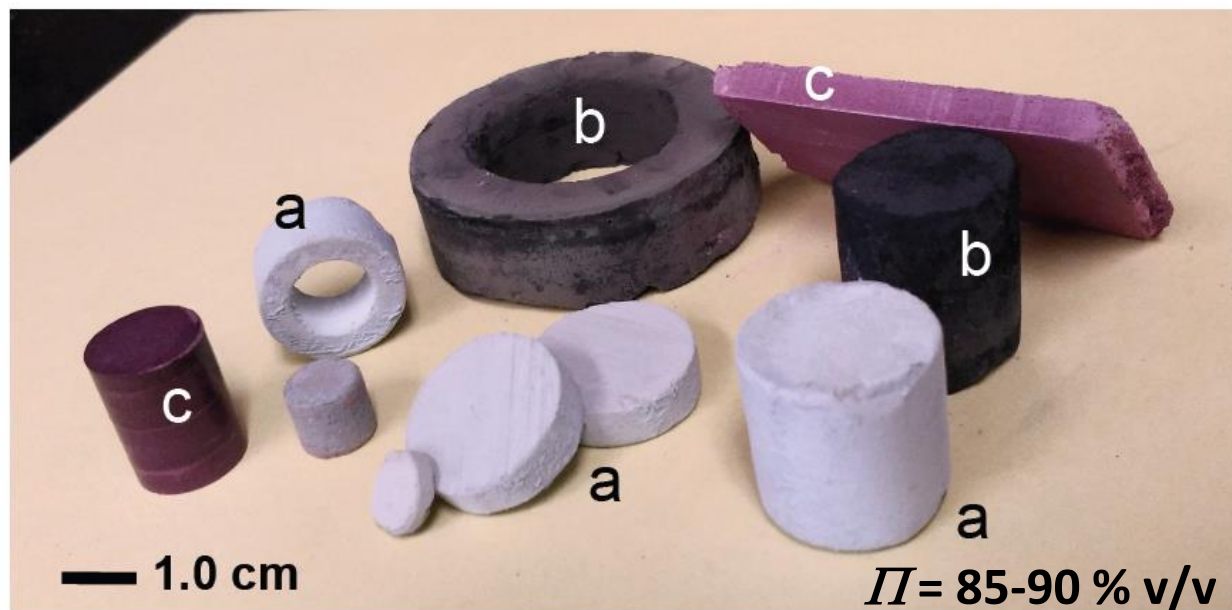
Applications of Polymer-Crosslinked (X-) Aerogels

1. Taking advantage of their mechanical strength:
 - in ballistic protection (armor)
 - seawater and wastewaters decontamination from organic solvents, diesel and selected heavy metals (Pb, Hg, U, Th, Eu)
2. Taking advantage of the intimate contact between the inorganic core and the polymer shell:
 - starting materials for ceramic, metal, C and graphite aerogels
3. Under optimal transparency, strength and thermal conductivity:
 - In daylighting (windows)
4. Since the mechanical properties of X-aerogels are dominated by the conformal polymer coating, nanoporous polymers with the structure and interparticle connectivity of X-aerogels should have similar properties

Applications of Polymer-Crosslinked (X-) Aerogels

Starting materials for monolithic ceramic aerogels

For example, SiC & Si₃N₄ aerogels from X-xerogel powder compacts



(a) SiC (b) Si₃N₄ (c) silica/polymer compact

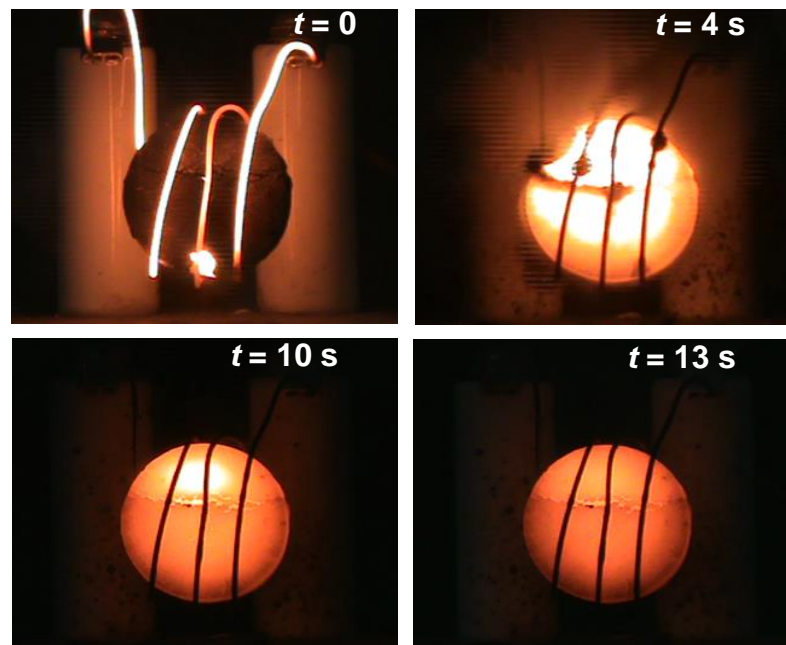
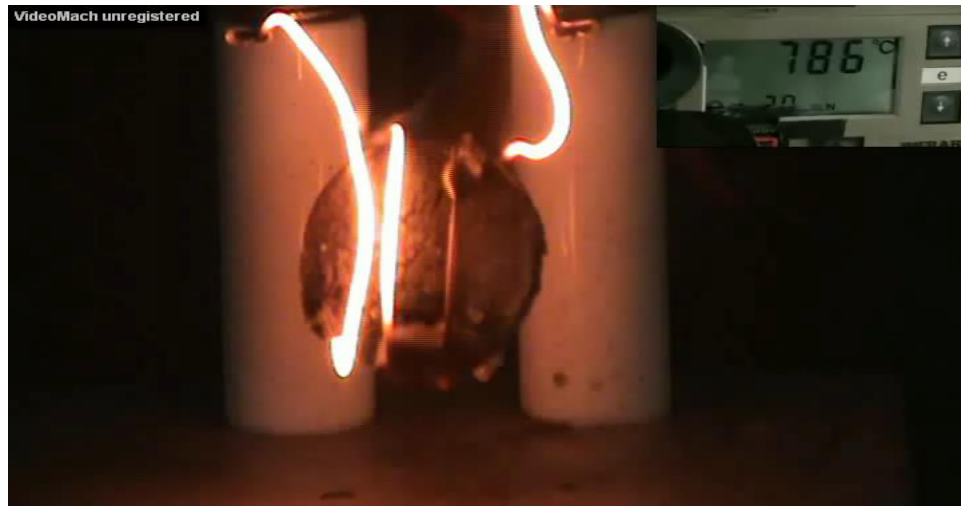


Applications of Polymer-Crosslinked (X-) Aerogels

Starting materials for monolithic ceramic aerogels

- Make metallic cobalt **aerogels** from **X-cobaltia xerogel powder compacts**
- Fill the porous space of cobalt aerogels with LiClO_4 from a melt
- The composite is a thermite reaching $>1500\text{ }^\circ\text{C}$

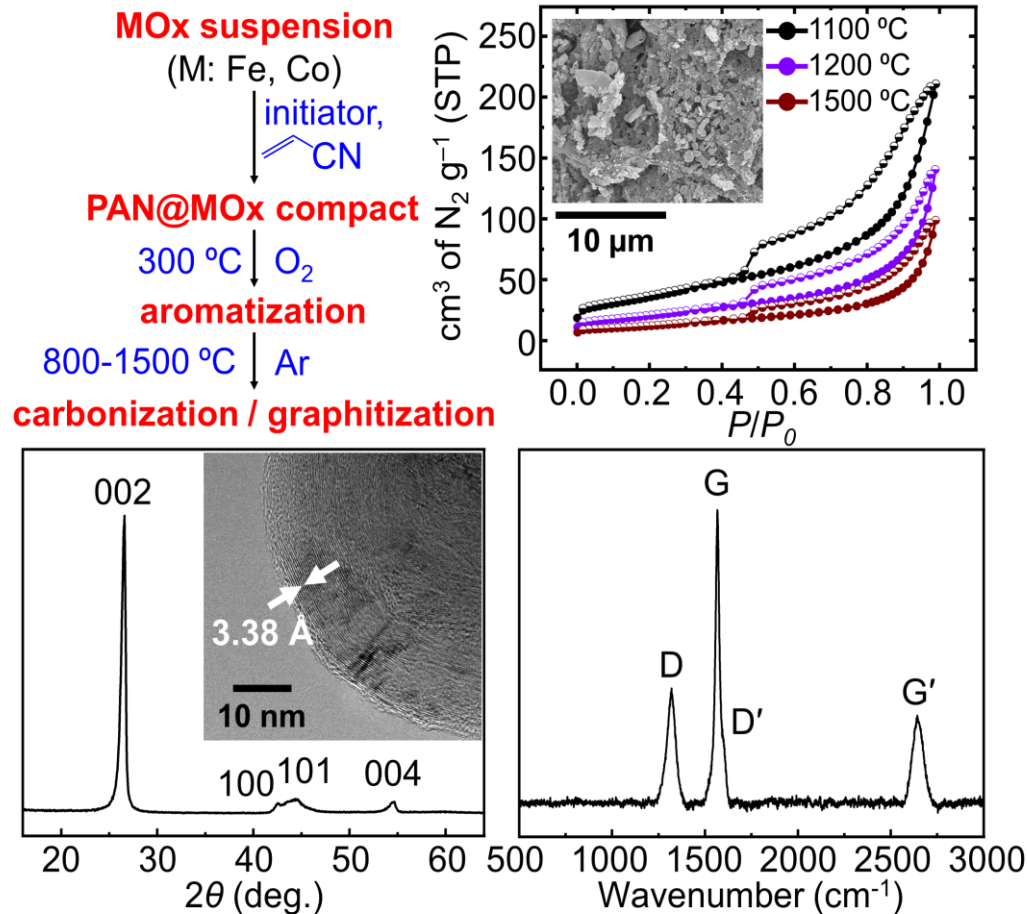
Ignition with an electric resistor



Applications of Polymer-Crosslinked (X-) Aerogels

Starting materials for carbon and graphite aerogels

- Formulate **X-xerogel compacts** to produce carbon in excess over MO_x
- After pyrolysis, remove the inorganic component with acid



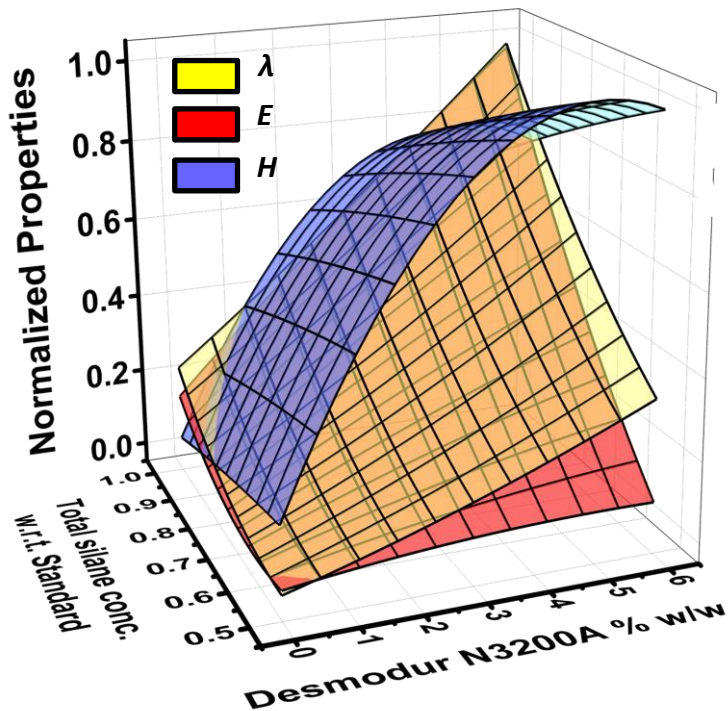
From **X-iron oxide**
or **X-cobaltia**
graphite **aerogels**

Applications of Polymer-Crosslinked (X-) Aerogels

In daylighting (windows) with X-silica aerogels

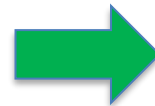
X-aerogels must be:

- ✓ Thermally Insulating
- ✓ Mechanically Strong
- ✓ Transparent



direct view

through an X-aerogel



Good sample:

$$\lambda = 22.5 \pm 0.8 \text{ mW m}^{-1} \text{ K}^{-1}$$

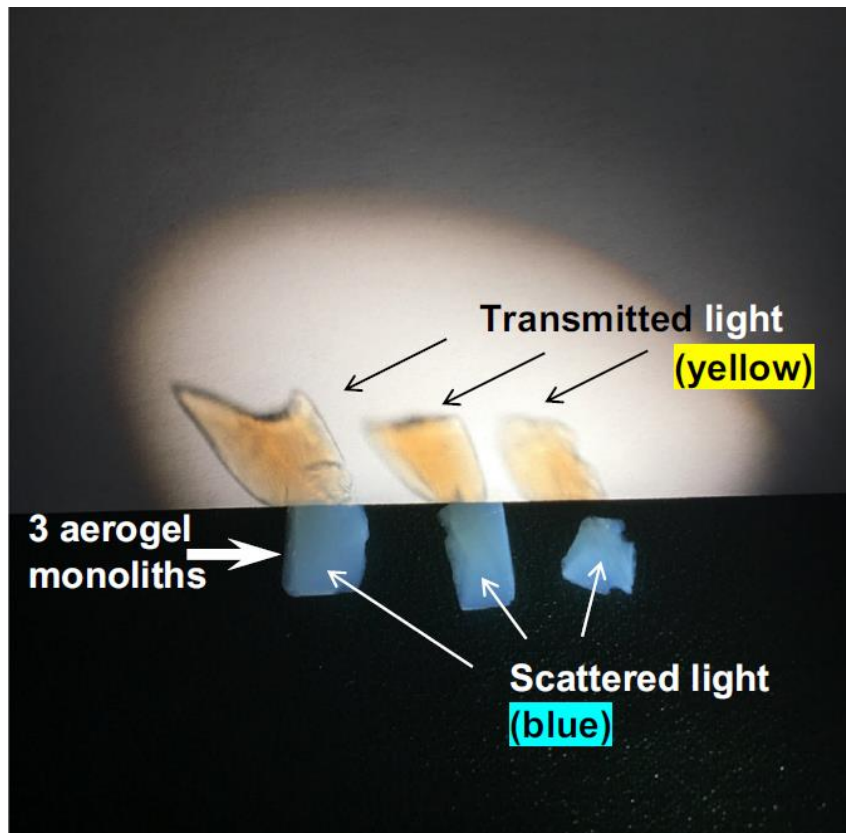
$$E = 70.29 \pm 2.94 \text{ MPa}$$

$$H = 10.5 \%$$

Applications of Polymer-Crosslinked (X-) Aerogels

In daylighting (windows) with X-silica aerogels

... blue is filtered off by
Rayleigh scattering



direct view

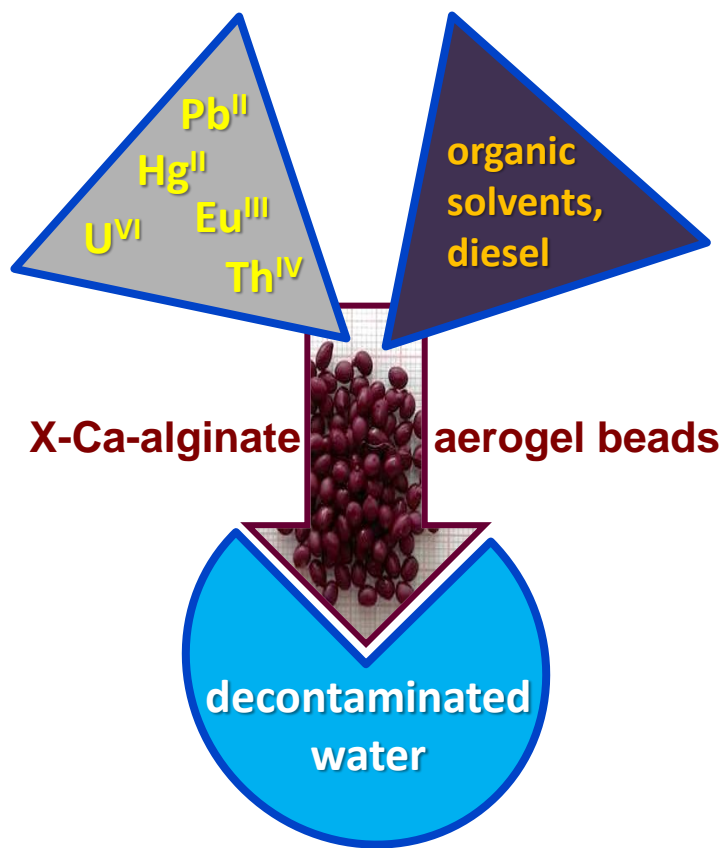
through an X-aerogel



Applications of Polymer-Crosslinked (X-) Aerogels

Environmental remediation with X-biopolymer aerogels

Seawater decontamination from organic solvents, oils and metal ions

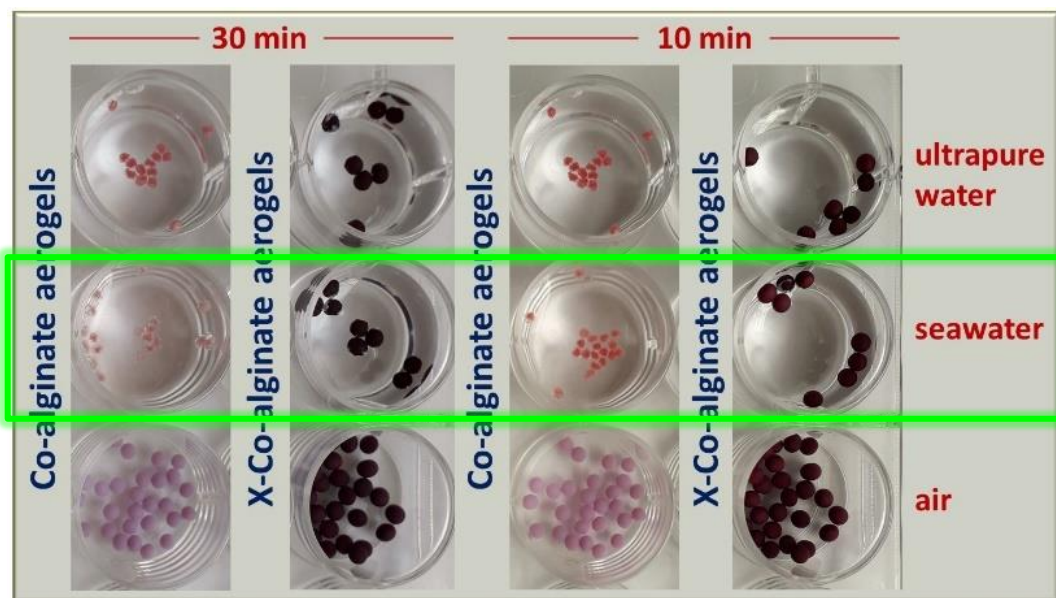
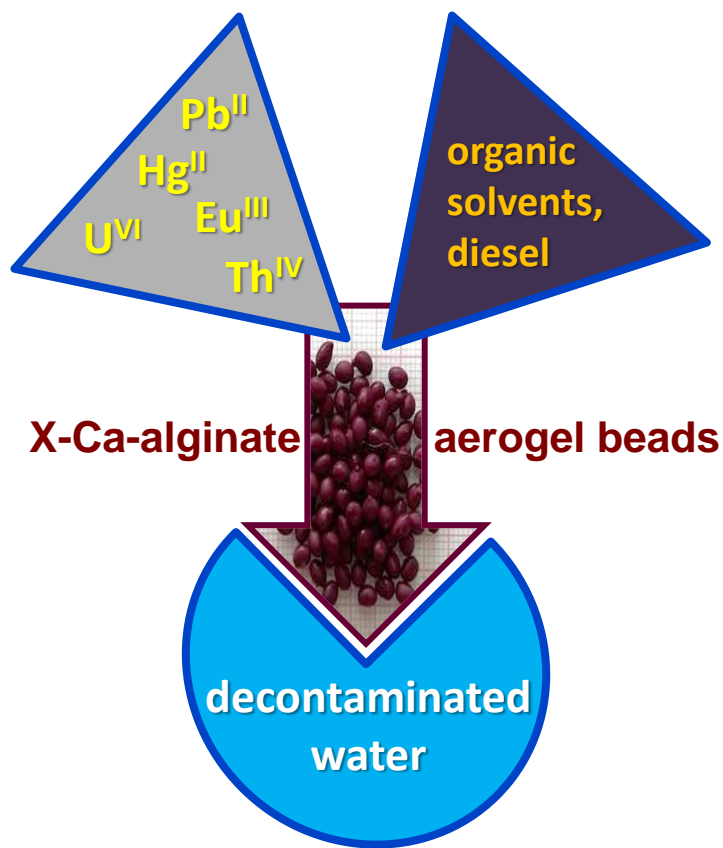


*high mechanical strength,
high stability in natural waters*

Applications of Polymer-Crosslinked (X-) Aerogels

Environmental remediation with X-biopolymer aerogels

Seawater decontamination from organic solvents, oils and metal ions

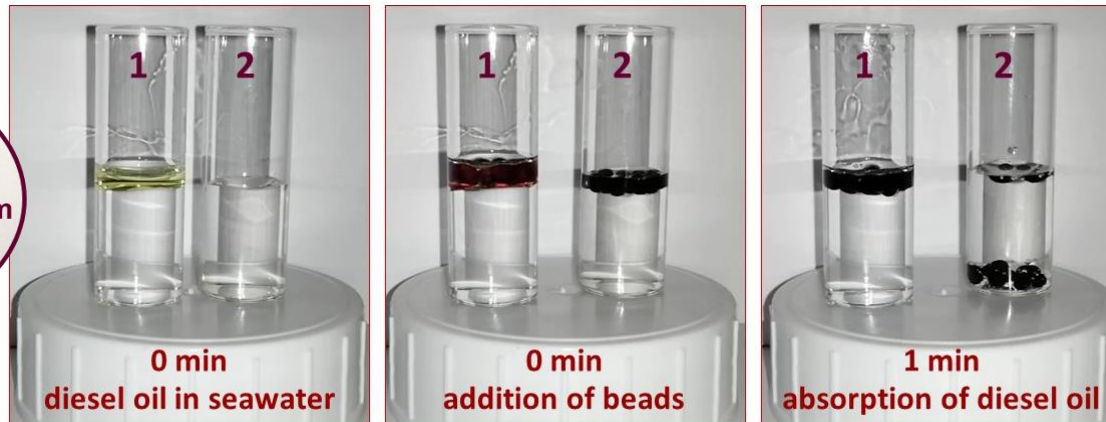
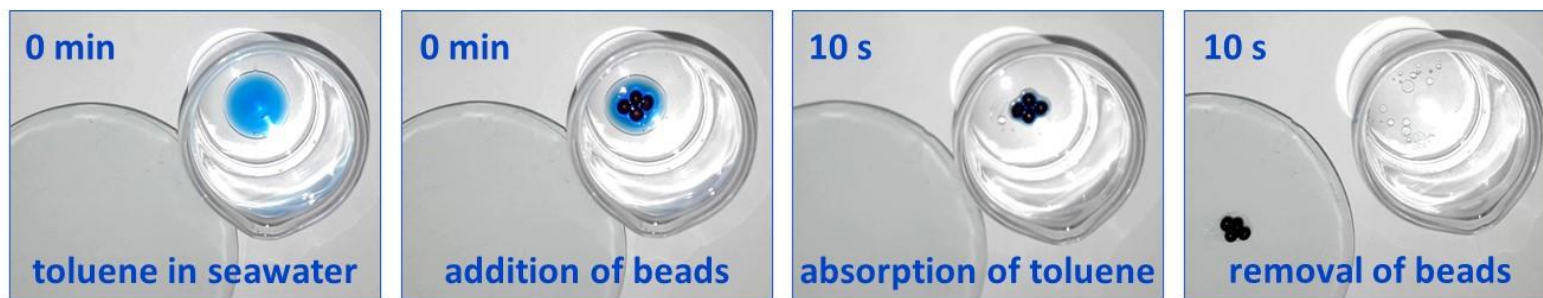


*high mechanical strength,
high stability in natural waters*

Applications of Polymer-Crosslinked (X-) Aerogels

Environmental remediation with X-biopolymer aerogels

Seawater decontamination from organic solvents and oils

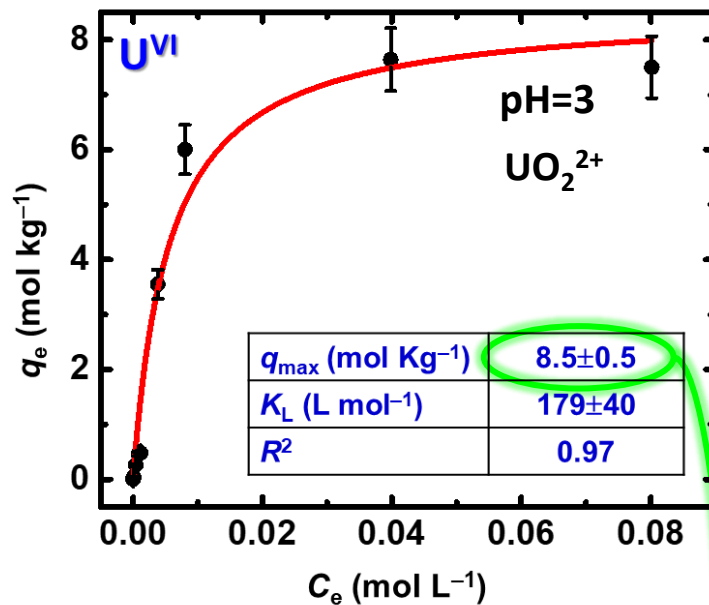
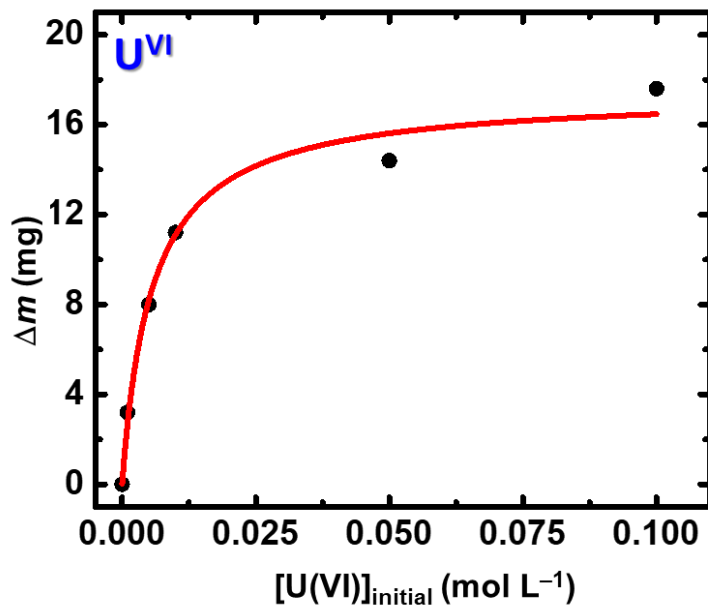


No desorption (leak) from the beads to the aqueous phase was observed even after 3 h.

Applications of Polymer-Crosslinked (X-) Aerogels

Environmental remediation with X-biopolymer aerogels

Water decontamination from U^{VI}

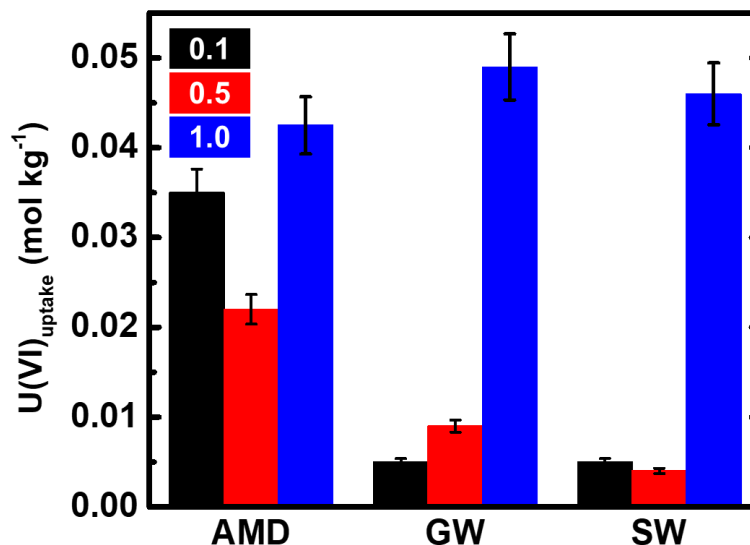


2000 g kg⁻¹
twice the mass
of the beads!!!

Applications of Polymer-Crosslinked (X-) Aerogels

Environmental remediation with X-biopolymer aerogels

Seawater and wastewater decontamination from U^{VI}



X-Ca-alginate: 0.1, 0.5, 1.0 g L^{-1}

AMD: acid mine drainage (pH=3)

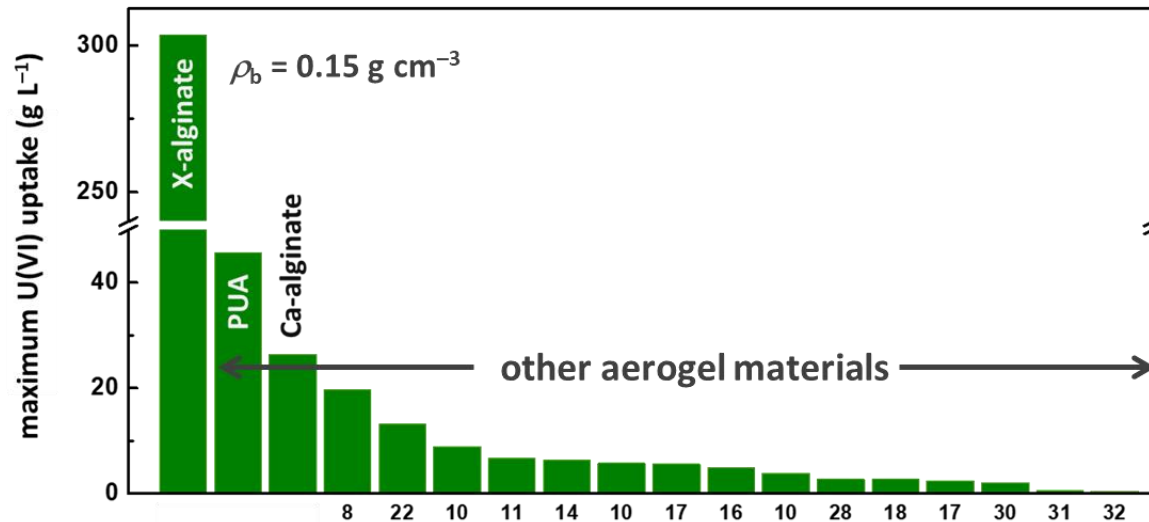
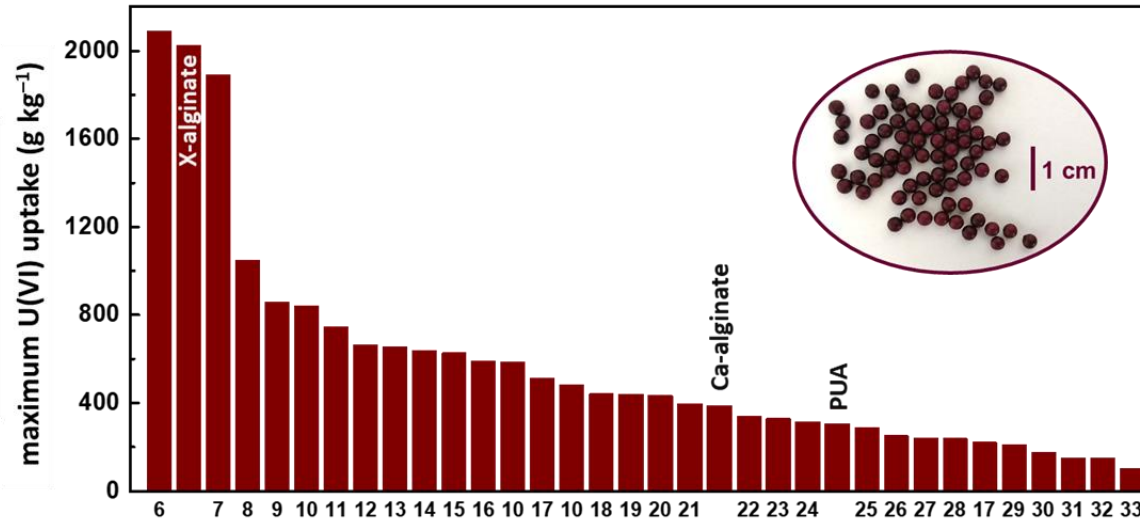
GW: ground water (pH=7.8)

SW: seawater (pH=8.3)

Applications of Polymer-Crosslinked (X-) Aerogels

Environmental remediation with X-biopolymer aerogels

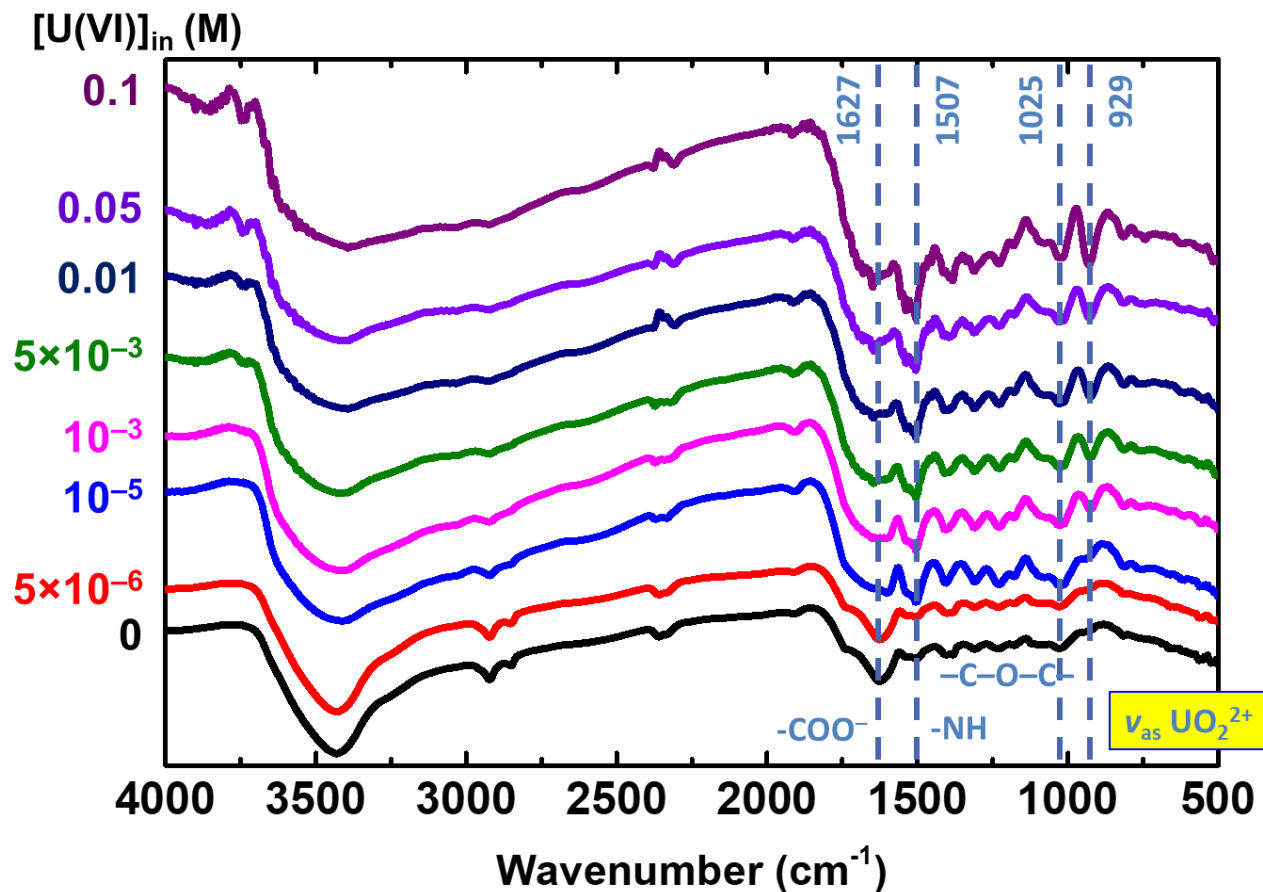
Water decontamination from U^{VI}



Applications of Polymer-Crosslinked (X-) Aerogels

Environmental remediation with X-biopolymer aerogels

Water decontamination from U^{VI}

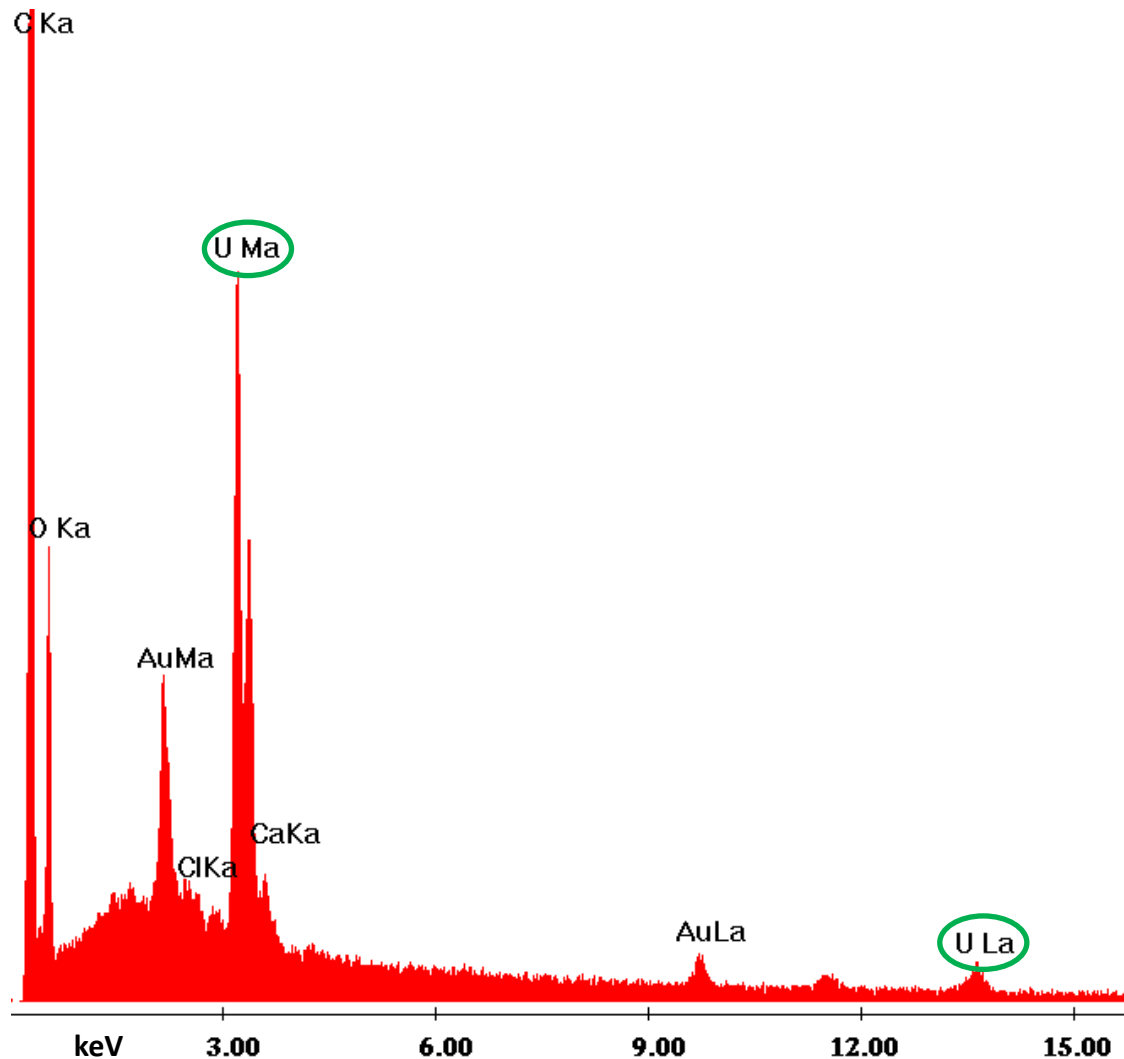


Applications of Polymer-Crosslinked (X-) Aerogels

All-polymer and carbon aerogels inspired by X-aerogels

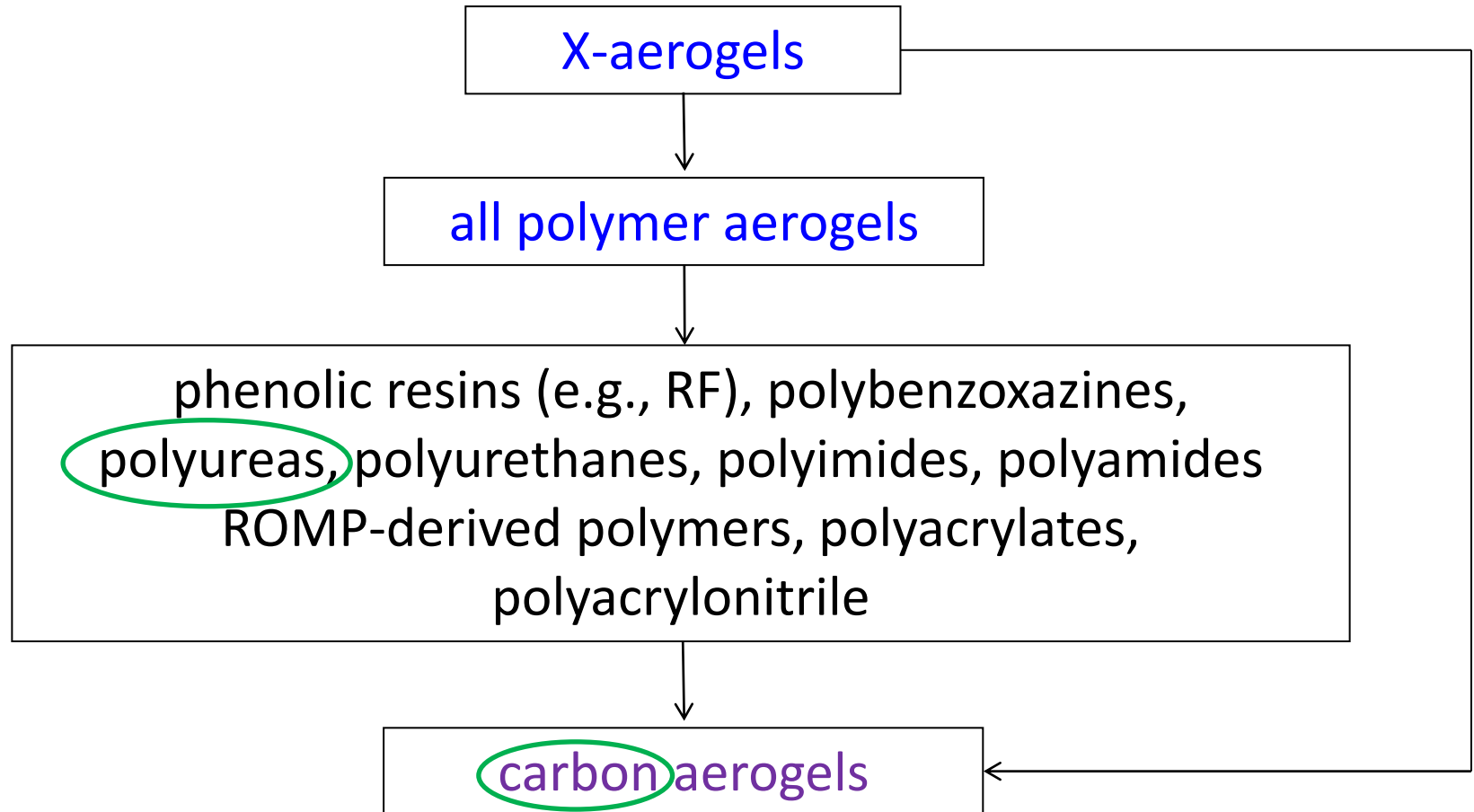
Water decontamination from U^{VI}

Energy Dispersive
Spectroscopy
(EDS)



Applications of Polymer-Crosslinked (X-) Aerogels

All-polymer and carbon aerogels inspired by X-aerogels



Applications of Polymer-Crosslinked (X-) Aerogels

Metal and N-doped carbons from X-biopolymer aerogels

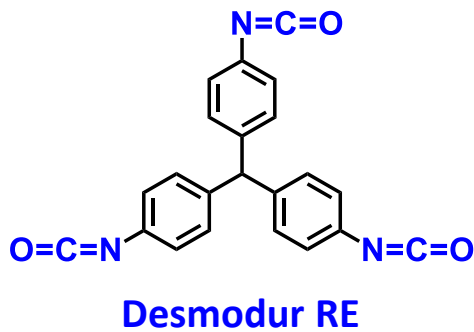
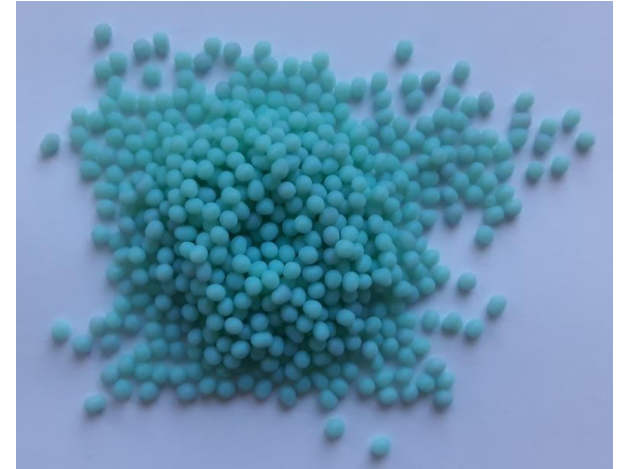
Co-alginate



Ni-alginate



Cu-alginate



X-linking with
a carbonizable
trisocyanate

X-M-alginate



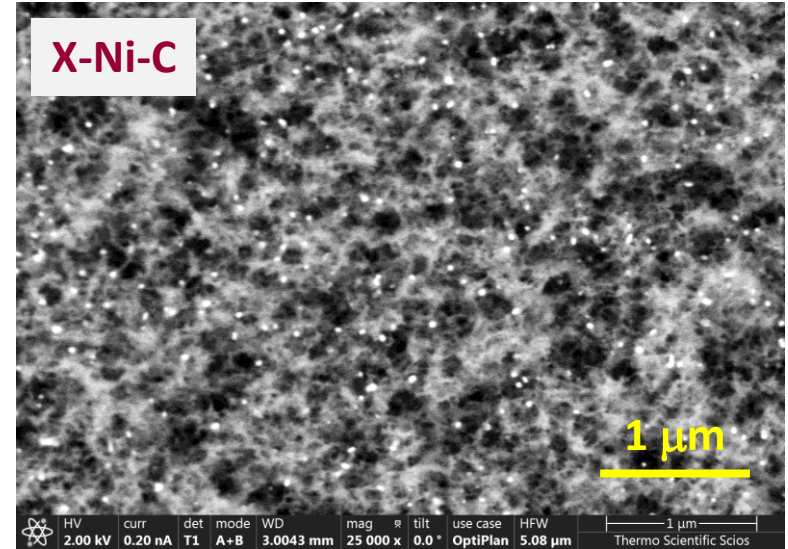
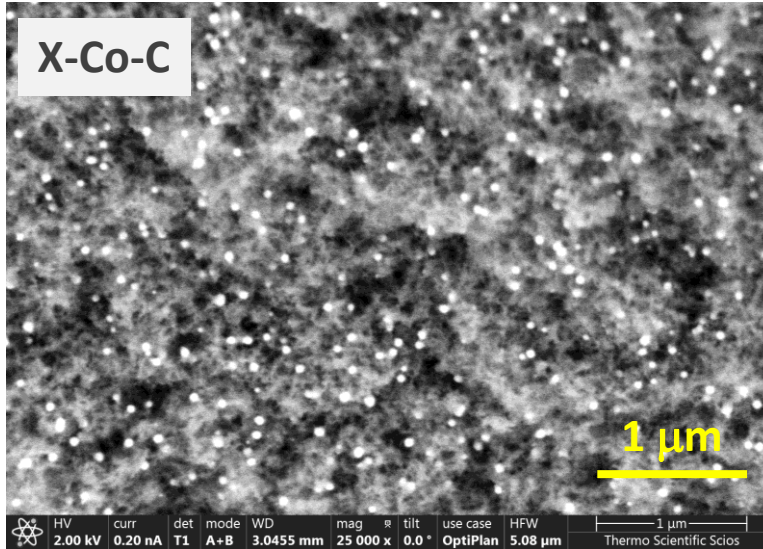
pyrolysis
under Ar

X-M-C

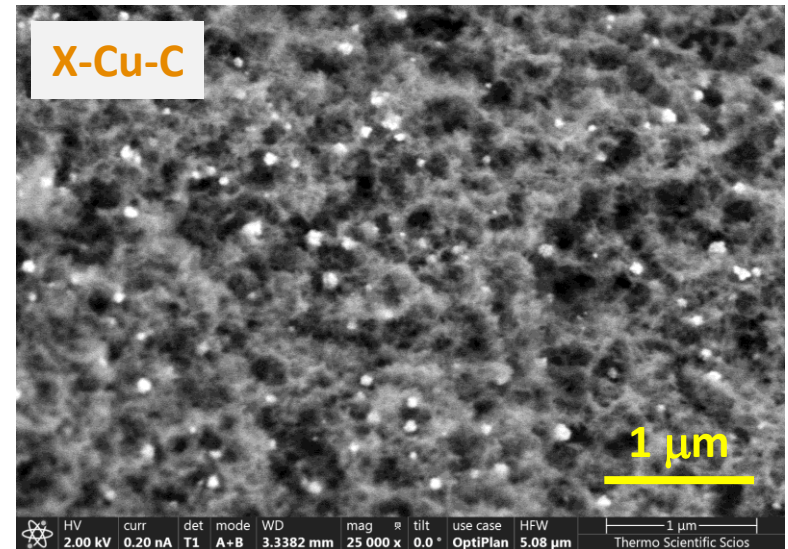


Applications of Polymer-Crosslinked (X-) Aerogels

Metal and N-doped carbons from X-biopolymer aerogels



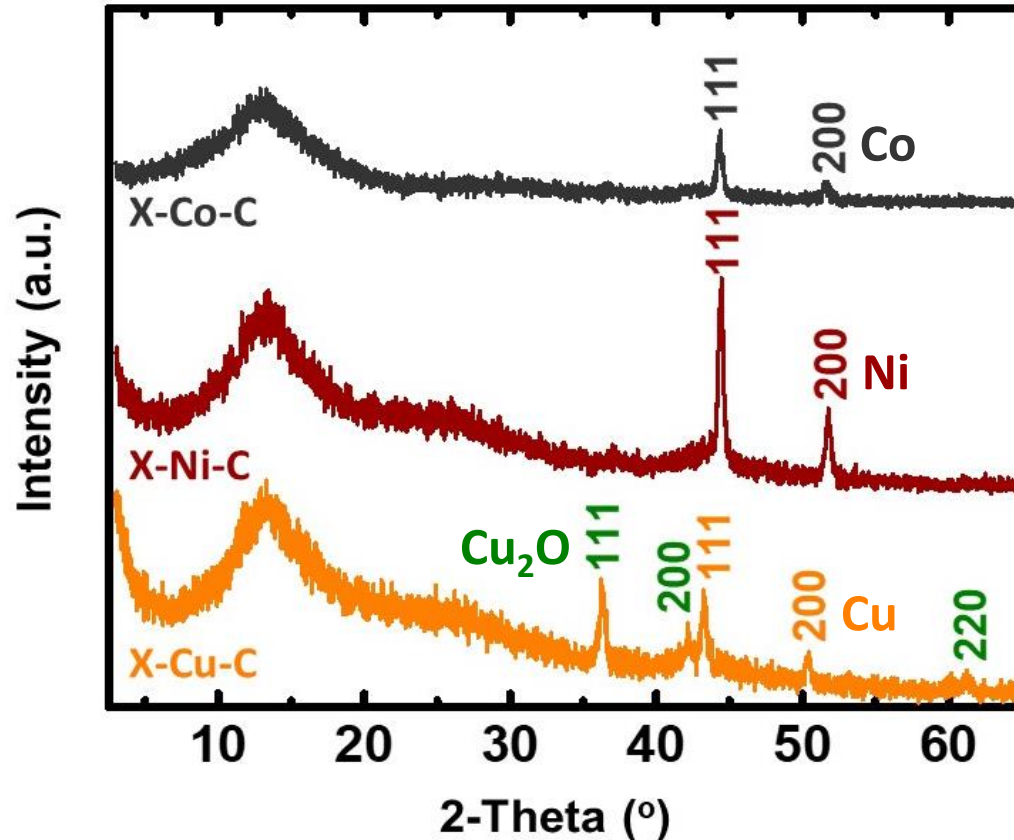
Focused Ion Beam
Scanning Electron
Microscopy
(FIB-SEM)



Applications of Polymer-Crosslinked (X-) Aerogels

Metal and N-doped carbons from X-biopolymer aerogels

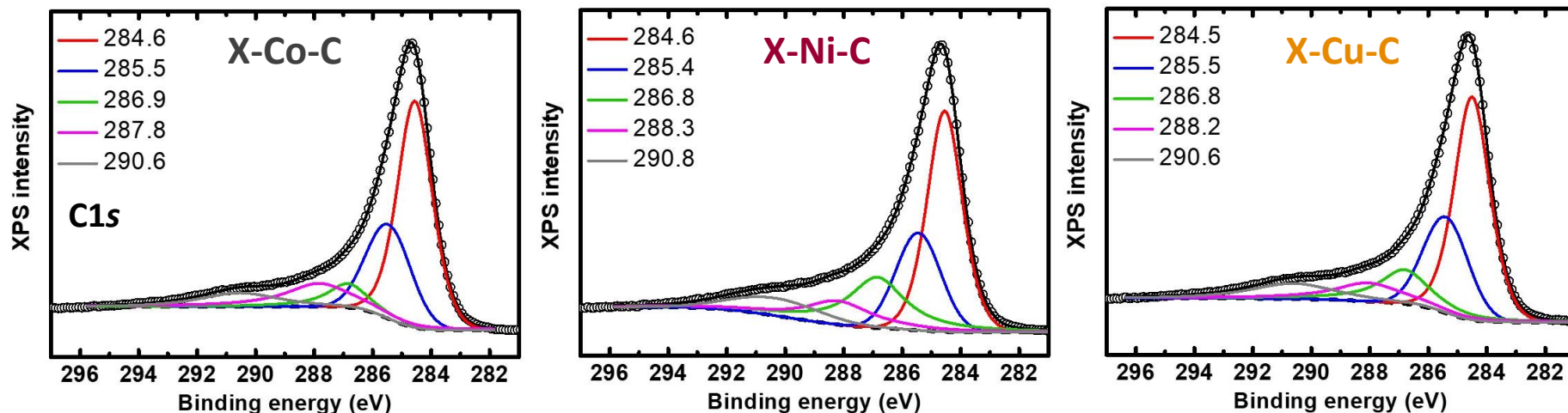
X-Ray Diffraction
(XRD)



The crystallite sizes were calculated at around 22 nm for all three metals.

Applications of Polymer-Crosslinked (X-) Aerogels

Metal and N-doped carbons from X-biopolymer aerogels

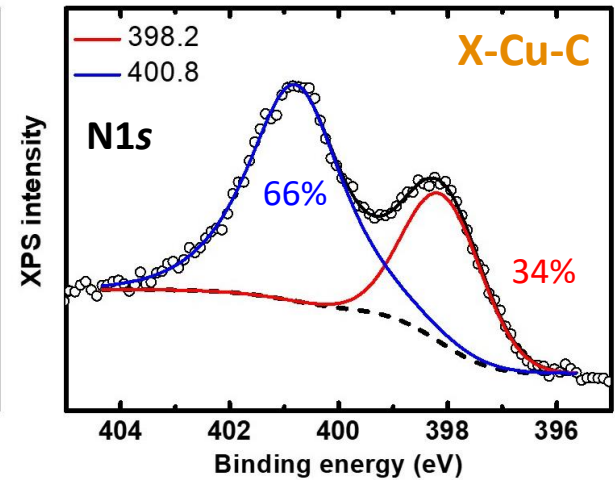
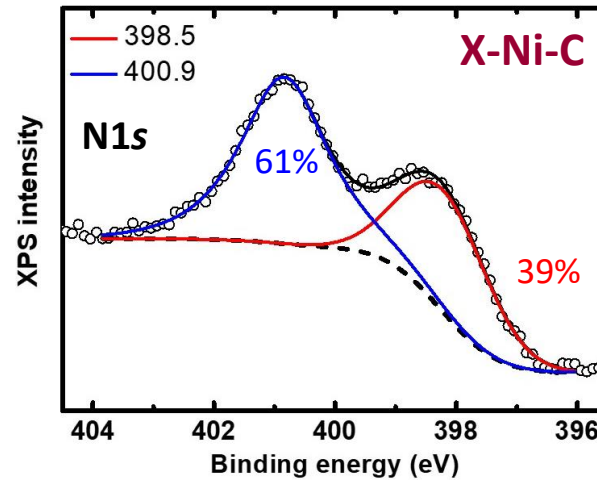
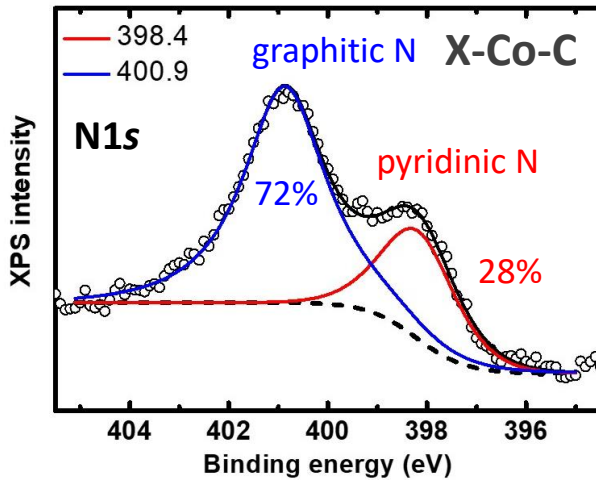


	Peak max. (eV)	X-Co-C	X-Ni-C	X-Cu-C
sp^2 C	284.5-284.6	47.70	39.84	45.00
sp^3 C	285.4-285.5	24.06	21.18	23.18
sp^2/sp^3		1.98	1.88	1.94
C-(O,N)	286.8-286.9	8.31	20.07	13.71
C=O	287.8-288.3	13.04	11.29	10.07
$\pi \rightarrow \pi^*$	290.6-290.8	7.97	7.62	8.03

X-Ray
Photoelectron
Spectroscopy
(XPS)

Applications of Polymer-Crosslinked (X-) Aerogels

Metal and N-doped carbons from X-biopolymer aerogels



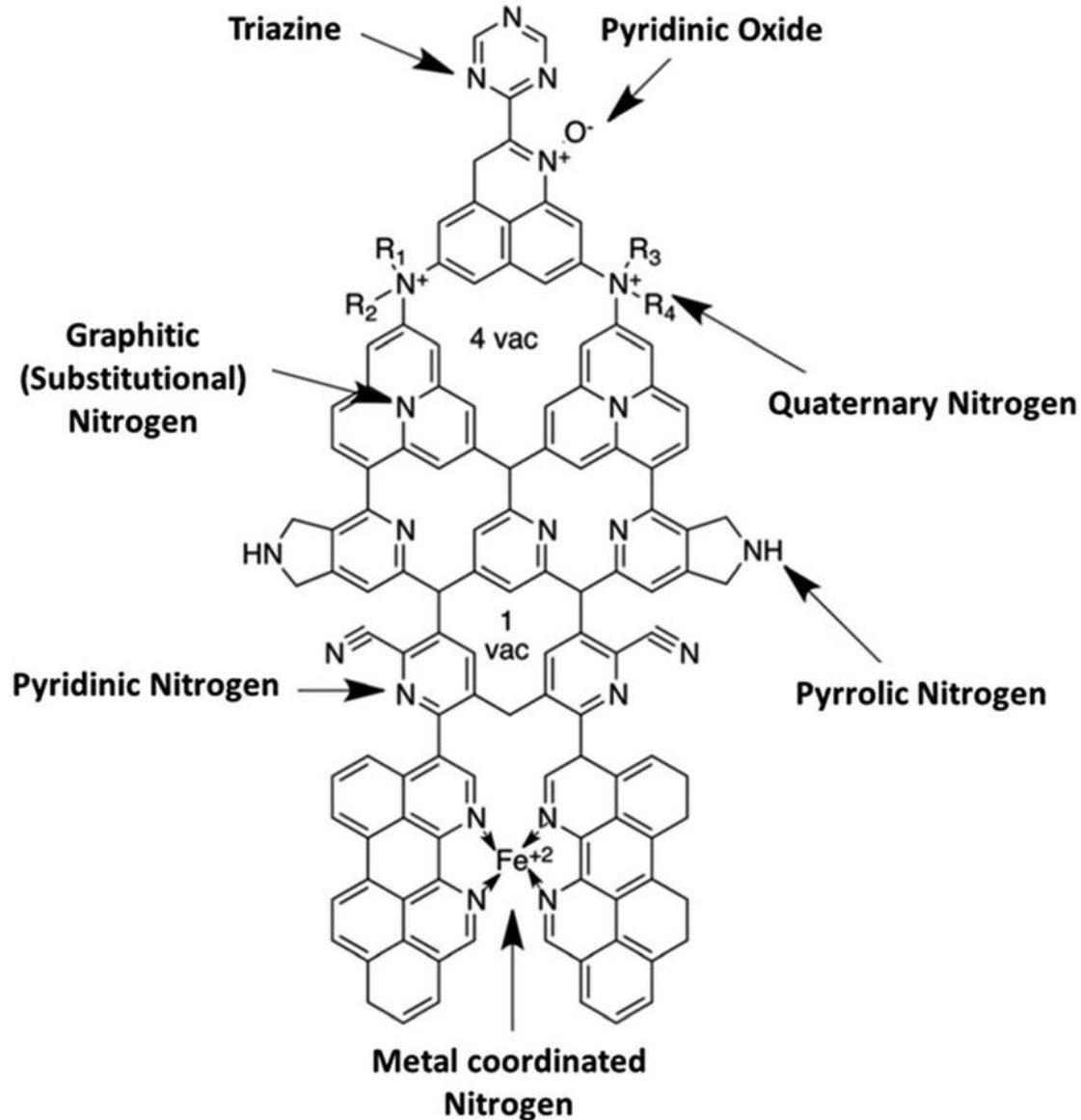
X-Ray
Photoelectron
Spectroscopy
(XPS)

Graphitic and pyridinic N are considered as active sites for the oxygen reduction reaction (ORR), while other N species (e.g., pyrrolic N) have a disputable role in the ORR.

Therefore, it is considered positive that X-M-C aerogels show only graphitic and pyridinic N, as opposed to most alginate-derived carbons from the literature.

Applications of Polymer-Crosslinked (X-) Aerogels

N-functionalities



Tuning the Nanomorphology of Aerogels

Polyurea aerogels

Triisocyanate + water + Et₃N
in anhydrous solvent

stir, 23 °C, 5 min

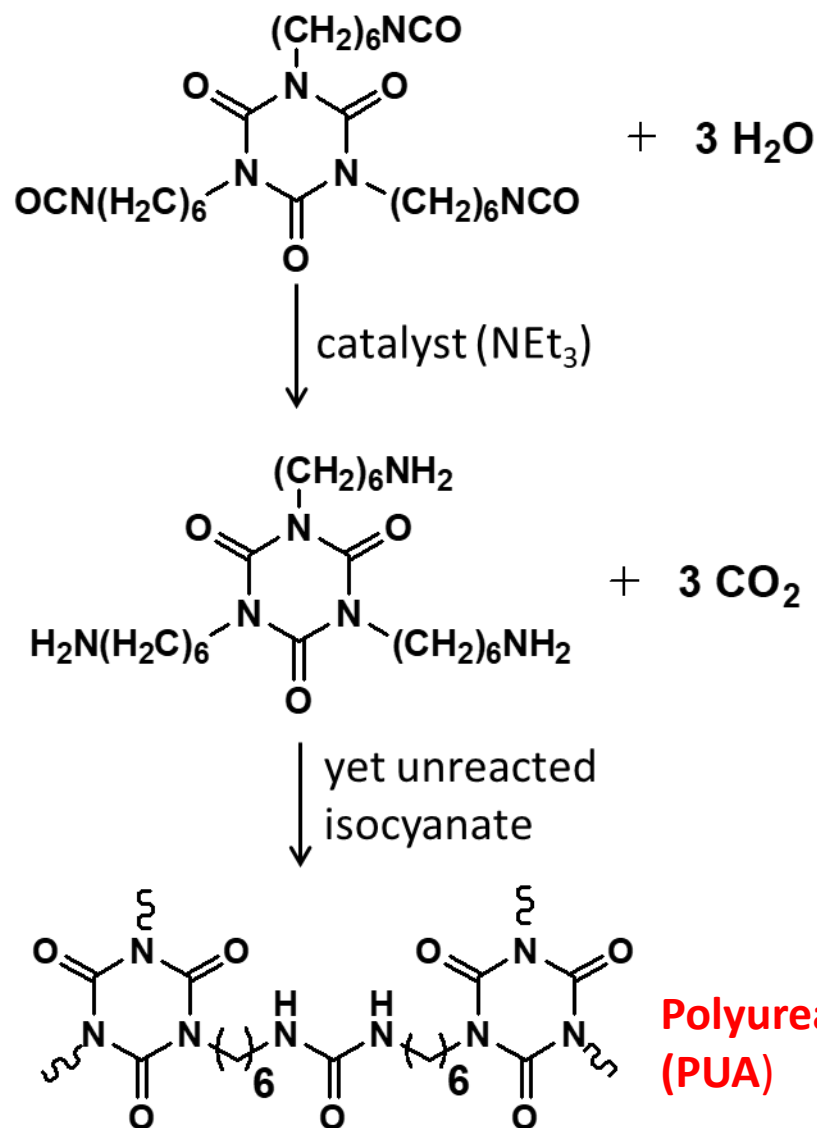
sol

pour in molds

PUA wet-gels

1. age, 23 °C, 24 h
2. wash with acetone, 4×8 h
3. dry with SCF CO₂

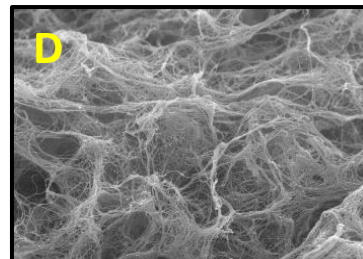
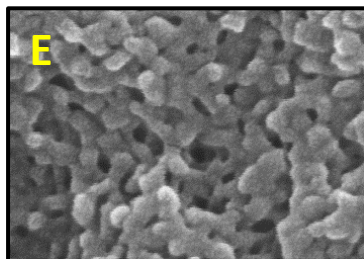
PUA aerogels



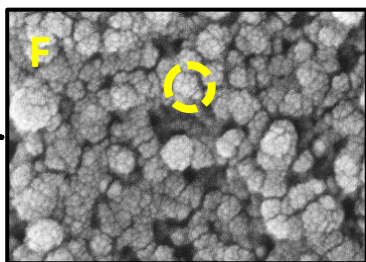
Tuning the Nanomorphology of Aerogels

Polyurea aerogels display rich & complex nanomorphology

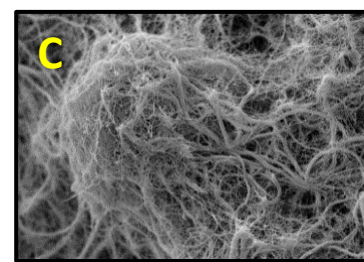
assembly
of fused
nanoparticles



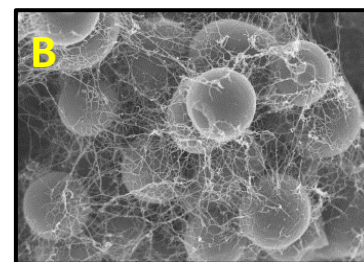
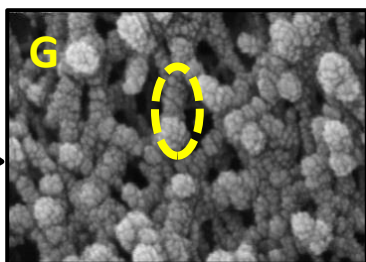
entangled
nanofibers



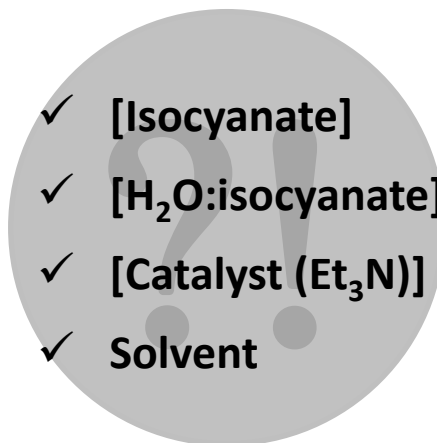
strings of
particles



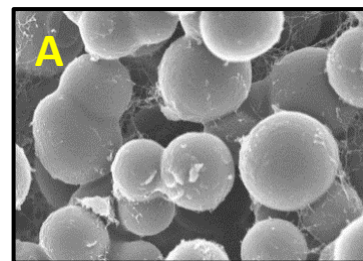
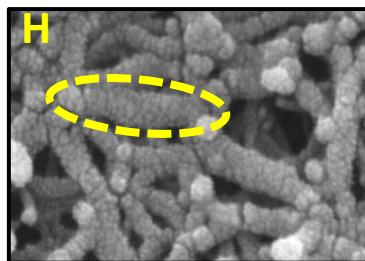
spheres
embedded
in fibers



micro-
spheres
in web



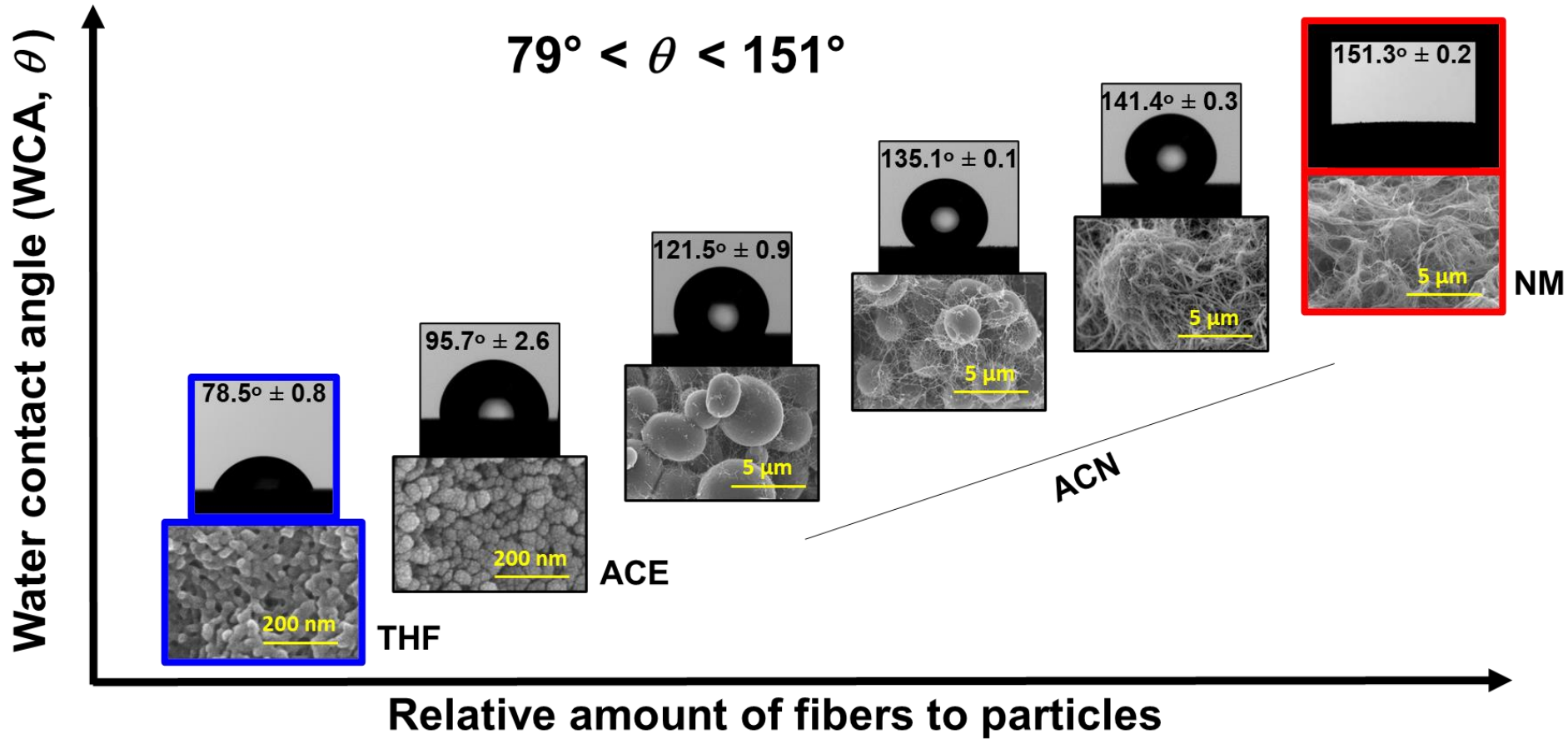
caterpillars
of nanoparticles



bald
microspheres

Tuning the Nanomorphology of Aerogels

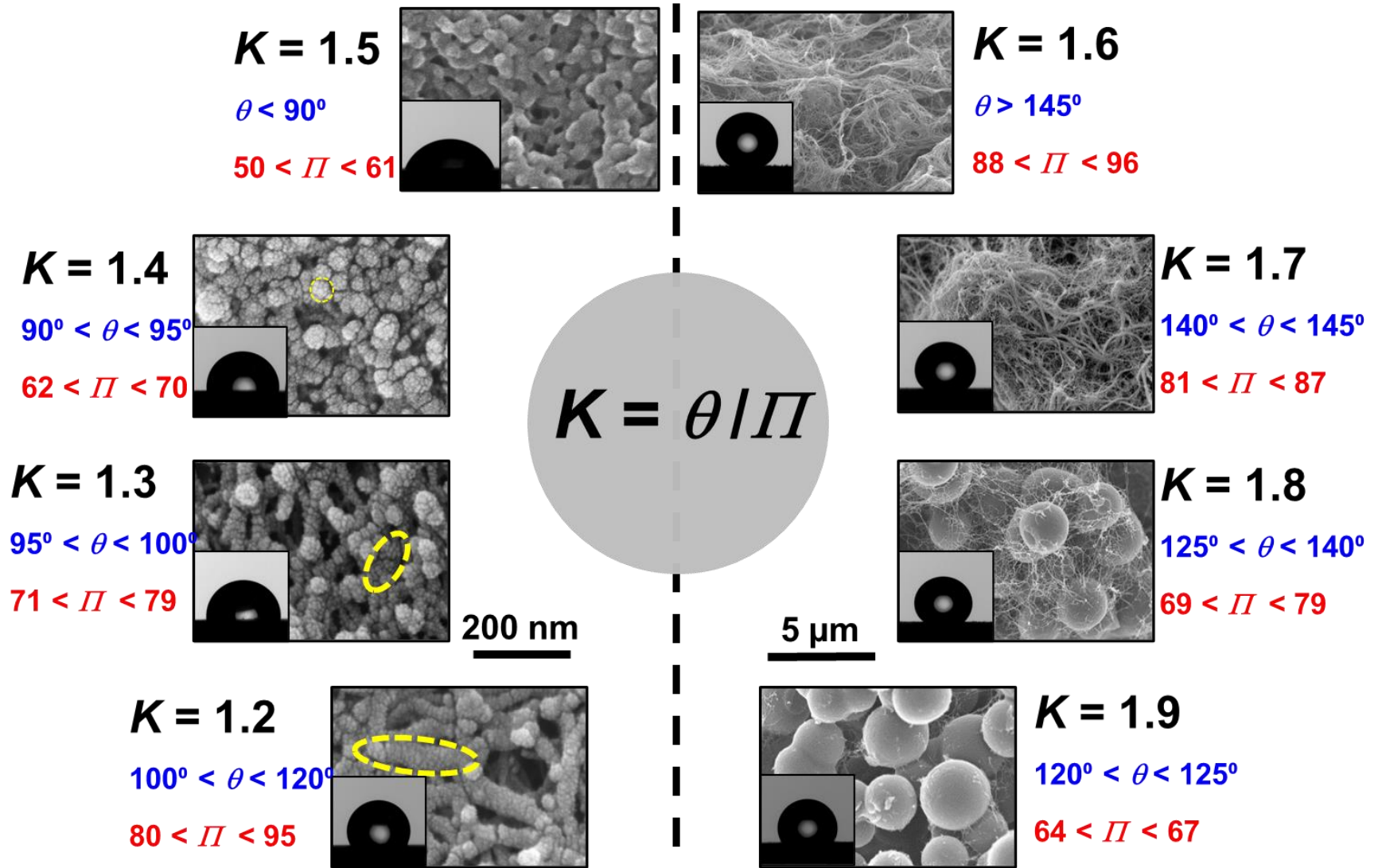
Water contact angle (θ) on PUA aerogels as a function of texture



Cassie-Baxter state, where water droplets touch only the apices of the surface roughness.

Tuning the Nanomorphology of Aerogels

Nanomorphology/properties correlation



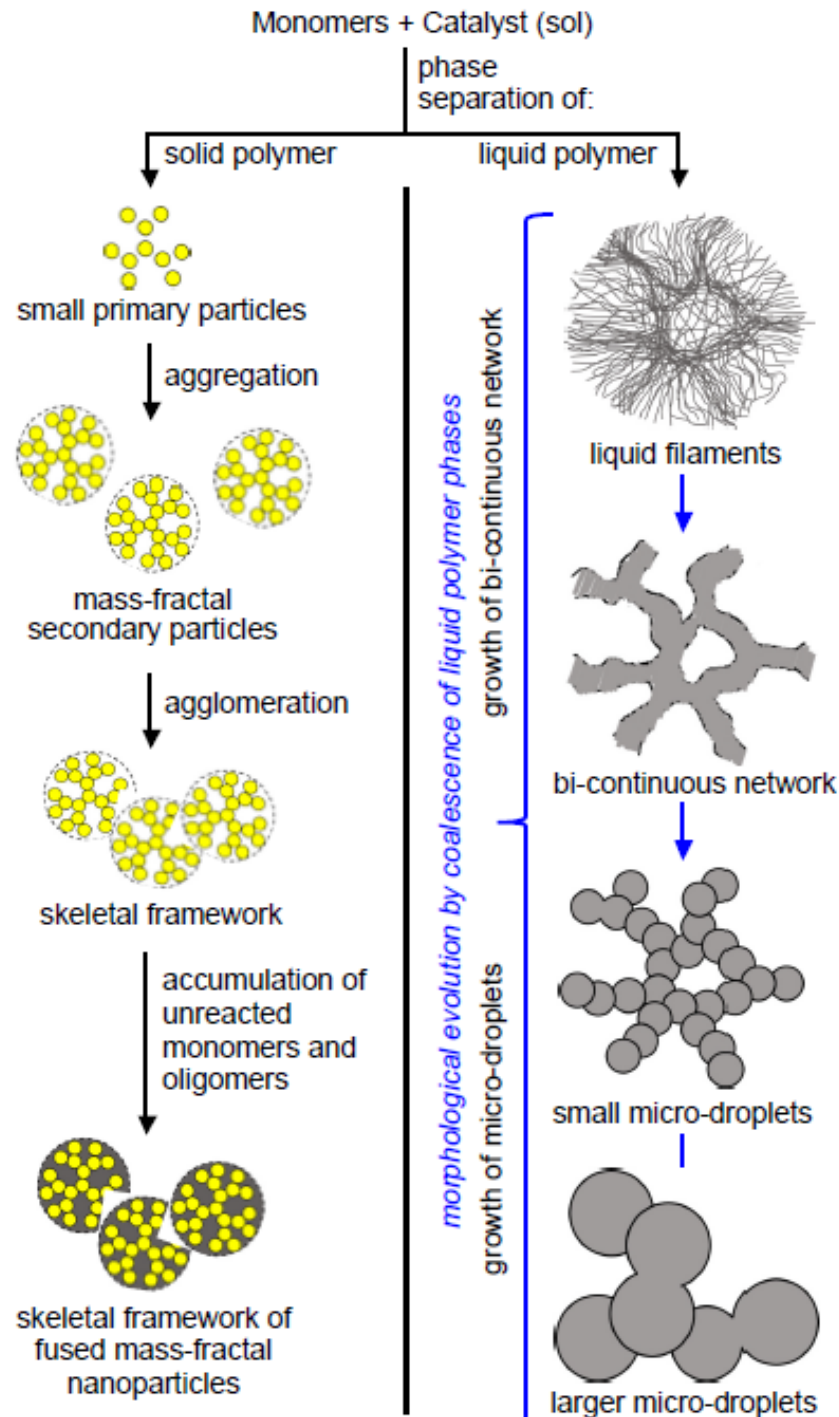
Tuning the Nanomorphology of Aerogels

Microscopically, aerogels can be hierarchical 3D assemblies of nanoparticles ...

... but not only!

In fact, aerogels comprise a convenient platform to study the properties of nano-structured matter!

The mechanism of aerogels formation we have already discussed.



Another mechanism, which does not involve formation of primary particles.

PART 3

ΜΕΘΟΔΟΙ ΧΑΡΑΚΤΗΡΙΣΜΟΥ

The gelation process

In principle, you can follow any property you want, in practice, however, two approaches stand out:

- Rheology
- *In situ* liquid NMR (^1H , ^{13}C , ^{29}Si etc.)

ΜΕΘΟΔΟΙ ΧΑΡΑΚΤΗΡΙΣΜΟΥ

Rheology

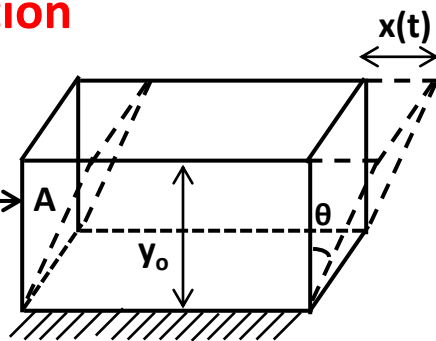
Rheology provides information about the structure of liquids by studying their deformation

Shear deformation

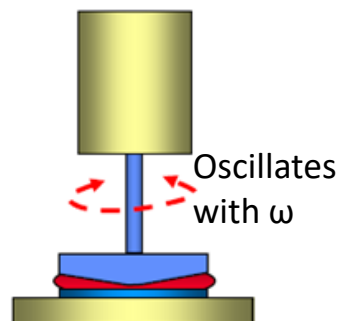
$$\text{Stress, } \tau = \frac{F}{A}$$

$$\text{Strain, } \gamma = \frac{x(t)}{y_0}$$

$$\text{Shear Modulus, } G = \frac{\tau}{\gamma}$$

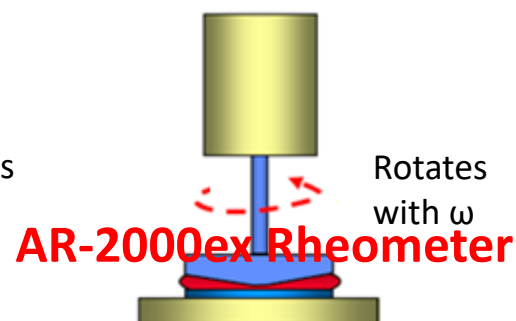


Oscillation mode



Cone and Plate deformation lags behind stress, depending how fast you oscillate

Flow mode



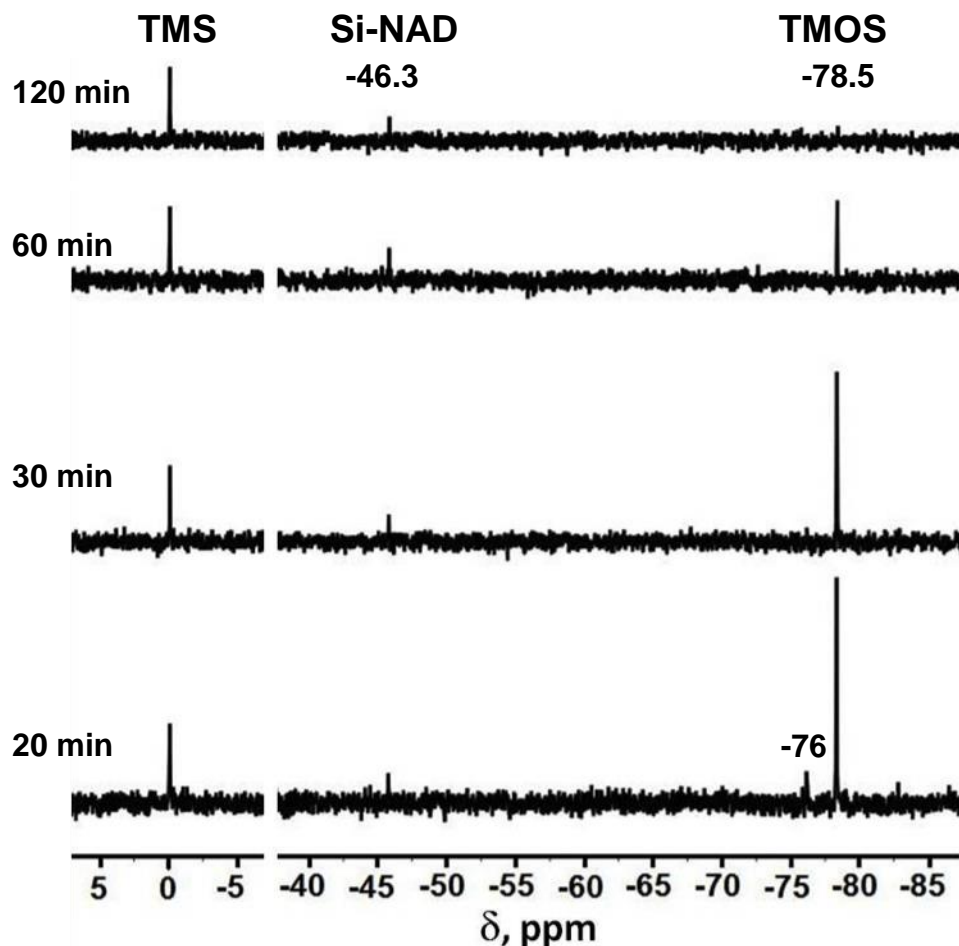
Cone and Plate



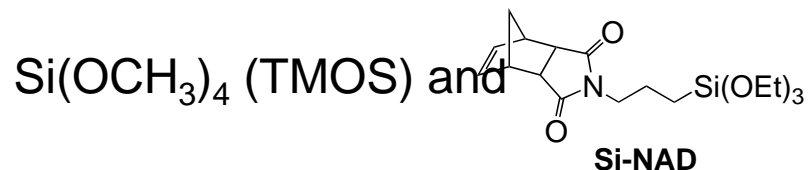
ΜΕΘΟΔΟΙ ΧΑΡΑΚΤΗΡΙΣΜΟΥ

In situ liquid NMR during gelation

You follow NMR signal of monomers in solution till signal is lost due to gelation



Co-gelation of:



TMOS signal disappears completely while **Si-NAD** signal is still present.

Conclusion: Primary network of TMOS, **Si-NAD** is added* to the particles afterwards.

* Confirmed by TGA as well as:
CPMAS ^{13}C and ^{29}Si NMR of the aerogel

ΜΕΘΟΔΟΙ ΧΑΡΑΚΤΗΡΙΣΜΟΥ

Bulk Characterization

In principle, you can follow any property you want, in practice, however, two approaches stand out:

- Mechanical properties
- Thermal conductivity
- Acoustic impedance

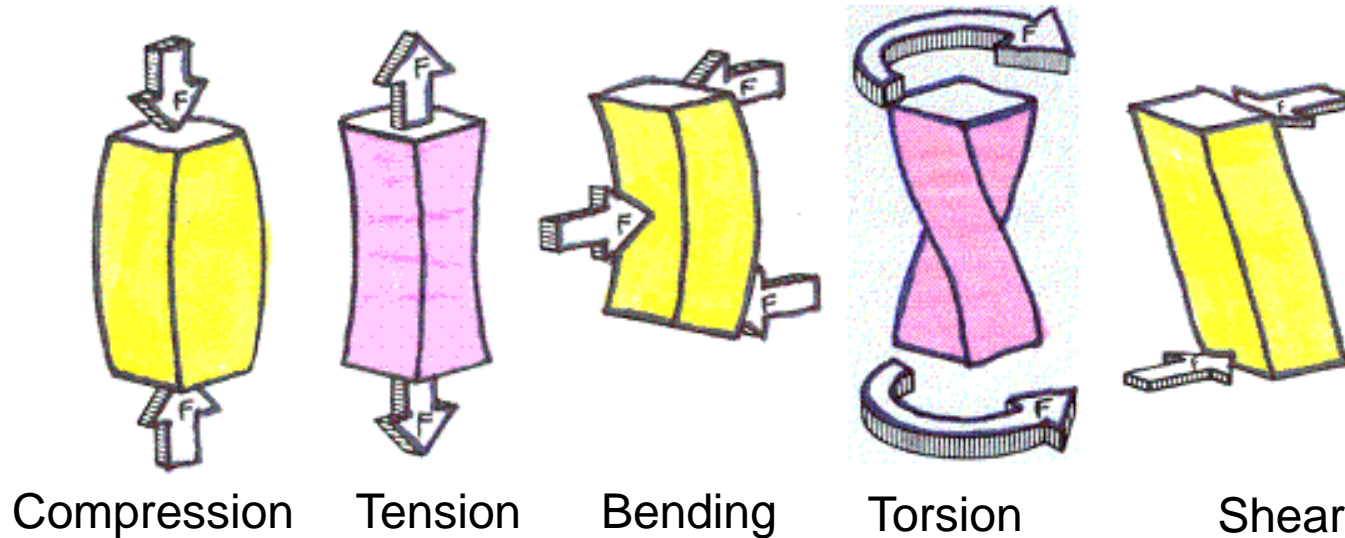
ΜΕΘΟΔΟΙ ΧΑΡΑΚΤΗΡΙΣΜΟΥ

Mechanical Properties

Mechanical properties are important for:

- (a) Practical reasons (strong lightweight materials)
- (b) Fundamental reasons (interparticle connectivity)

Possible mechanical deformations of materials:

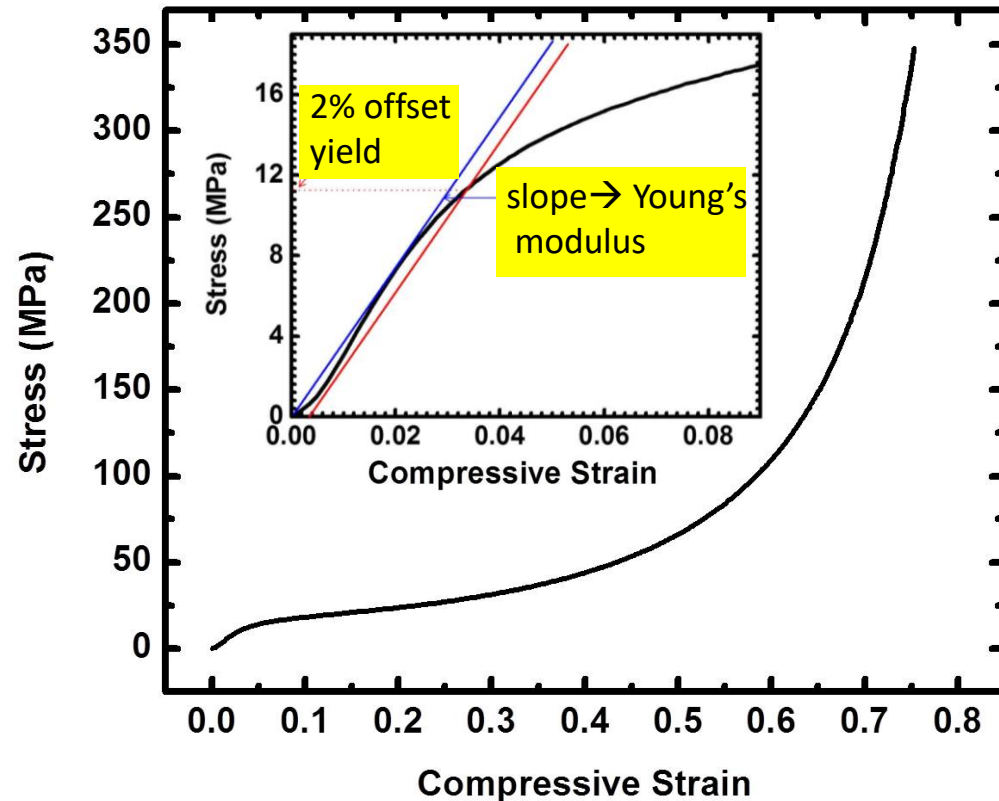
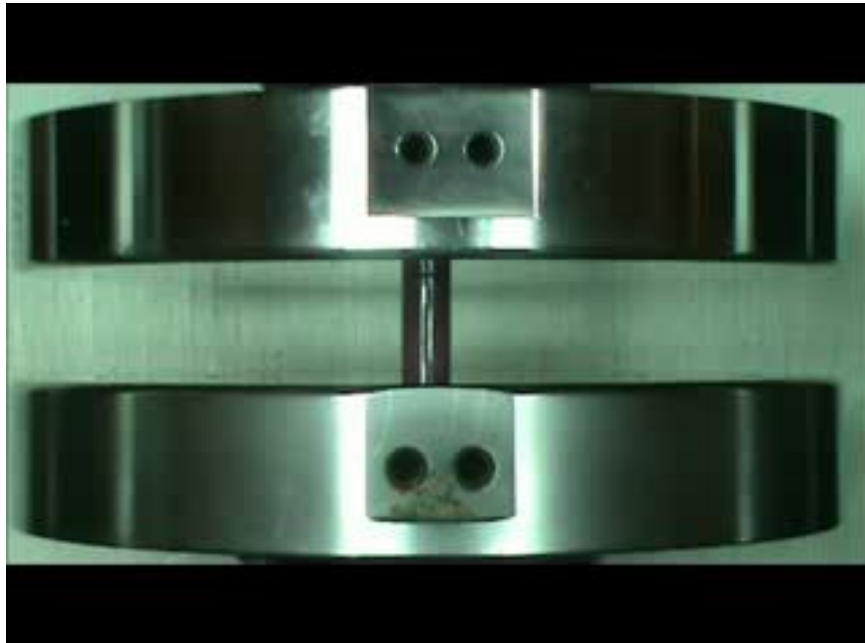


...of those, compression and tension are the most commonly used.

ΜΕΘΟΔΟΙ ΧΑΡΑΚΤΗΡΙΣΜΟΥ

Mechanical Properties

Polyurethane aerogels under compression



Quantities of interest:

Initial slope => elastic modulus (stiffness)

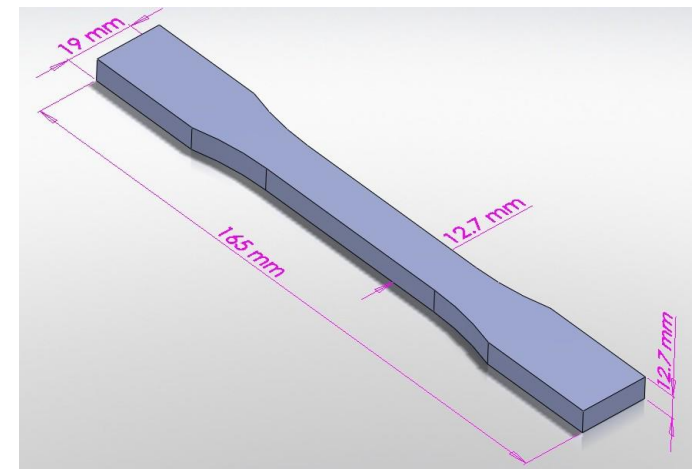
Ultimate compressive stress per unit mass (strength)

Area under the stress-strain curve (energy absorption-toughness)

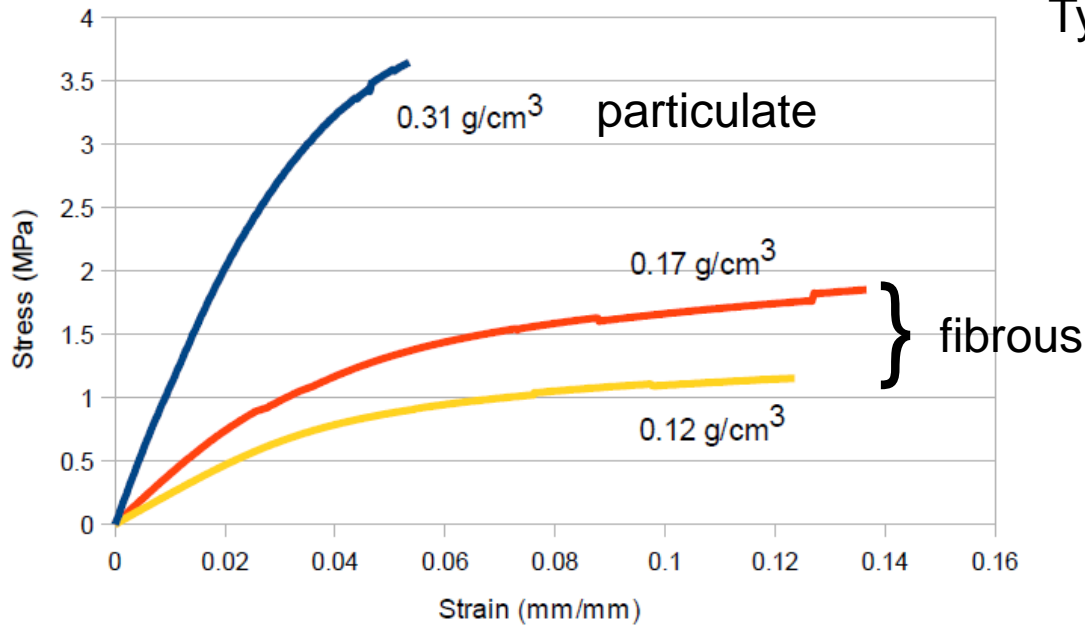
ΜΕΘΟΔΟΙ ΧΑΡΑΚΤΗΡΙΣΜΟΥ

Mechanical Properties

Polyurea aerogels under tension



Typical tension specimen (dog-bone)



Tensile testing set-up

ΜΕΘΟΔΟΙ ΧΑΡΑΚΤΗΡΙΣΜΟΥ

Thermal Conductivity

The ability of a material to conduct heat

$$\lambda(T) - \lambda_{\text{radiation}} = \lambda_{\text{gas_conduction}} + \lambda_{\text{skeletal_conduction}} = \rho_b(T) \times C_p(T) \times R(T)$$

λ = thermal conductivity

ρ_b = bulk density

C_p = heat capacity

R = thermal diffusivity (using **Laser Flash method**)

Higher λ : used as heat sink

Lower λ : used as thermal insulator

ΜΕΘΟΔΟΙ ΧΑΡΑΚΤΗΡΙΣΜΟΥ

Porous Structure

- **Nitrogen sorption porosimetry**

- probes <2 nm to ~300 nm

You can use it with anything

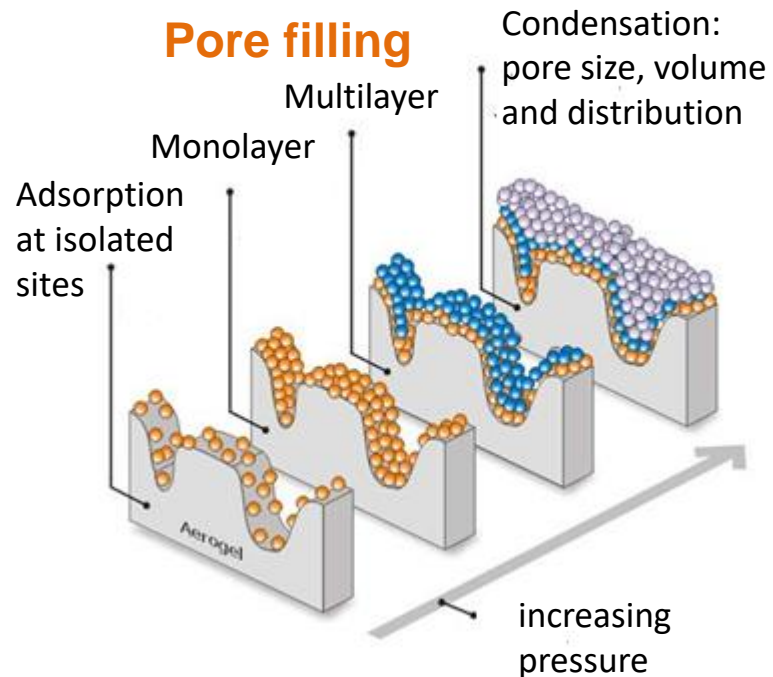
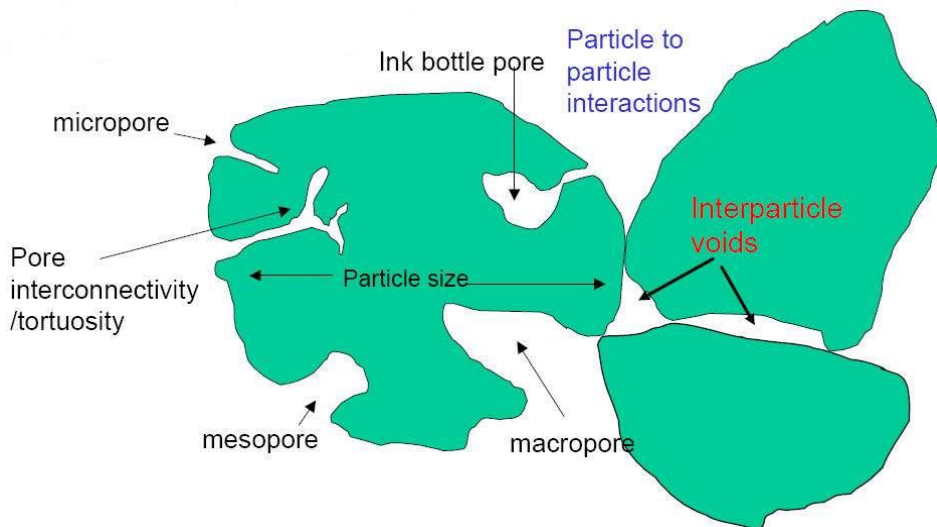
- **Mercury intrusion porosimetry**

- probes 3 nm to 1 mm

You cannot use it with soft materials

ΜΕΘΟΔΟΙ ΧΑΡΑΚΤΗΡΙΣΜΟΥ

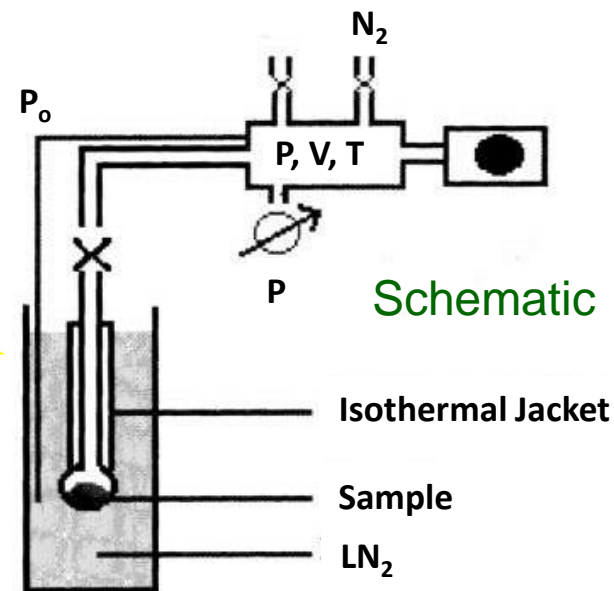
Nitrogen sorption porosimetry



- Micropores $d < 2 \text{ nm}$
- Mesopores $2 \text{ nm} < d < 50 \text{ nm}$
- Macropores $d > 50 \text{ nm}$

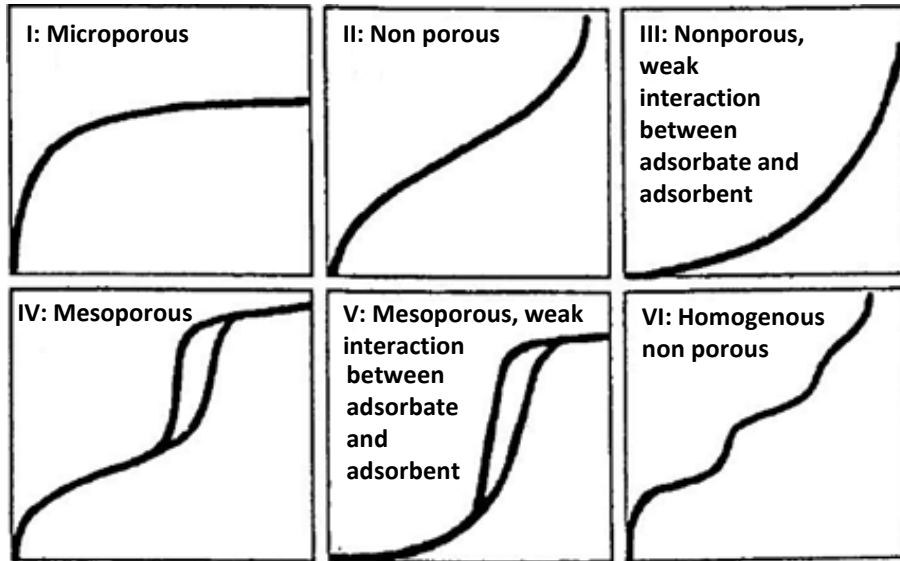
Pore size classification
by IUPAC (1984)

Operating principle:
In small pores N_2 gas
condenses to liquid
 N_2 at $< 1 \text{ atm}$

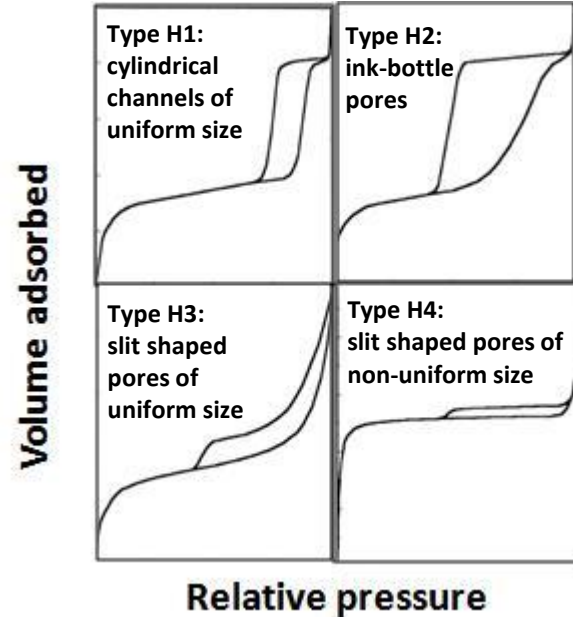


Nitrogen sorption porosimetry

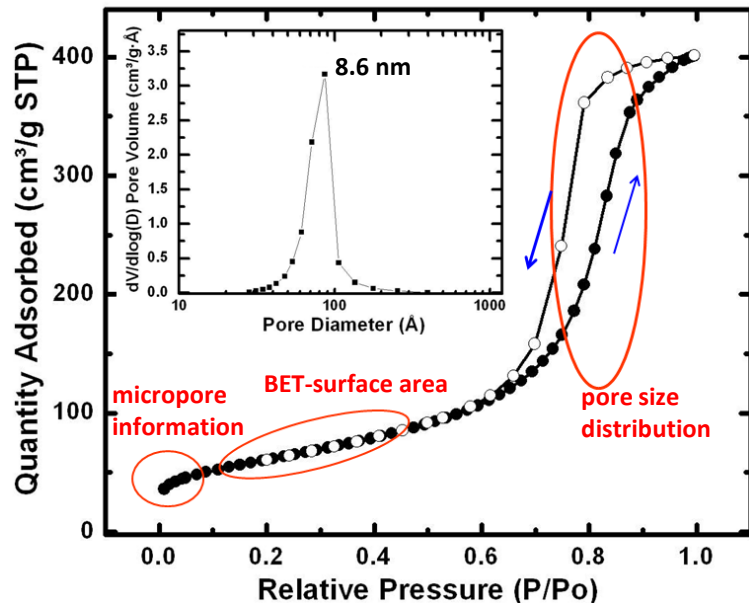
Classical adsorption isotherm models



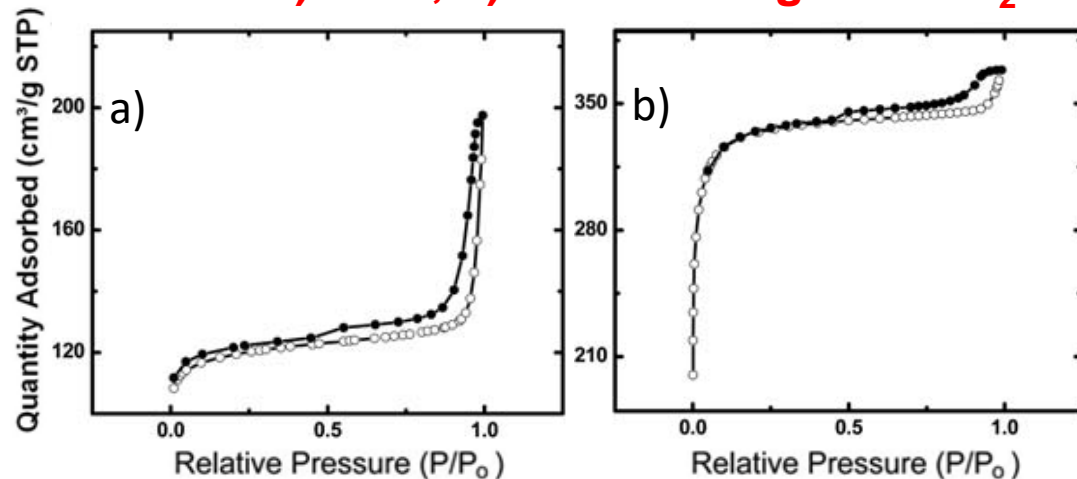
Types of hysteresis curves



Typical sorption isotherm (Silica-Alumina Ref.)

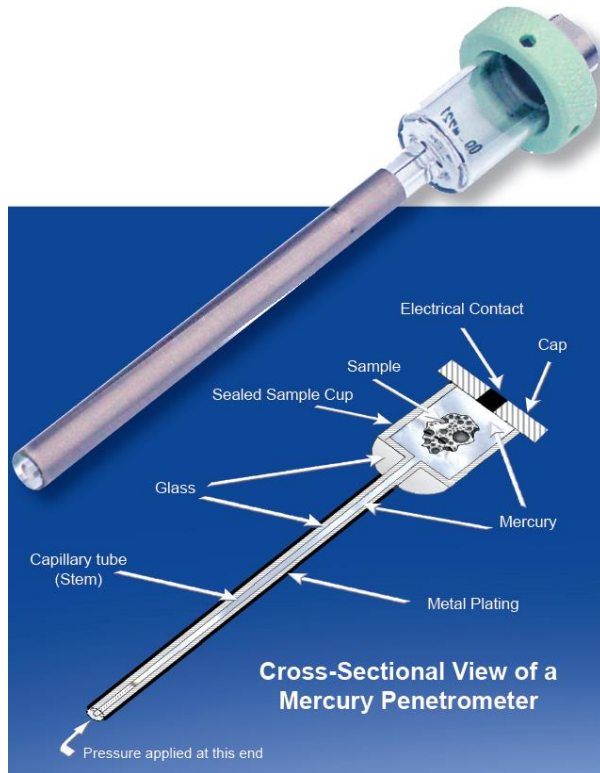


Sorption isotherm of Polyimide derived carbon a) as is, b) after etching with CO_2

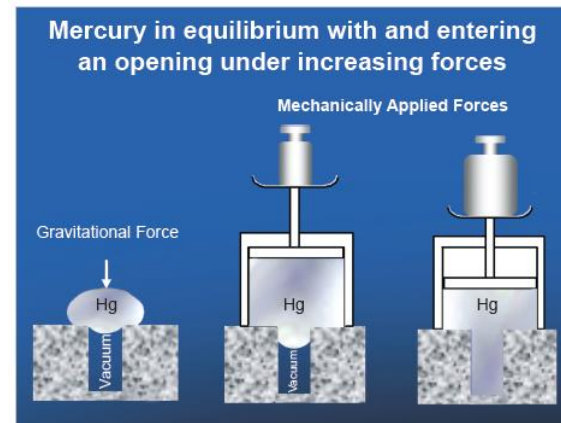


ΜΕΘΟΔΟΙ ΧΑΡΑΚΤΗΡΙΣΜΟΥ

Hg Intrusion porosimetry



- Works by applying various levels of pressure to samples immersed in mercury
- Can be used to determine broad pore size distribution 3 nm to ~1 mm

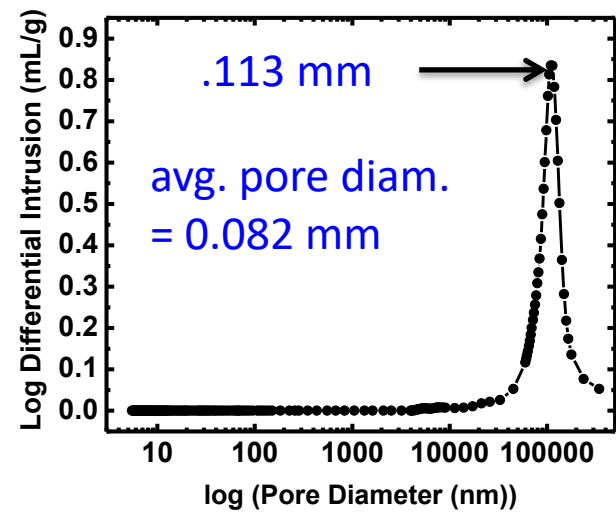
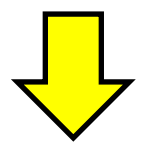
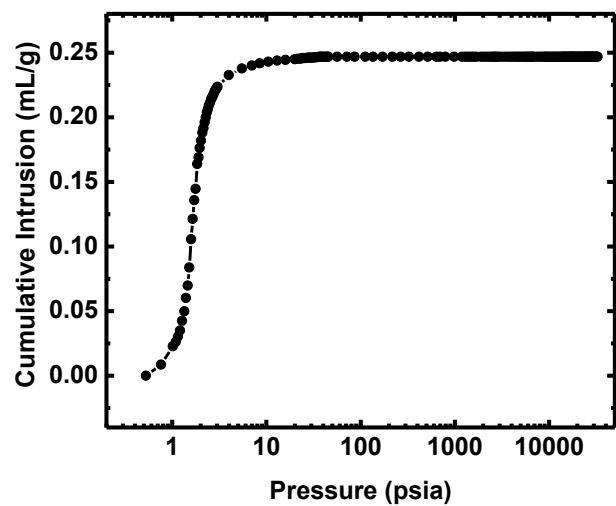


Since Hg doesn't wet most substances, it doesn't penetrate into pores by capillary action. Hence it is forced into the pores by applying external pressure (up to 60,000 psi).

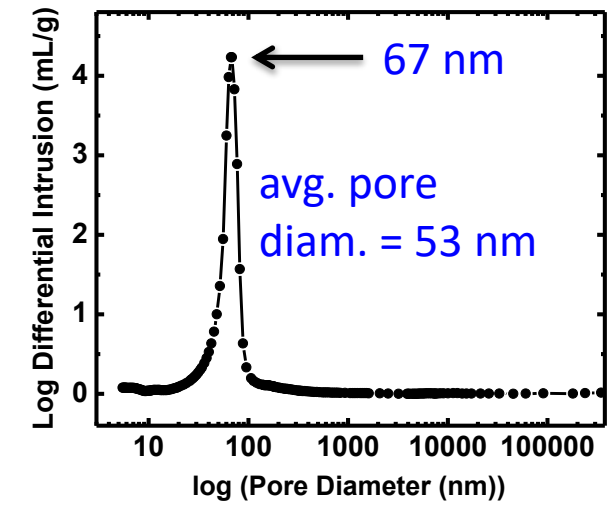
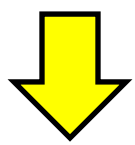
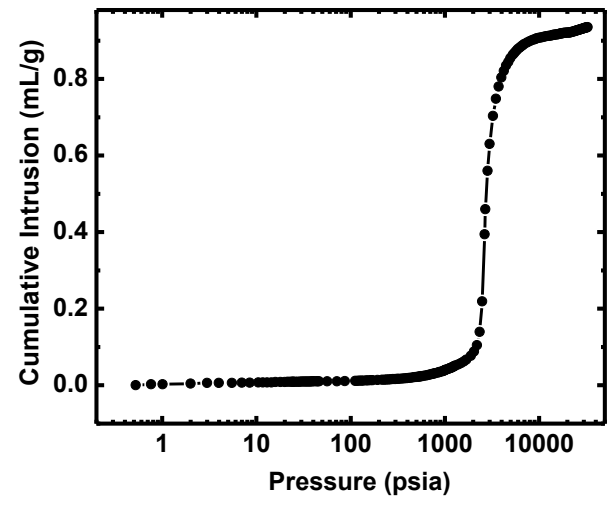
The pressure is inversely proportional to the size of the pores.

Pore size distribution by Hg intrusion

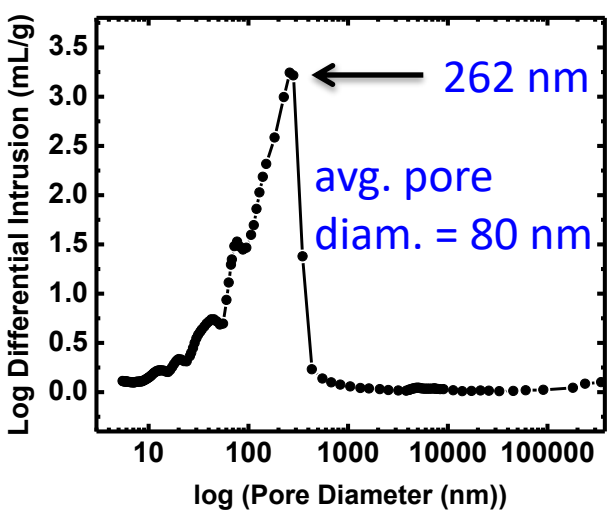
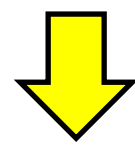
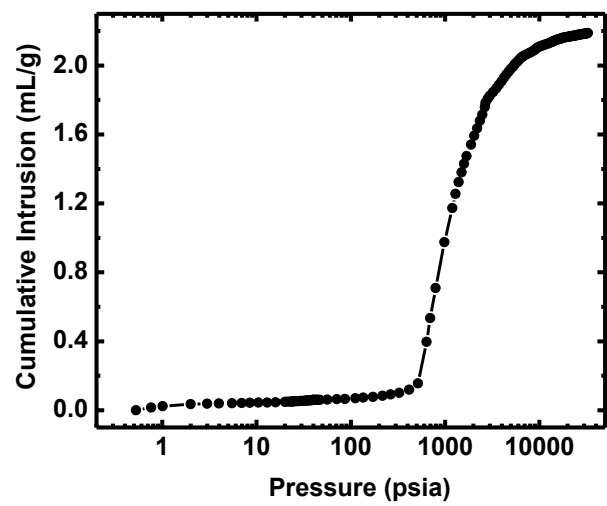
sand



PU aerogel



Example of collapsed structure (PU aerogel)



ΜΕΘΟΔΟΙ ΧΑΡΑΚΤΗΡΙΣΜΟΥ

Skeletal Framework – Molecular Level Characterization

Basically, we adopt polymer characterization methods:

- Solid-state CPMAS NMR (mainly ^{13}C)
- Gel Permeation Chromatography (GPC; polymer MW)
- Differential Scanning Calorimetry (DSC; glass transition, T_g , binding on surface)
- Dynamic Mechanical Analysis (DMA)
- X-ray diffraction (XRD; for establishing crystallinity)

And also macroscopic mechanical testing:

- Compression (establishing interparticle connectivity)

ΜΕΘΟΔΟΙ ΧΑΡΑΚΤΗΡΙΣΜΟΥ

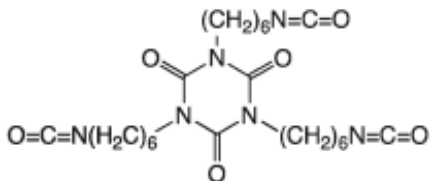
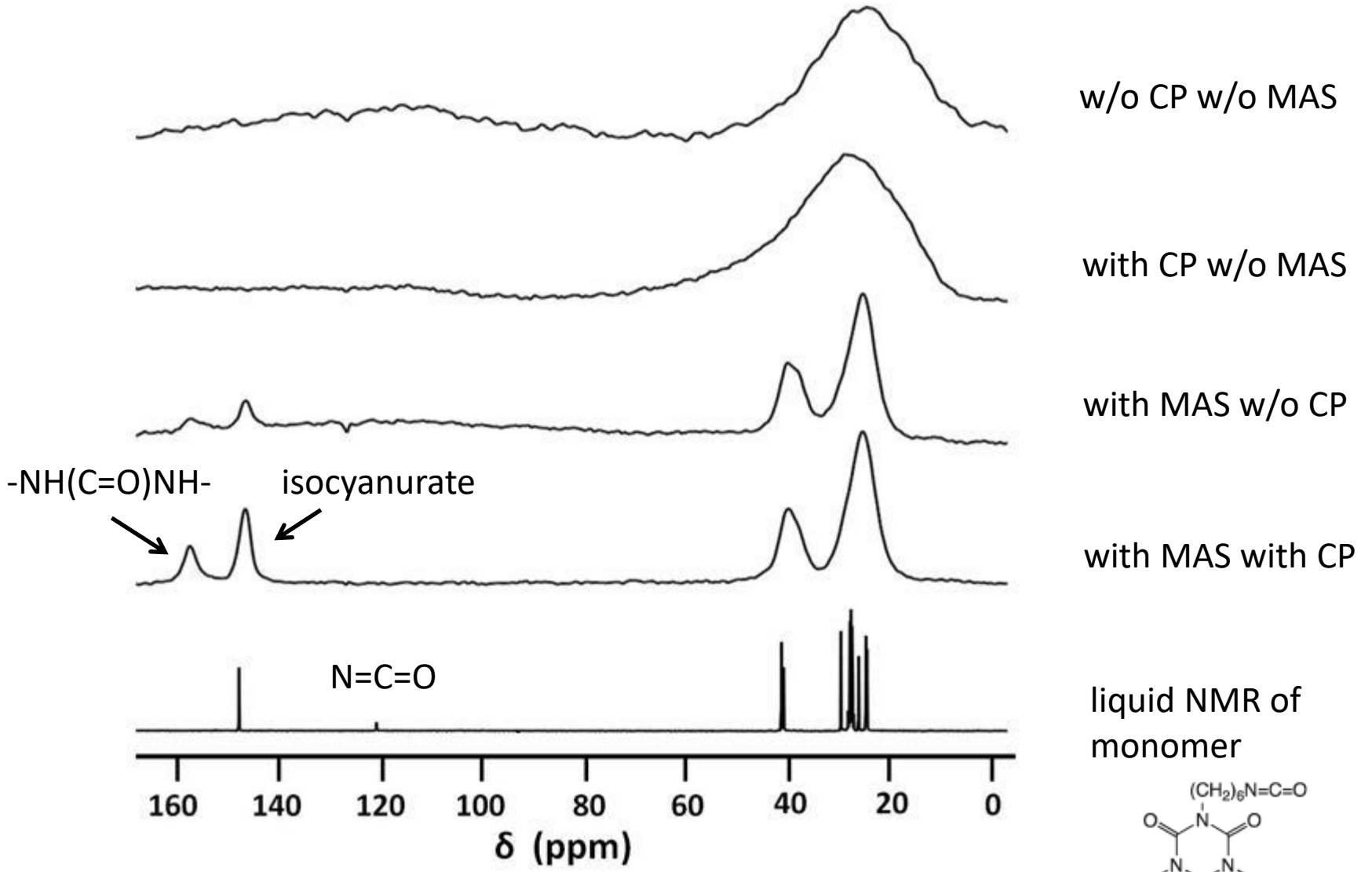
Solid-state CPMAS NMR (mainly ^{13}C)

- Running solids with a liquid NMR instrument gives very broad signal.
 - Not interpretably useful.
- To improve resolution we use dedicated solid NMR instruments and we apply:
 - Magic Angle (54.74°) Spinning (MAS), and
 - Cross Polarization (CP) for improving relaxation and increased signal to noise

Once those are implemented, one obtains almost liquid-like resolution and peaks can be integrated just as in familiar NMR in solution

Solid-state CPMAS NMR

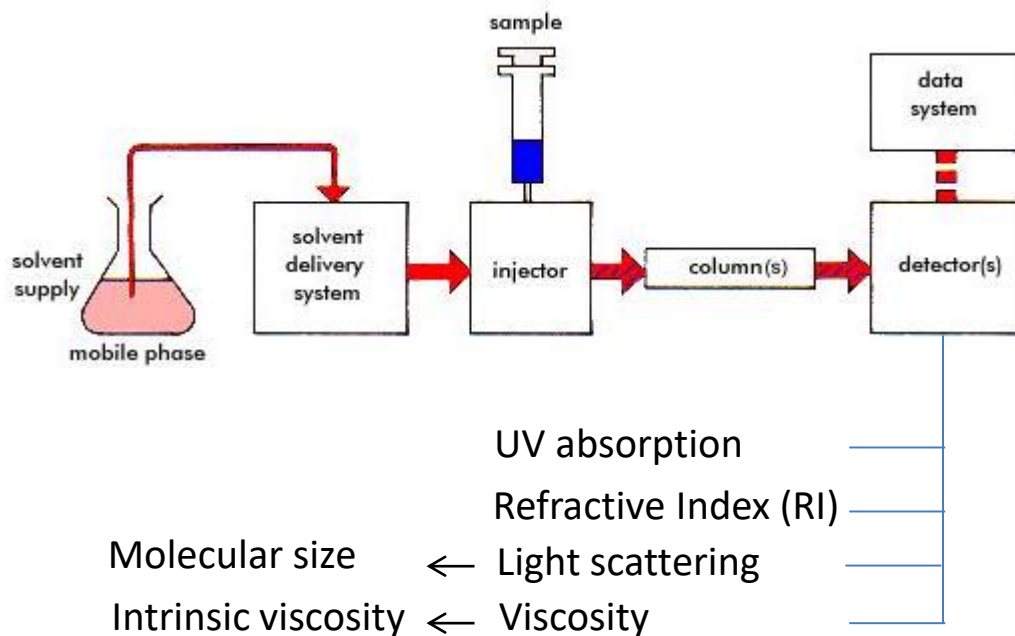
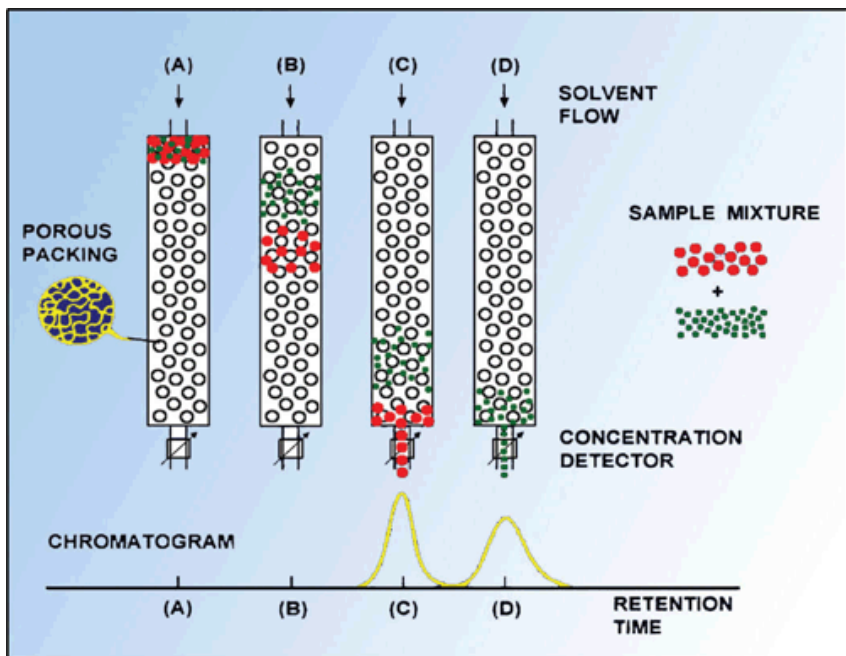
The effect of CP and MAS on solid-state ^{13}C NMR spectrum of polyurea aerogels



ΜΕΘΟΔΟΙ ΧΑΡΑΚΤΗΡΙΣΜΟΥ

Gel Permeation Chromatography (GPC)

GPC (or SEC-size exclusion chromatography) is a method that separates components based on their size (hydrodynamic radius (R_h)).



Larger molecule → higher molecular weight (MW) → shorter retention time

Smaller molecule → lower molecular weight (MW) → longer retention time

ΜΕΘΟΔΟΙ ΧΑΡΑΚΤΗΡΙΣΜΟΥ

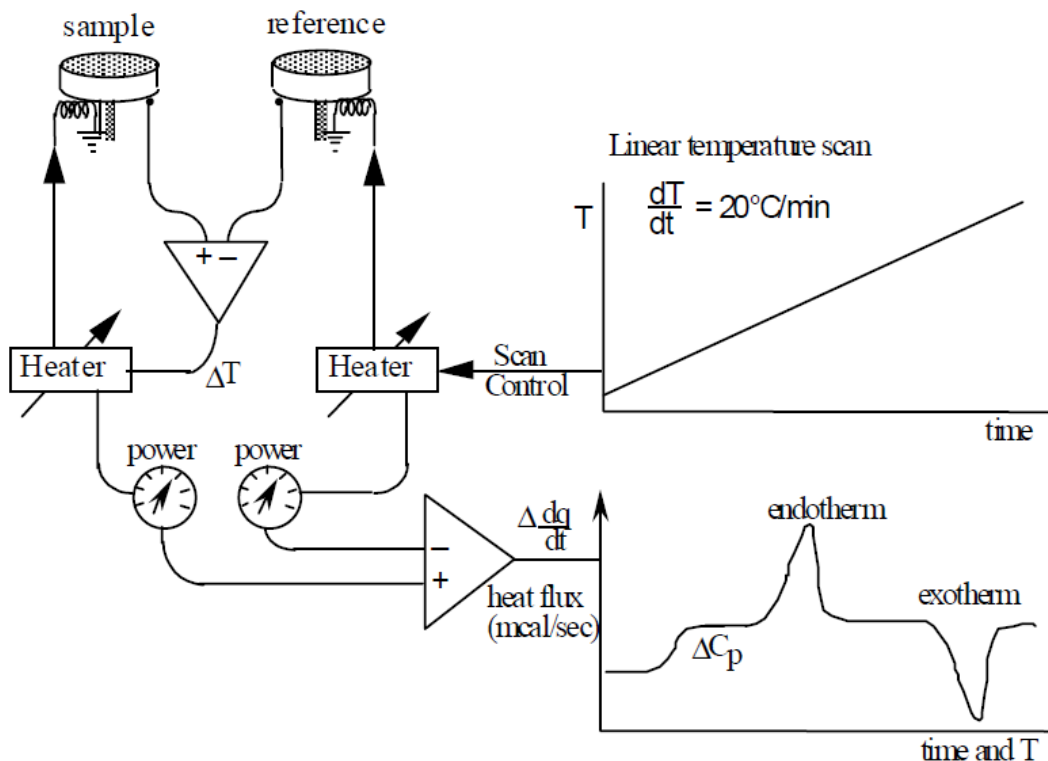
Differential Scanning Calorimetry (DSC)

Differential: Measures the heat flow difference between a sample and a reference

Scanning: Temperature or time scan

Calorimetry: Measurement of heat (or heat flow)

Monitors heat effects associated with phase transitions and chemical reactions



Since DSC is at constant pressure, heat flow is equivalent to enthalpy changes.

$$\left(\frac{dq}{dt}\right)_p = \frac{dH}{dt}$$

$$\Delta \frac{dH}{dt} = \left(\frac{dH}{dt}\right)_{\text{sample}} - \left(\frac{dH}{dt}\right)_{\text{reference}}$$

- Reference: Empty pan or alumina
- Temperatures of both sample and reference are increased at constant rate.
- Monitor the heat flow difference between sample and reference

Differential Scanning Calorimetry (DSC)

- ✓ Glass transitions
- ✓ Melting and boiling points
- ✓ Crystallization time and temperature
- ✓ Percent crystallinity
- ✓ Heats of fusion and reactions
- ✓ Specific heat
- ✓ Oxidative/Thermal stability
- ✓ Rate and degree of cure
- ✓ Reaction kinetics

$$\Delta H = C_p \Delta T$$
$$dH/dt = C_p dT/dt + \text{thermal events}$$

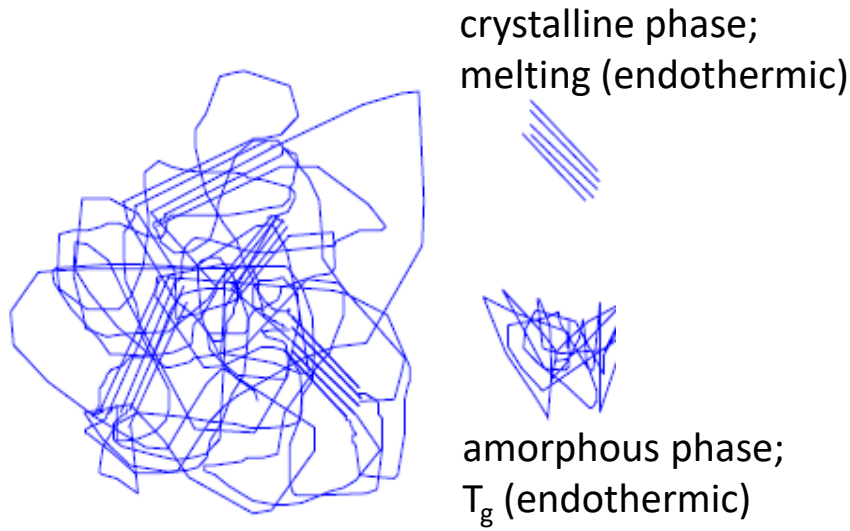
C_p = specific heat (J/g °C)

T = Temperature

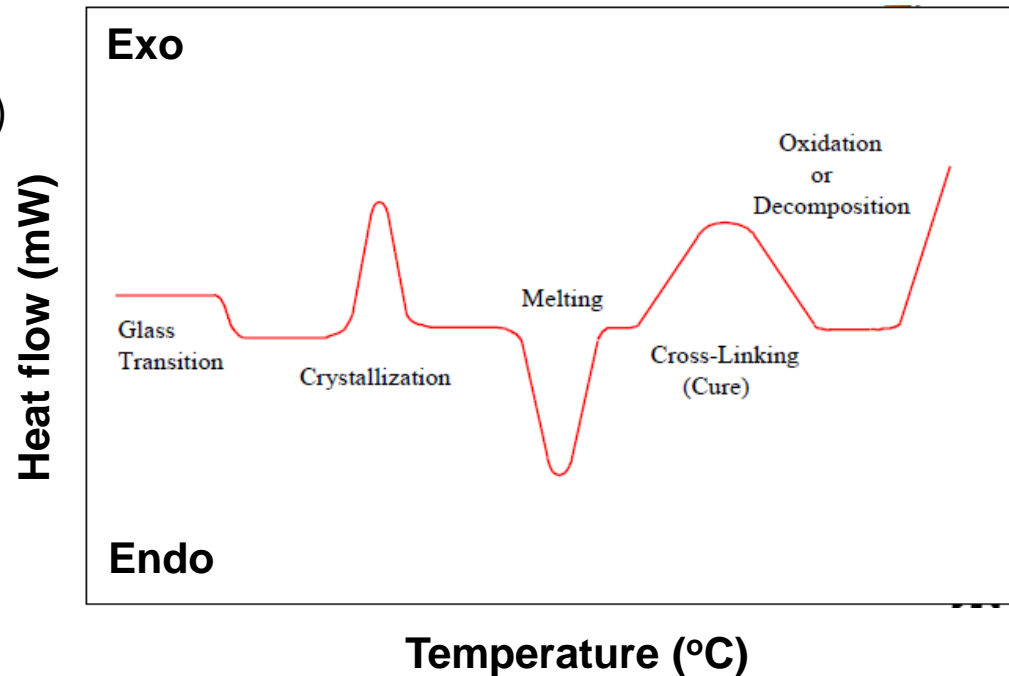
H = heat (J)

dH/dt = heat flow (mW)

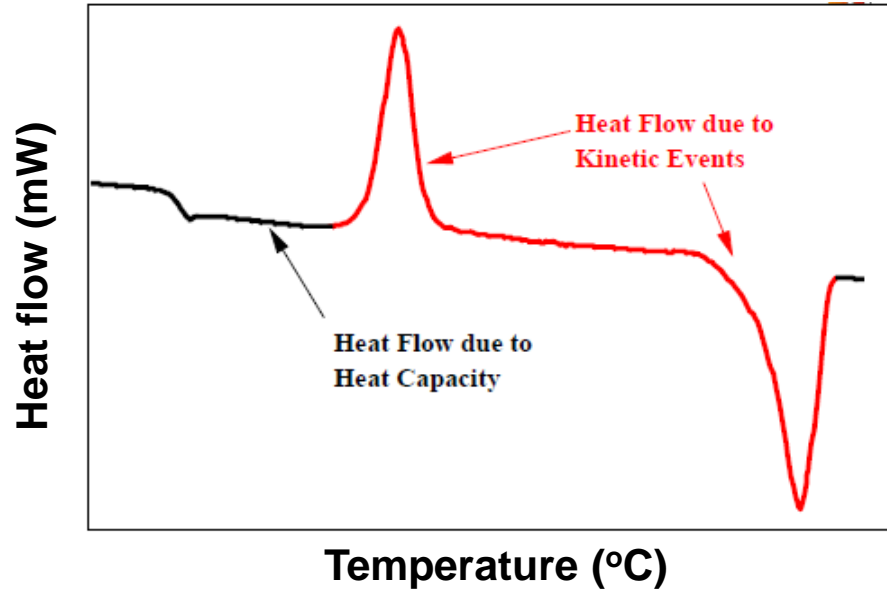
dT/dt = heating rate (°C/min)



Typical DSC transitions



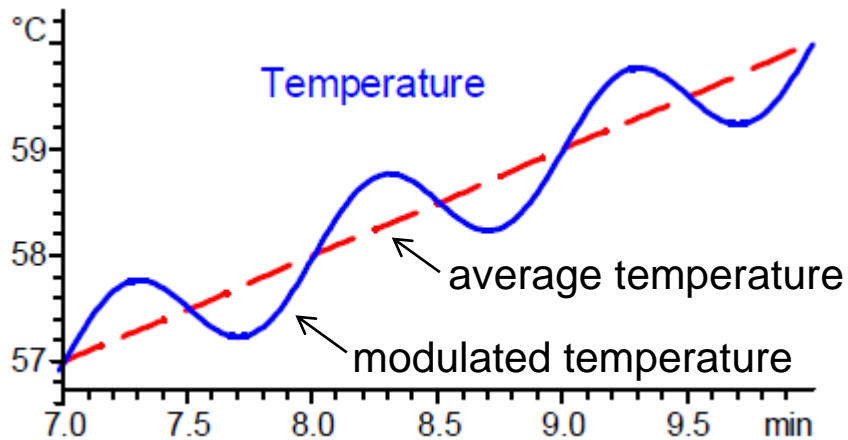
Modulated Differential Scanning Calorimetry (MDSC)



$$\frac{dH}{dt} = C_p \frac{dT}{dt} + f(T, t)$$

One problem with regular DSC is that you do not know what part of the heat flow is due to glass transition, melting, or reaction and which part is due to the heat capacity....

...so you apply a sine temperature wave on top of the linear sweep...



Total heat flow = in phase + 90° off phase
In phase heat flow: reversible (C_p , T_g , T_m)
90° off phase: irreversible (kinetic slow-down)

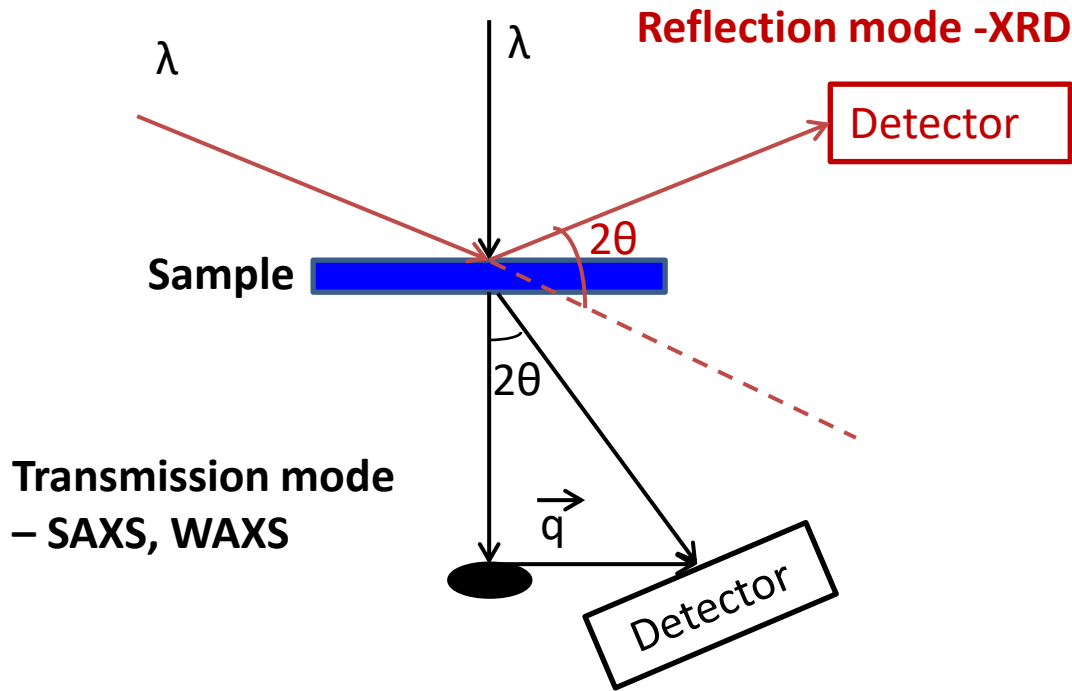
- Relatively slow technique
- Improved sensitivity, resolution, accuracy
- Separates overlapping transitions

ΜΕΘΟΔΟΙ ΧΑΡΑΚΤΗΡΙΣΜΟΥ

Skeletal Framework – Nano-scopic level characterization

- Small angle X-ray or neutron scattering (SAXS and SANS)
- Electron Microscopy
 - Scanning electron microscopy (SEM)
 - Transmission electron microscopy (TEM)

X-ray Diffraction



$$n\lambda = 2d \sin \theta$$

n : integer representing the order of diffraction

λ : wavelength of the x-ray

d : interplane distance

θ : scattering angle

Scherrer's equation

$$t = K\lambda / B \cos \theta$$

t : thickness of the crystallite

λ : wavelength of the x-ray

K : constant

θ : scattering angle

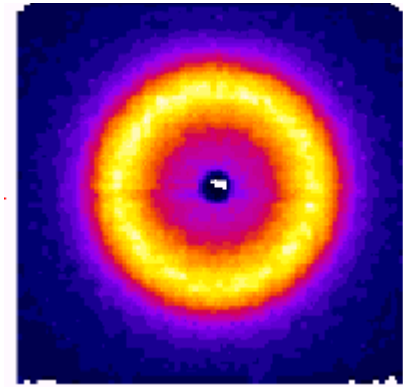
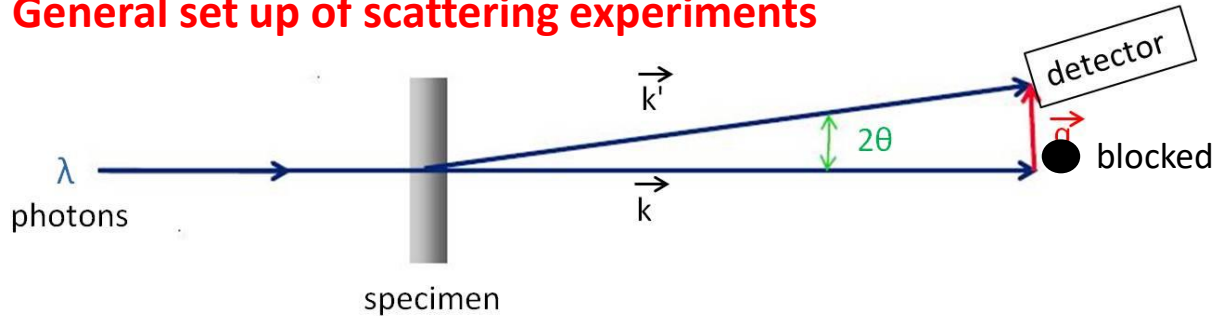
B : FWHM (full width at half maxima)

XRD

- Phase composition of sample (degree of crystallinity)
- Unit cell lattice parameters
- Crystal structure
- Orientation
- Crystallite size and microstrain

Small angle X-ray scattering (SAXS)

General set up of scattering experiments



Scattering vector: $q = \frac{4\pi}{\lambda} \sin \theta$

λ : wavelength of incident beam

θ : Half of the scattering angle

Equation for one structural level:

$$I(q) \simeq G \exp(-q^2 R_g^2/3) + B(1/q^*)^P$$

where $q^* = q/[\text{erf}(kR_g q/\sqrt{6})]^3$

G : Guinier prefactor

B : power-law prefactor

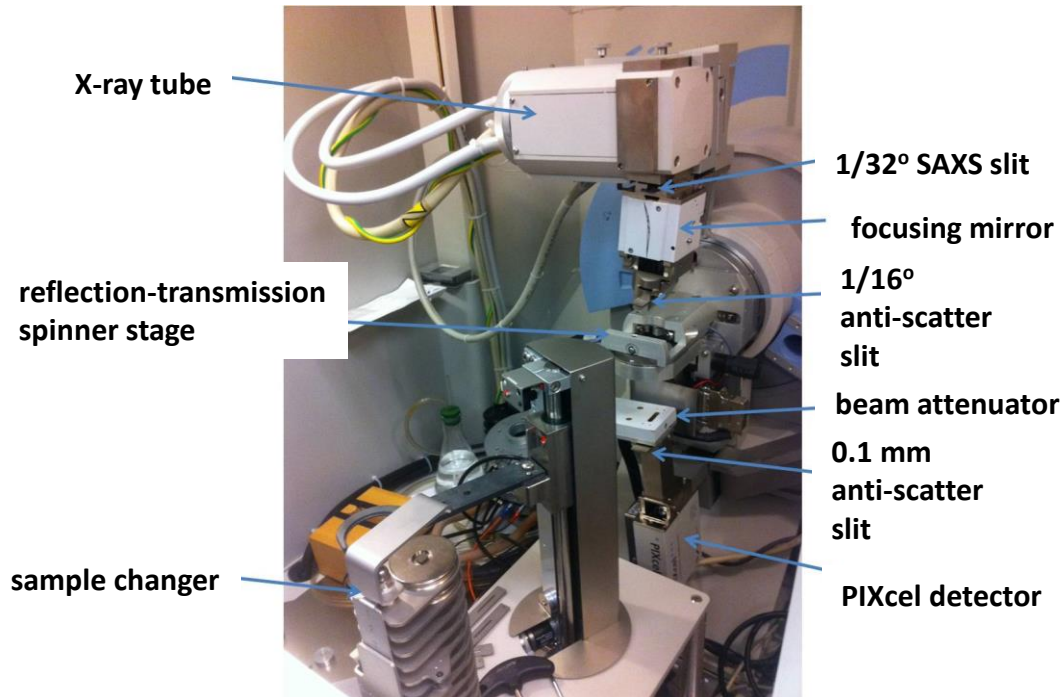
R_g : radius of gyration

k : approximation involved in the description of the low- q power-law limit

P : fractal dimension, for surface fractals $4 > P > 3$, for mass fractals $P < 3$ and for diffuse interfaces $P > 4$

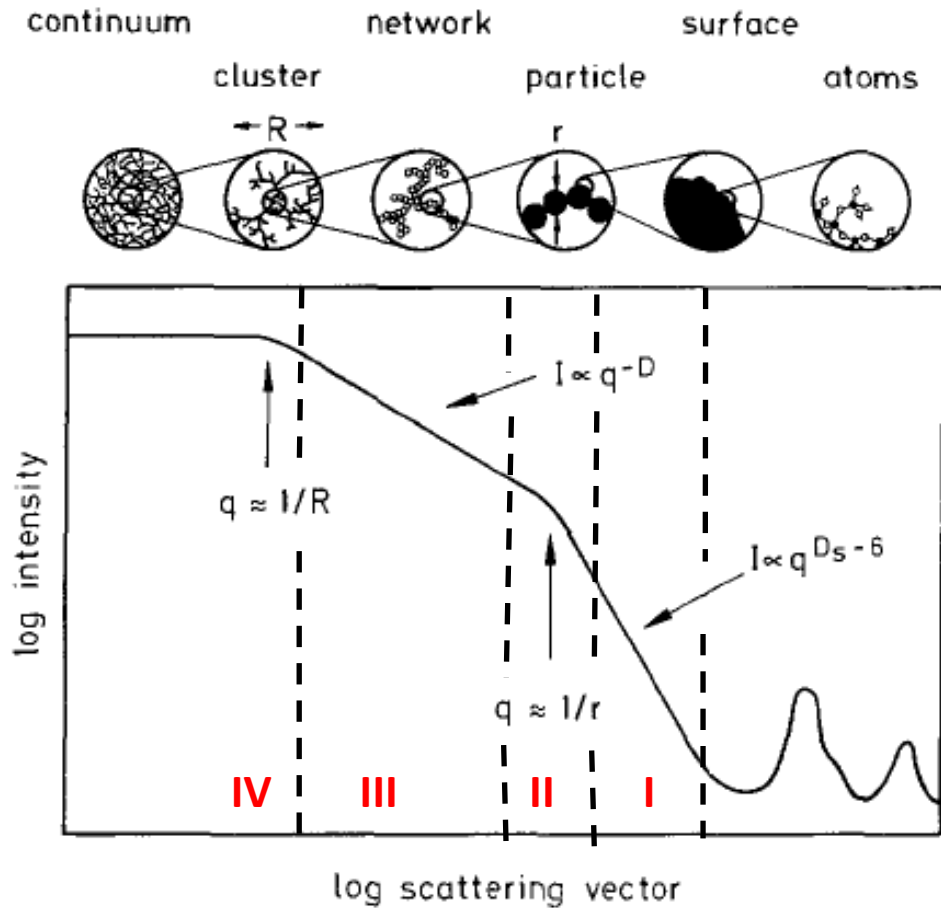
Beaucage, G. J. *Appl. Cryst.* **1996**, 29, 134-146

PANalytical X'Pert Pro Multi-Purpose Diffractometer (MPD) - configured for SAXS



Small angle X-ray scattering (SAXS)

Idealized small angle scattering profile from aerogels and information extracted



Region I

Porod region: Slope = -4.0

If Slope < -4.0 \implies interface density gradients

Region II

Guinier knee: radius of gyration of primary particles

Region III

Power law: $I \propto q^{-D_m}$ or $I \propto q^{D_s-6}$

D_m : mass fractal dimensions of the clusters

D_s : surface fractal dimensions

For smooth surfaces ($D_s = 2$) and for fractal surfaces ($D_s = 2-3$)

Region IV

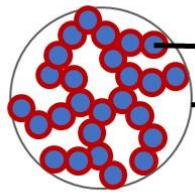
Radius of gyration of secondary particles

$$R = (5/3)^{0.5} \times R_G$$

R: radius of sphere

Small angle X-ray or neutron scattering (SAXS and SANS)

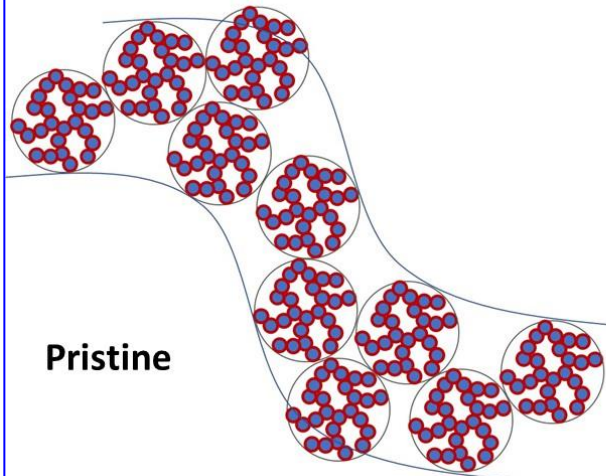
X-Ca-*alg*-N3300



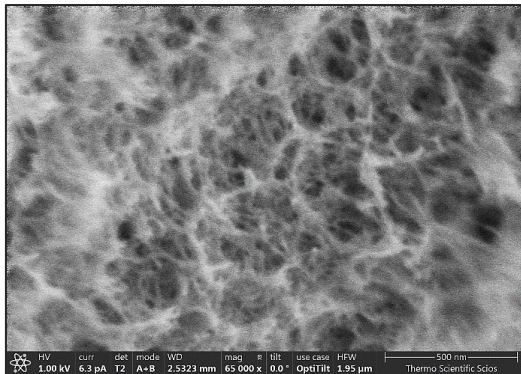
primary particles of X-Ca-alginate aerogel coated with polyurea; *radius* = 8.8 nm

secondary particle of X-Ca-alginate aerogel
- space within the secondary particle **NOT** filled with polyurea

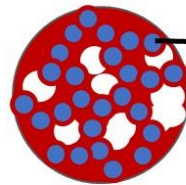
alginate/polyurea aerogels



Pristine

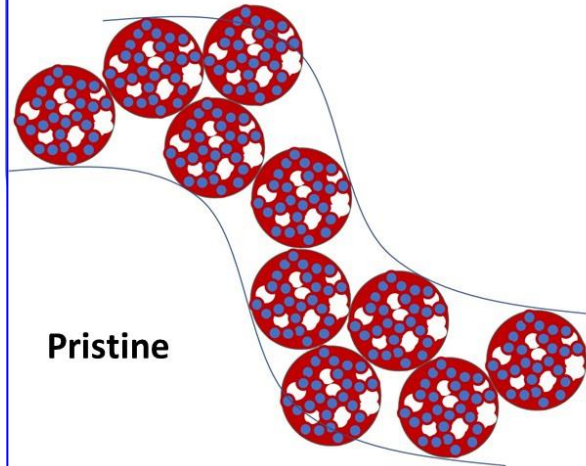


X-Ca-*alg*-RE

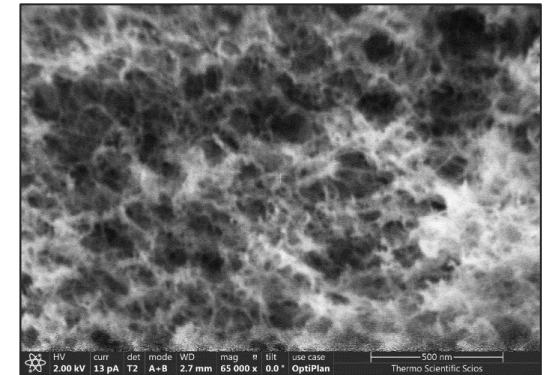


primary particles of X-Ca-alginate aerogel embedded in polyurea; *radius* = 10 nm

secondary particle of X-Ca-alginate aerogel
- space within the secondary particle **PARTIALLY** filled with same-density, or less-dense polyurea – minor closed porosity



Pristine

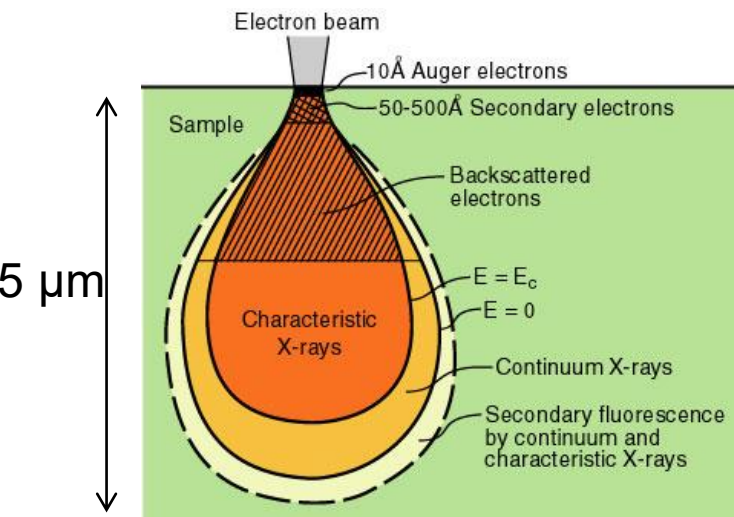


ACS Appl. Nano Mater.
2021, 4, 10575–10583

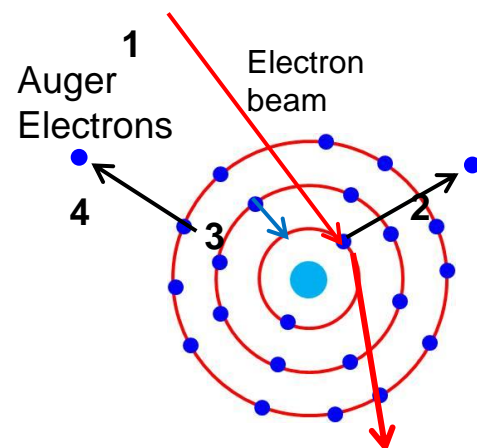
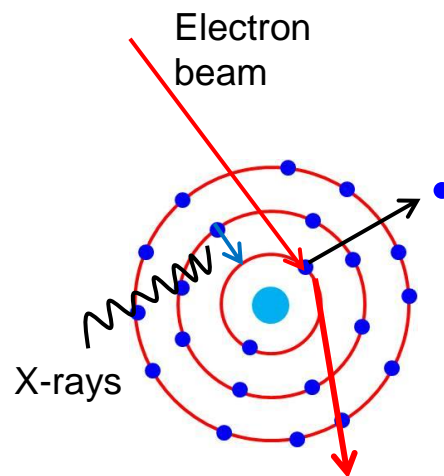
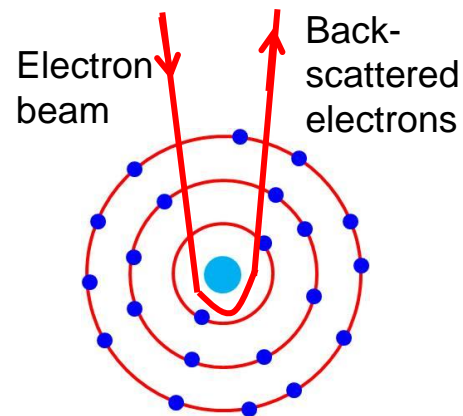
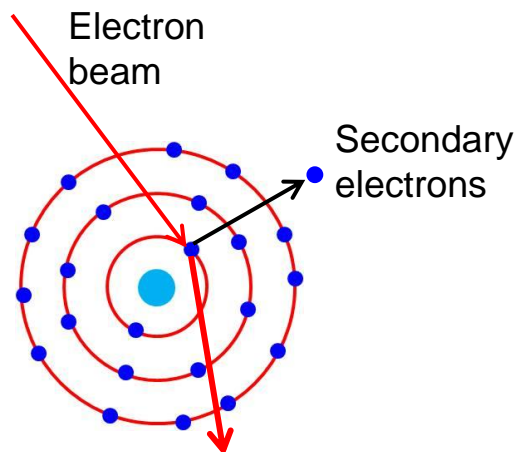
ΜΕΘΟΔΟΙ ΧΑΡΑΚΤΗΡΙΣΜΟΥ

Scanning electron microscopy (SEM)

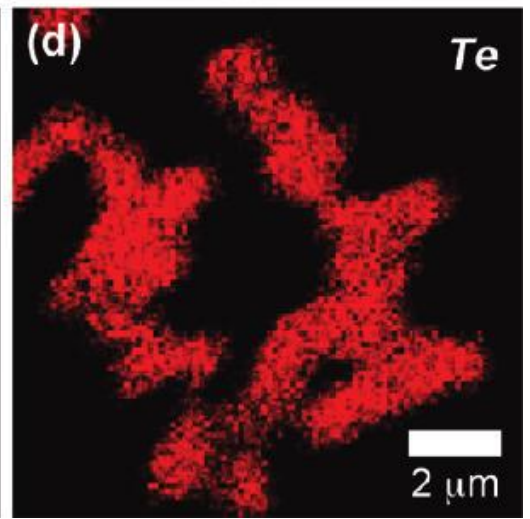
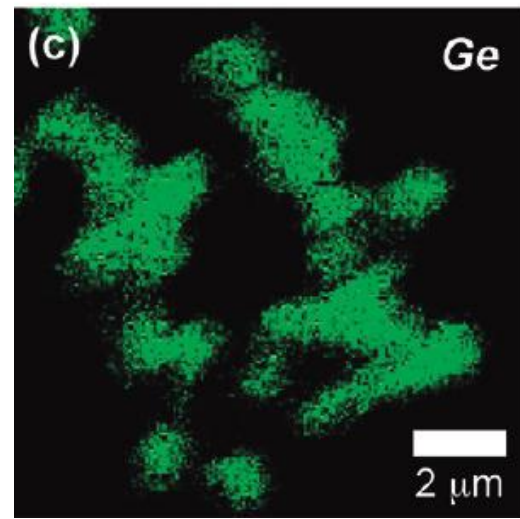
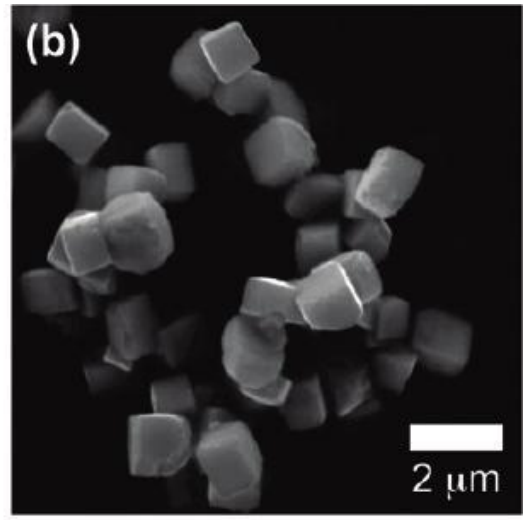
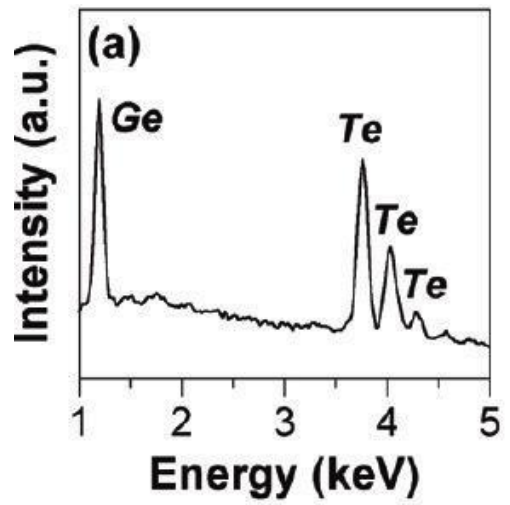
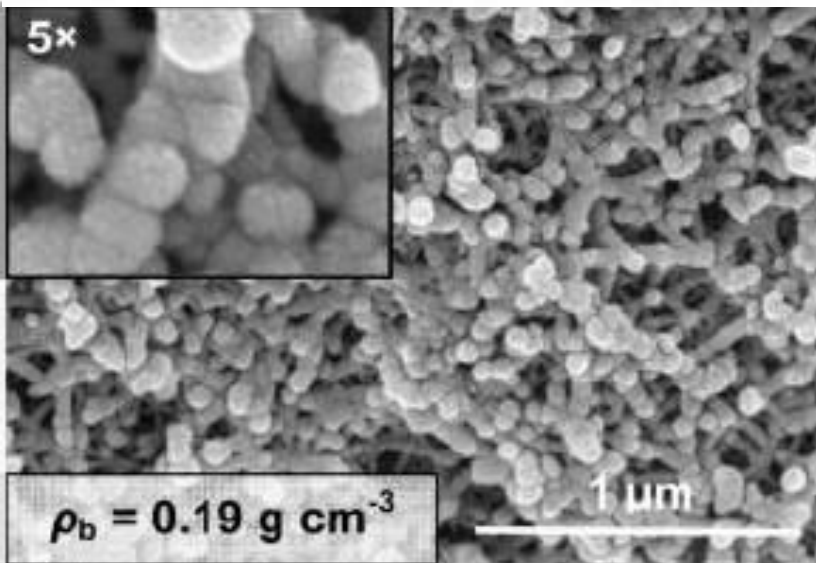
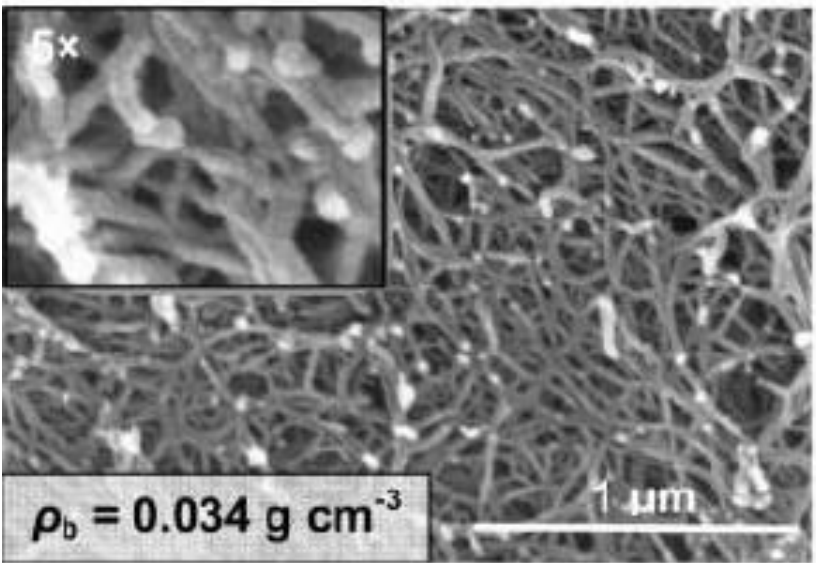
Beam-sample interaction volume



Different signal generation mechanism



Scanning electron microscopy (SEM) and Electron dispersive spectroscopy (EDS)

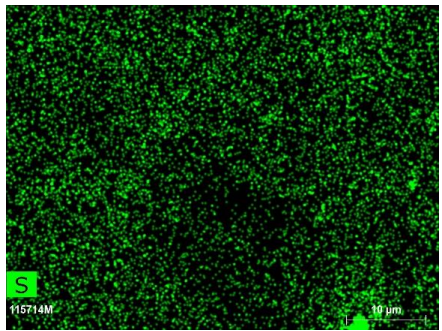
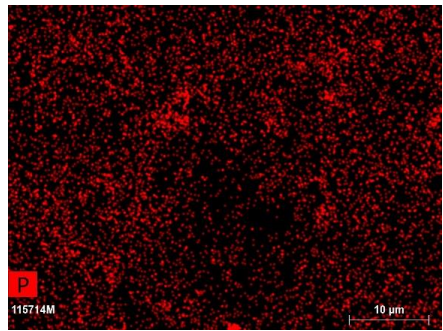
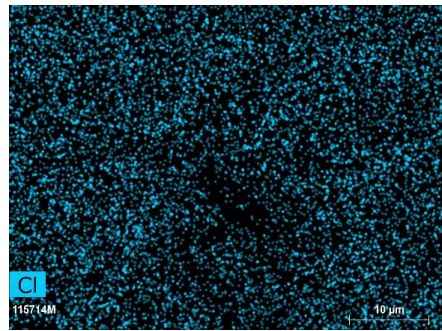
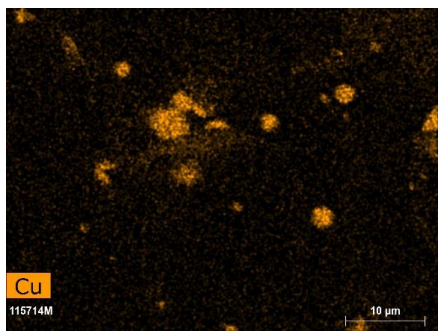
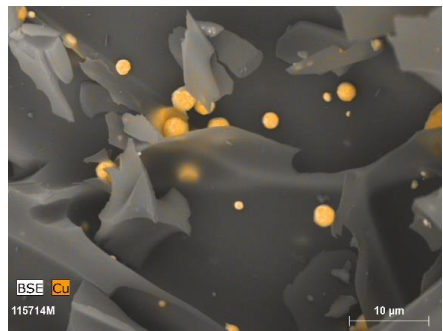
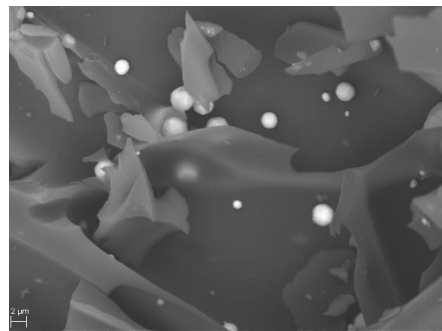
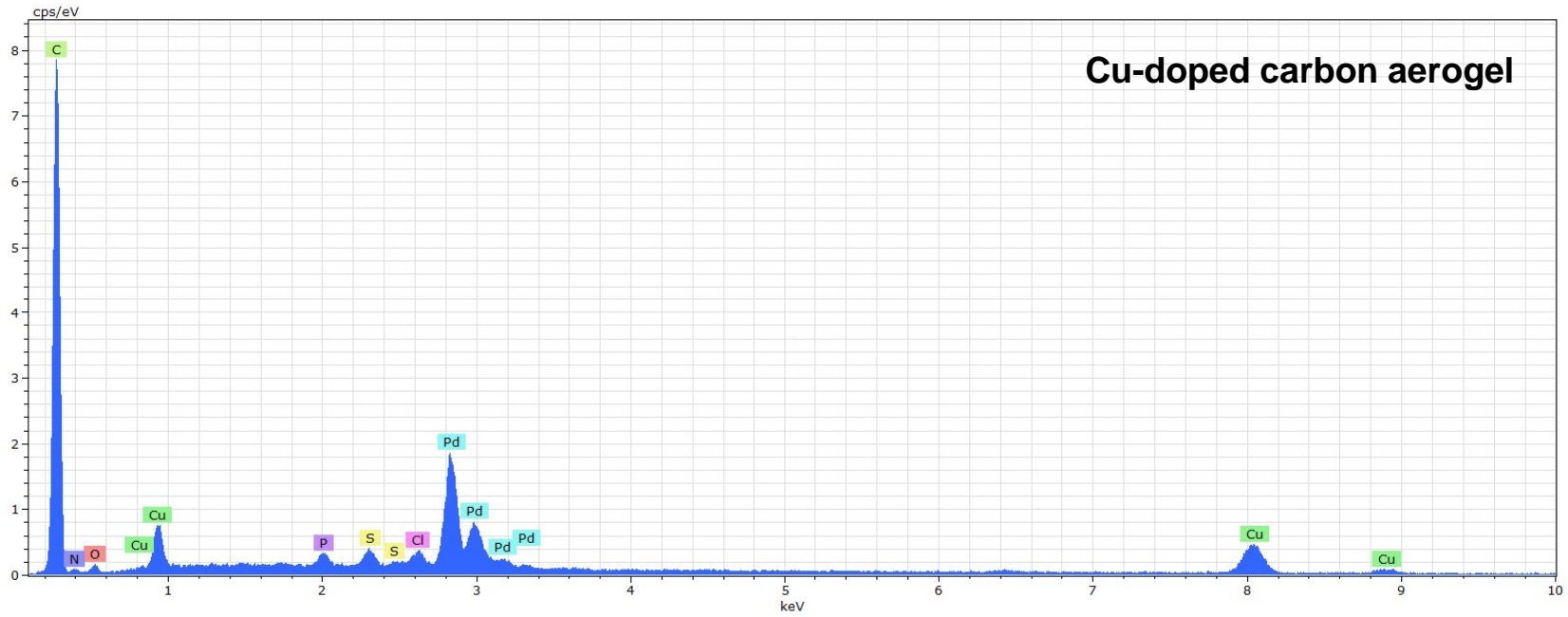


(a) EDS spectrum and (b) SEM image of the GeTe microcrystals, along with the associated EDS element mapping data showing uniform distribution of (c) Ge and (d) Te throughout each particle.

SEM of polyurea (a) 2.75 g (b) 16.5 aerogels

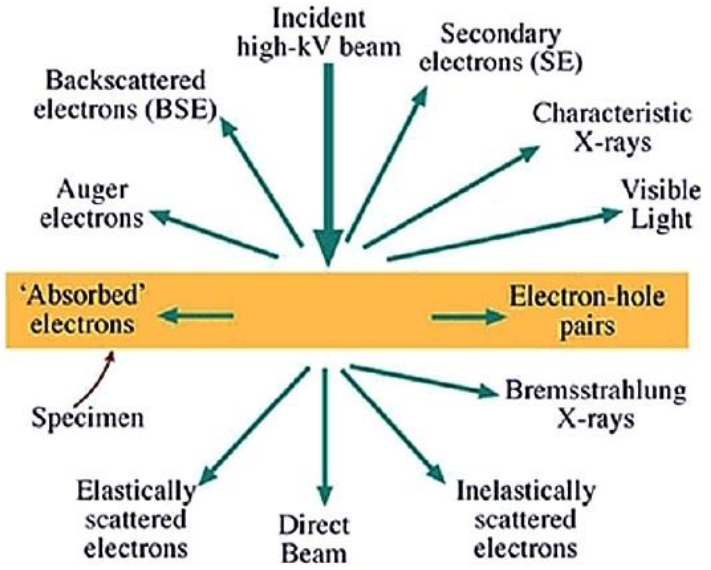
Scanning electron microscopy (SEM) and Electron dispersive spectroscopy (EDS)

Cu-doped carbon aerogel



Transmission electron microscopy (TEM)

Electron-sample interaction



Secondary e⁻: SEM (Topographical information)

Backscattered e⁻: Atomic number and topographical information

Auger e⁻: surface sensitive composition information

Characteristics x-rays: Through-thickness composition information

Direct beam: TEM (Sample morphology)

Inelastically scattered e⁻: EELS (Electron energy loss spectrum)

Elastically scattered e⁻: Major of contrast in TEM image and formation of DPs

Bremsstrahlung X-rays: XEDS (x-ray Energy dispersive spectra)

Optical Microscope (OM)

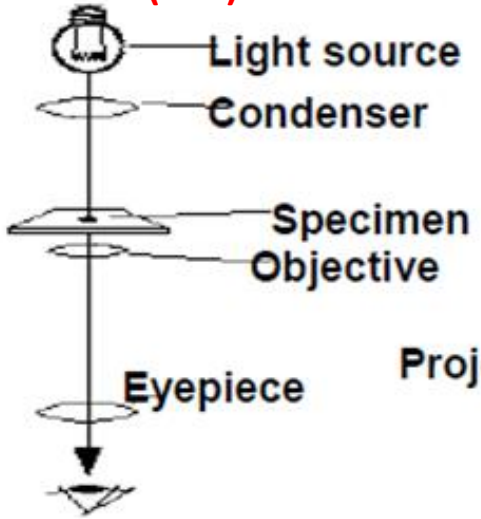


Image viewed directly

Transmission Electron Microscope (TEM)

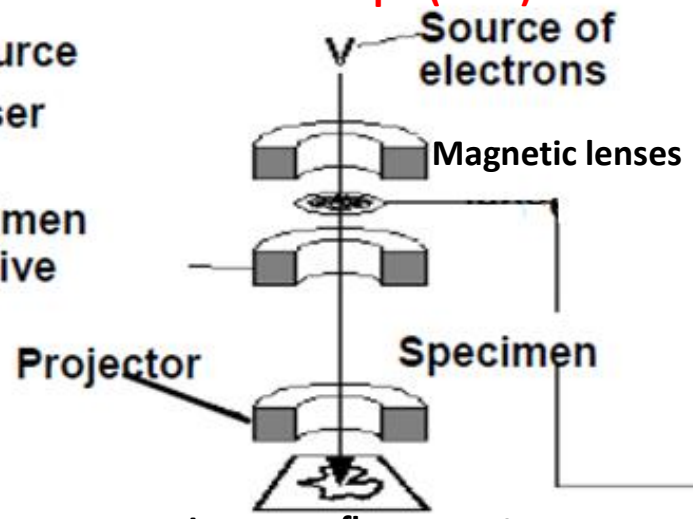
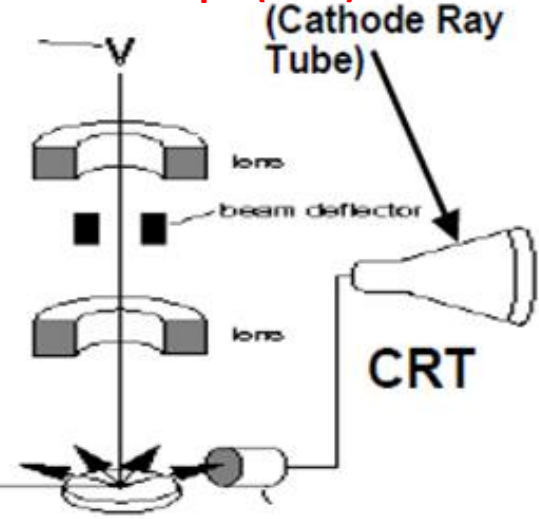


Image on fluorescent screen

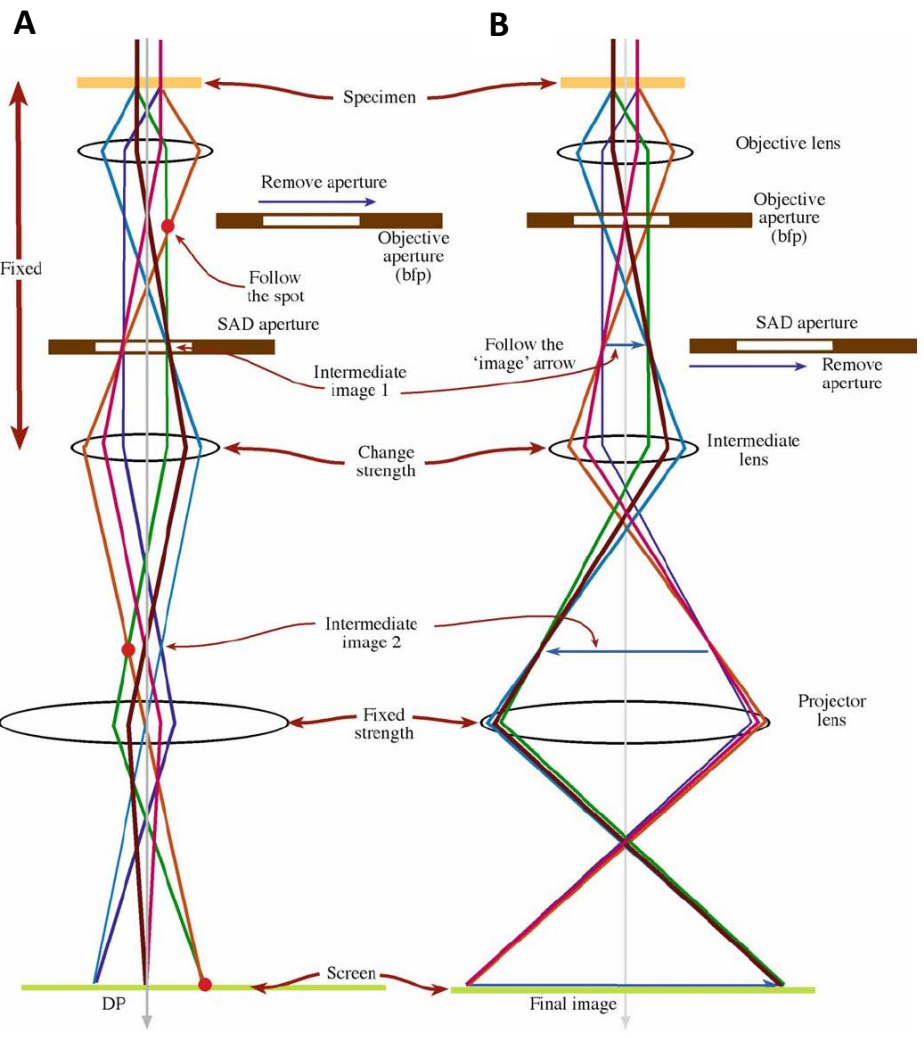
Scanning Electron Microscope (SEM)



Detector

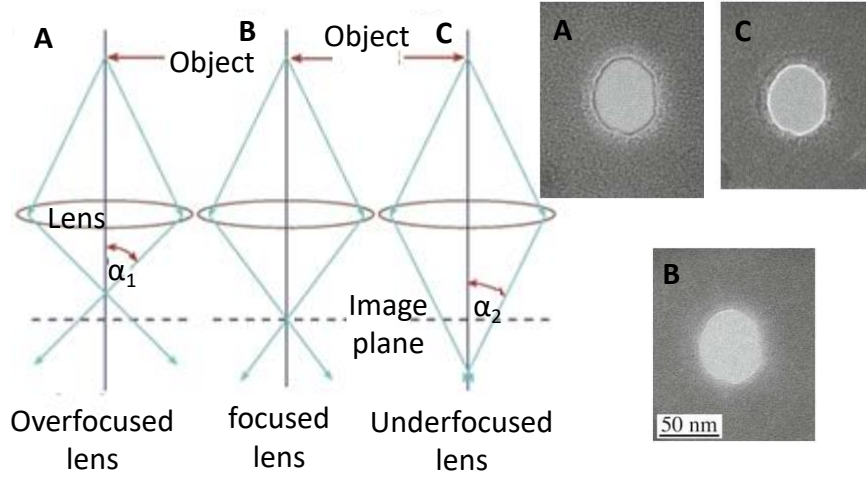
Transmission electron microscopy (TEM)

Modes of TEM operation

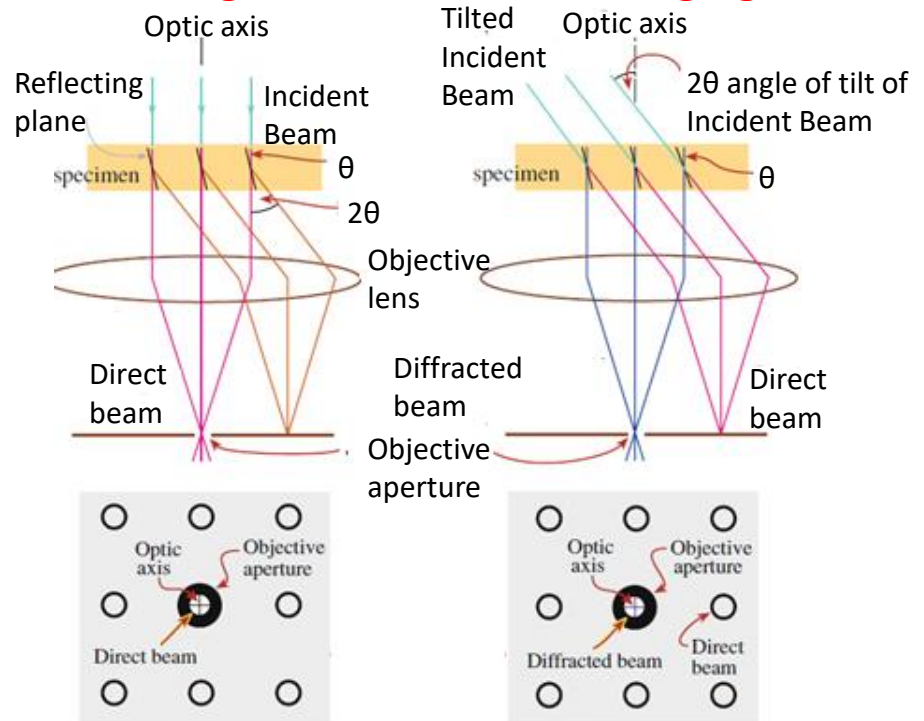


A) Projecting the diffraction pattern,
 B) Projecting the image. The intermediate lens selects either the Back Focal Plane or the image plane of the objective lens.

Lens focusing and resulting image

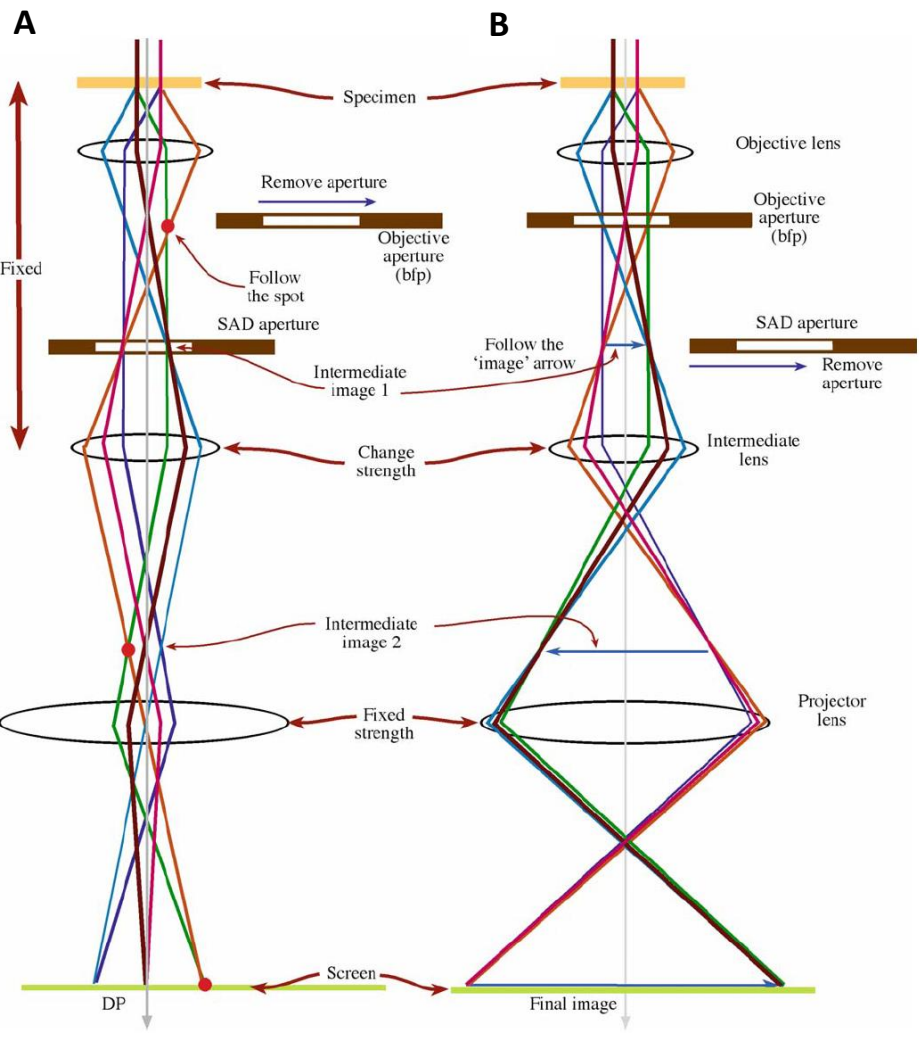


Bright field-Dark field imaging



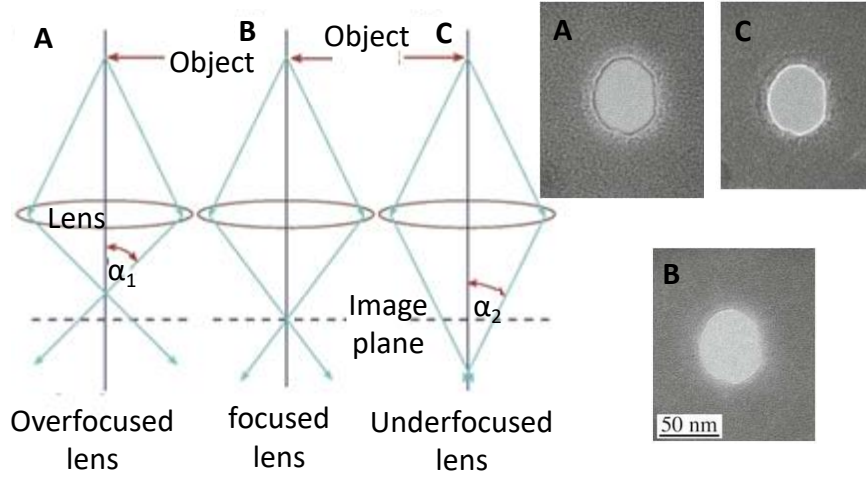
Transmission electron microscopy (TEM)

Modes of TEM operation

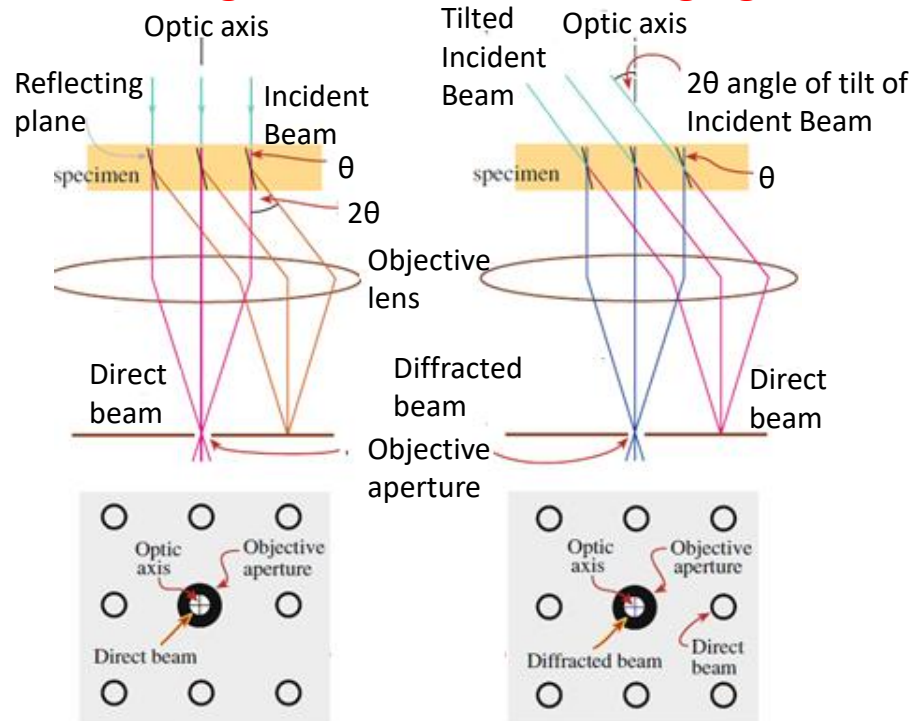


A) Projecting the diffraction pattern,
 B) Projecting the image. The intermediate lens selects either the Back Focal Plane or the image plane of the objective lens.

Lens focusing and resulting image



Bright field-Dark field imaging



Transmission electron microscopy (TEM)

